Seismic Behavior of Steel Framed Structures with Infill Walls - Analytical Study

Elif Nazlı Akbaş

Submitted to the
Institute of Graduate Studies and Research
in partial fulfillment of the requirements for the degree of

Master of Science
in
Civil Engineering

Eastern Mediterranean University
September 2017
Gazimağusa, North Cyprus

Approval of the Institute of Graduate Studies and Research

Assoc. Prof. Dr. Ali Hakan Ulusoy
Acting Director

I certify that this thesis satisfies the requirements as a thesis for the dgree of Master of Science in Civil Engineering.

Assoc. Prof. Dr. Serhan Şensoy
Chair, Department of Civil Engineering

We certify that we have read this thesis and that in our opinion it is fully adequate in scope and quality as a thesis for the degree of Master of Science in Civil Engineering.

Assoc. Prof. Dr. Mürüde Çelikağ
Supervisor

Examining Committee

1. Assoc. Prof. Dr. Mürüde Çelikağ _____

2. Assoc. Prof. Dr. Mehmet Cemal Geneş _____

3. Asst. Prof. Dr. Abdullah Fettahoğlu _____

ABSTRACT

The objective of this numerical study was the investigation of the seismic behavior of steel framed structures with infill walls. The equivalent diagonal struts and shear spring model based finite element software SeismoStruct was employed for this purpose. The experimental test setup and the data obtained from the experiments were used to verify the two basic analytical models by using SeismoStruct software. Then, six new groups of frame models were formed by using the validated simple frame structures. The number of bays and stories were increased, and infill walls were introduced in alternative steel frames. The global structural performance parameters of top displacement, base shear, fundamental time period, out-of-plane displacement and local parameters of inter-story drift ratio and member deformation capacities were obtained for all models. These parameters were compared in each group of models to detect symmetry/asymmetry and vertical discontinuity based effects due to presence or absence of infill walls. From this study, it is concluded that infill walls can increase strength and stiffness of the systems depending on the location of them. Also, the orientation of vertical frame members have significant advantages such as decreased fundamental time period, zero-out-of-plane displacement for minor axis frame models.

Keywords: steel frame, infill wall, infill panel, infilled steel frame, static-pushover analysis, moment frame

ÖZ

Bu nümerik çalışma ile dolgu duvarların çelik çerçeve yapı sistemlerinin sismik davranışına etkileri araştırılmıştır. Bu amaç için çerçeve yapılardaki dolgu panellerin doğrusal olmayan davranışlarını modellemede eşdeğer basınç ve kesme çubuğu yaklaşımını esas alan sonlu elemanlar programı SeismoStruct kullanılmıştır. SeismoStruct kullanılarak referans olarak alınan bir deneysel çalışmanın yarı ölçekli örnekleri bilgisayar ortamında bire bir aynısı oluşturularak test edilmiştir. Daha sonra deneysel çalışmada kullanılan örneklerin açıklık ve kat sayıları artırılmış ve dolgu panellerin yerleri değiştirilerek altı adet yeni model grubu oluşturulmuştur. Bu modeller genel performans parametreleri olan yatay yer değiştirme, taban kesmesi, yapının serbest titreşim periyodu, düzlem dışı yer değiştirme ve lokal parametreler olan katlar arası rölatif deplasman ile eleman kapasiteleri açısından incelenmiştir. Dolgu duvarların varlığı ve simetrik/asimetrik yerleşimleri nedeniyle planda ve düşey düzlemde oluşan düzensizliklerin bu parametrelere etkisi her grup kendi içerisinde ve tüm gruplar karşılaştırılarak çıkarımlar yapılmıştır. Yapılan çalışma neticesinde dolgu duvarların konumuna bağlı olarak rijitlik ve sağlamlığı artırdığı sonucuna varılmıştır. Ayrıca, düşey taşıyıcı elemanların yerleşim yönlerinin yapının serbest titreşim periyodunu düşürmek ve düzlem dışı yer değiştirmeyi azaltmak gibi avantajları olduğu gözlemlenmiştir.

Anahtar Kelimeler: çelik çerçeve, dolgu duvar, statik itme (pushover) analizi

DEDICATION

To my dear family and especially to my one and only NEPHEW…

TABLE OF CONTENTS

LIST OF TABLES

LIST OF FIGURES

LIST OF SYMBOLS AND ABBREVIATIONS

$\varepsilon_{\mathbf{m}}$	Stain at maximum stress
$\varepsilon_{\mathbf{ult}}$	Ultimate stain
$\varepsilon_{\mathbf{cl}}$	Closing strain
$\varepsilon_{\mathbf{1}}$ & $\varepsilon_{\mathbf{2}}$	Strut area reduction strain
γ_{pr} or γ_{plr}	Reloadin stiffness factor
γ_{plu}	Starting unloading stiffness factor
α_{re}	Strain reloading factor
α_{ch}	Strain inflection factor
β_a	Complete unloading strain factor
β_{ch}	Stress inflection point
μ	Coefficient of friction or mean value
τ_{max}	Maximum shear stress
τ_o	Shear bond strength
α_s	Reduction shear factor
γ_s	Proportion of Stiffness Assigned to Shear
σ	Standard deviation
A_1	Strut Area 1
A_2	Strut Area 2
b_w	Equivalent strut width
c.o.v.	Coefficient of variation
disp.	Displacement
d_m	Masonry panel diagonal length

E_m	Elastic Modulus
e_{x1}	Plastic unloading stiffness factor
e_{x2}	Repeated cycle strain factor
$f_m\theta$	Compressive Strength
f_t	Tensile strength
h_z	Equivalent Contact Length
infmFB	Inelastic force-based frame element
MAJ-1B-1S	1 bay 1 story bare major axis frame (validation model)
MAJ-1B-1S-INF	1 bay 1 story major axis frame with infill (validation model)
MAJ-1B-2S	1 bay 2 story bare major axis frame
MAJ-1B-2S-GRINF	1 bay 2 story major axis frame with infill in the ground story only
MAJ-1B-2S-INF	1 bay 2 story major axis frame with infill
MAJ-1B-2S-UPINF	1 bay 2 story major axis frame with infill in the upper story only
MAJ-2B-1S	2 bay 1 story bare major axis frame
MAJ-2B-1S-INF	2 bay 1 story major axis frame with infill
MAJ-2B-1S-LINF	2 bay 1 story major axis frame with infill in the left bay only
MAJ-2B-1S-RINF	2 bay 1 story major axis frame with infill in the right bay only
MAJ-2B-2S	2 bay 2 story bare major axis frame
MAJ-2B-2S-ASYM1	2 bay 2 story major axis frame with asymmetrically placed infill
MAJ-2B-2S-ASYM2	2 bay 2 story major axis frame with asymmetrically placed infill

MAJ-2B-2S-GRINF	2 bay 2 story major axis frame with infill in the ground story only
MAJ-2B-2S-INF	2 bay 2 story major axis frame with infill
MAJ-2B-2S-LINF	2 bay 2 story major axis frame with infill in the left bay only
MAJ-2B-2S-RINF	2 bay 2 story major axis frame with infill in the right bay only
MAJ-2B-2S-UPINF	2 bay 2 story major axis frame with infill in the upper story only
MIN-1B-1S	1 bay 1 story bare minor axis frame (validation model)
MIN-1B-1S-INF	1 bay 1 story minor axis frame with infill (validation model)
MIN-1B-2S	1 bay 2 story bare minor axis frame
MIN-1B-2S-GRINF	1 bay 2 story minor axis frame with infill in the ground story only
MIN-1B-2S-INF	1 bay 2 story minor axis frame with infill
MIN-1B-2S-UPINF	1 bay 2 story minor axis frame with infill in the upper story only
MIN-2B-1S	2 bay 1 story bare minor axis frame
MIN-2B-1S-INF	2 bay 1 story minor axis frame with infill
MIN-2B-1S-LINF	2 bay 1 story minor axis frame with infill in the left bay only
MIN-2B-1S-RINF	2 bay 1 story minor axis frame with infill in the right bay only
MIN-2B-2S	2 bay 2 story bare minor axis frame
MIN-2B-2S-ASYM1	2 bay 2 story minor axis frame with asymmetrically placed infill
MIN-2B-2S-ASYM2	2 bay 2 story minor axis frame with asymmetrically placed infill

MIN-2B-2S-GRINF	2 bay 2 story minor axis frame with infill in the ground story only
MIN-2B-2S-INF	2 bay 2 story minor axis frame with infill
MIN-2B-2S-LINF	2 bay 2 story minor axis frame with infill in the left bay only
MIN-2B-2S-RINF	2 bay 2 story minor axis frame with infill in the right bay only
MIN-2B-2S-UPINF	2 bay 2 story minor axis frame with infill in the upper story only
RC	Reinforced Concrete
sits	Symmetric I or T section
stl_bl	Bilinear steel model
t_w	Infill panel thickness
Y_{oi} and X_{oi}	Horizontal offset
z	Contact length

Chapter 1

INTRODUCTION

1.1 Introduction

The reaction of masonry infill walls during an earthquake is complex and unpredictable due to variations in material properties and their brittle force-displacement behaviour. This yields to infill walls being ignored during design and analysis of new structures and capacity evaluation of the existing buildings. However, field observations after recent earthquakes e.g. Adana-Ceyhan (1998), Bam-Kerman (2003) and L'Aquila (2009), show that structures with infill walls experience in-plane and out-of-plane wall failures, frame failures and formation of soft and weak story (Fig.1.1) which affects strength, stiffness and ductility of the system.

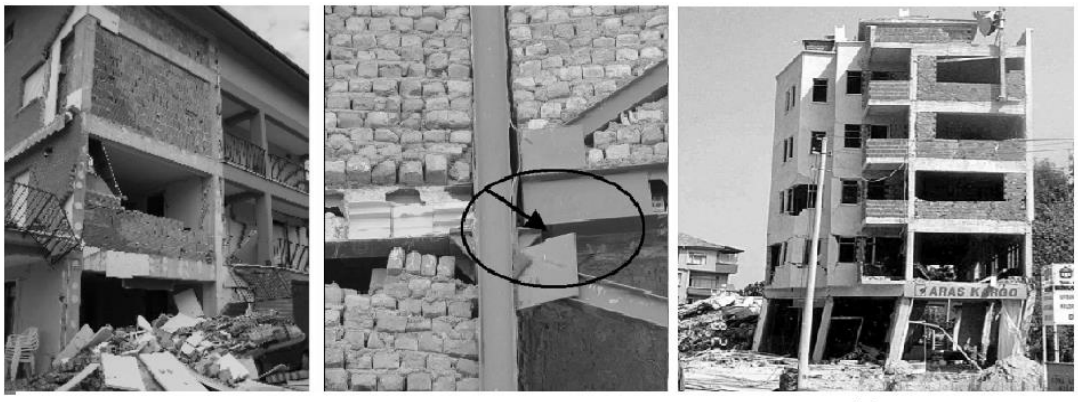

(a) (b) (c)

Figure 1.1: (a) Failure of infill walls, (b) frame failure and, (c) formation of a soft and weak story from L'Aqulia (2009), Bam-Kerman (2003) and Gölcük-Kocaeli (1999) earthquakes respectively [1, 2, 3]

The presence of infill walls alters the lateral-load transfer mechanism by developing alternative load paths through infills. Studies on reinforced concrete (RC) frames showed that introduction of masonry infill changes the behaviour of structure from frame action to truss action that creates higher axial forces and lower bending moments in the structural members [4] (Fig.1.2) This can be related to so called equivalent compressive strut actions of infill walls.

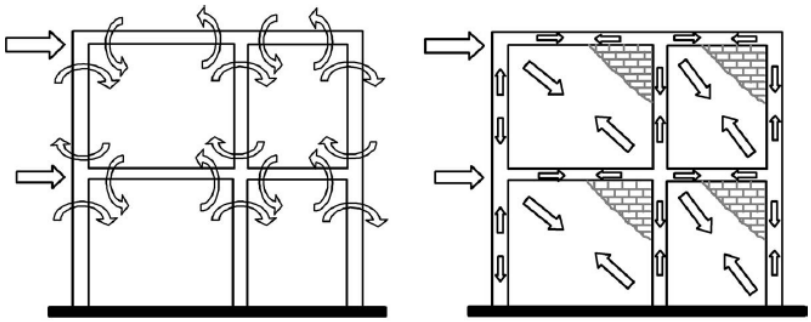

Figure 1.2: Change in the lateral-load transfer mechanism due to masonry infills [5].

Uncertain positions of infill walls and openings in them can create irregularities in plan and elevation. Also, regular structures can become irregular by rearrangement of infills according to changing functional requirements of the occupants without considering the structural effects of these changes. Thus, construction of a regular building as well as sustaining its design during its service life is a difficult issue (Fig. 1.3).

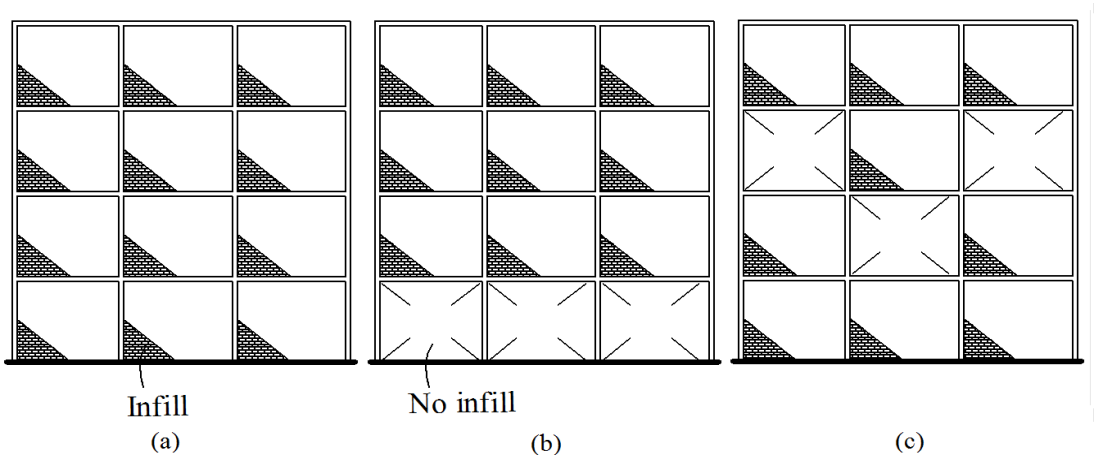

Figure 1.3: Different arrangement of infill walls; (a) fully infilled, (b) only upper stories infilled and, (c) asymmetrically placed infills in structures.

The significance of infill walls has been recognized after the results of broad scientific research and in the light of these studies, two earthquake resistant design approaches were suggested. [6]. The first one proposed to isolate infill walls from the frame in which they are located to neglect their effects. In the second one, infill walls are taken into account in the design, detailing and construction by proper introduction of them inside the surrounding frames. Despite the former approach, the second one allows to predict and determine global and local impacts of these stiff and brittle components. These approaches have been adopted by a number of available national codes and design guidelines such as FEMA 306 [7], FEMA 273 [8] and Eurocode 8 [9] which are intended for evaluation and rehabilitation of earthquake prone and damaged buildings to enclose infill walls but they differ greatly from a seismic performance viewpoint [4]. Thus, infill walls are treated as non-structural elements such as partition, finishing and isolation, in practice. However, they are required to receive more attention for a reliable design.

1.2 Significance and Objective of this Research

More study is necessary to understand how the presence and location of the infill walls affect the behaviour of structural systems. Although, a broad study has been done on infilled RC framed structures, there is considerably less study on infilled steel framed structures. Also, in these studies, the effects of infill walls on strength, stiffness and energy absorption capacity have been studied but symmetry/asymmetry and plan/vertical discontinuity due to presence or absence of infill walls has not been investigated comparatively yet.

In addition, it is believed that level of interaction between the infill and its surrounding frame is affected by the type of material they are made (e.g. concrete BIMs or clay bricks and RC or steel). Thus, it might not be convenient to assume that the behaviour of steel frames will be in similar manner as the RC frames [10].

This thesis is aimed to provide more information about structural performance of masonry infilled steel framed structures by introducing infill walls at different locations of the frame to include plan and vertical irregularities and symmetrical/asymmetrical placement of them. For this purpose the experimental test setup and data of Milad [11] was used to verify the analytical models prepared by using SeismoStruct programme. Upon completion of the validation of models then new group of models were created by using SeismoStruct programme to investigate effects of infill walls to steel frames.

1.3 Organization of the Thesis

This thesis is composed of five chapters, also, table of content, list of figures, tables, symbols, abbreviations and references are provided to fulfil an easy access to required information.

Chapter 1 presents general information about infill walls, significance and objective of the study and content of the thesis.

Chapter 2 provides a broad literature review including frame types, seismic methods of analysis, failure modes of infill walls and frames, soft/weak story formation and modelling of infill walls.

In Chapter 3, reference experimental study of Milad [11] was mentioned briefly and then the validation of this study was done by SeismoStruct created models.

In Chapter 4, new groups of models having different infill wall locations and column orientations are analyzed and their results are given. Finally, the conclusions and suggestions for future research are provided in Chapter 5.

Appendix A gives load-displacement curves, global and local performance parameters of validation models.

Appendix B gives the location of plastic hinges for all model groups.

It should be noted that the terms infill wall, infill panel and infills will be used interchangeably for masonry infill walls throughout this thesis according to terminology.

Chapter 2

LITERATURE REVIEW

2.1 Introduction

Masonry walls with many other kinds of infill walls are commonly used as partition walls to separate interior spaces or as finishes on the exterior surface of the buildings for aesthetic purposes [12]. Despite their extensive use, infill walls in both RC and steel frames are treated as non-structural elements, hence contribution of these elements on the behaviour of structures are neglected at design phase. Furthermore, their contribution to the system is ignored in the assessment of the existing buildings [13]. These two approaches are due to lack of universally accepted scientific information that provides sufficient specifications on design practices by describing the extent of infill-frame interaction when loads are present. As a result, surrounding frames are designed to bear both gravity and lateral loads [14] which yields the need of decent isolation of infills from the surrounding frame to prevent their large in-plane stiffness that is incorporated in the lateral load resisting system of the structure. This approach may lead to uneconomical design practices since daily design practices proportionate structural components of buildings with respect to displacement and strength requirements [1]. On the other hand, when infill walls are designed to participate in the load carrying capacity and tightly placed into surrounding frame for this purpose without considering their contribution to the strength and stiffness of the frame system, unsafe designs practices arise [14]. This is because of the fact that, due to interaction between infill walls and load resisting

structural members (e.g. beams, columns) dynamic characteristics (e.g. strength, stiffness, ductility) of the system changes, either positively or negatively [15].

Infill walls have both advantageous and disadvantageous effects but researchers have failed to form a common ground on which side it outweighs. Increment in overall strength and stiffness of the frames are considered as positive effects of infill walls. On the other hand torsional motion and soft-story/weak-story formation are considered as negative effects resulting from irregular placement of them in plans and upright direction respectively.

Other changes in the structural behaviour includes, increment of received seismic forces in structural elements, i.e. columns, due to increased structural stiffness and increased out-of-plane vulnerability of infill walls due to rising in-plane shear demands [16]. In addition, interaction between the infill and its surrounding frame causes formation of plastic hinges at the column ends due to crushed wall on the corners. This undesirable phenomena is known as short column formation which jeopardises the designs because strong column-weak beam configuration is aimed by the codes [15].

Referring to the available analytical and experimental data from past research, failure modes related with infill and surrounding frames can be categorized as infill failure (in-plane, out-of-plane infill failure), frame failure (column and beam elements failure), and soft/weak storey formation [17]. Thus, if infills are neglected during the design, lateral stability of the frame can be affected at serious levels. Hence, for a reliable design, it is essential to know the contribution of infills to the stiffness and strength of the infill-frame system [14,18]. However, due to its composite nature (composed of mortar, bricks etc.), many uncertainties of infill walls arise which

eventually causes them to be considered with their insulating, aesthetic and finishing aspects rather than their structural contribution to the behaviour of the system. Nevertheless, there have been a numerous researches investigating the effects of infills on the structural behaviour of the systems. For this purpose two modelling techniques are used for infills: micro models and macro models. The first one gives more detailed information than the latter due to large number of elements considered in the analysis. Also it provides a better understanding of the local effects despite macro models. In the macro modelling case, often structural responses of infill walls are examined by replacing them with equivalent diagonal strut(s) for simplicity [16].

2.2 Frame Types

Structural frames are chosen to resist the particular loads they are expected to be exposed during their service lives. Two principal categories of lateral load resisting systems of moment-resisting frames and dual systems are accommodated when lateral and gravity loads are considered. The main aim of structural engineers is to provide a system with regular mass and stiffness throughout the structure for continuous flow of loads to the foundation. However, vertical discontinuities and irregularities hinder this goal which can be solved by the continuity of stiff structural elements down to the foundation [19].

2.2.1 Moment-Resisting Frames

The design of moment resisting frames (Fig. 2.1) is based on strong column weak beam configuration that aims plastic hinges to develop at the beam ends prior to column ends (Fig. 2.2). In addition, sufficient strength and stiffness should be provided to resist seismic forces and inter-story drifts respectively while sustaining beam-column joint rotation [19]. Thus, these frames resist lateral loads by the flexure

in beams, columns and joints. Ductility develops by flexural yielding of beams, shear yielding of column panel zones and flexural and axial yielding of columns.

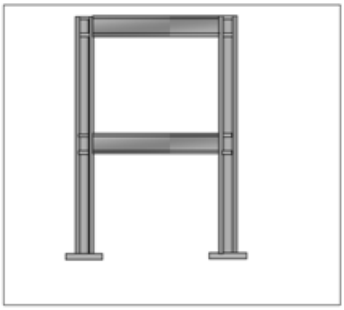

Figure 2.1: Moment resisting frame [20].

The columns are subjected to zero moment at their mid-heights as well as shear distribution. Also, inter-storey drifts and shear forces develop proportional to the moments of inertia of the columns under lateral forces. These frames are sometimes referred to as shear systems due to latter two actions.

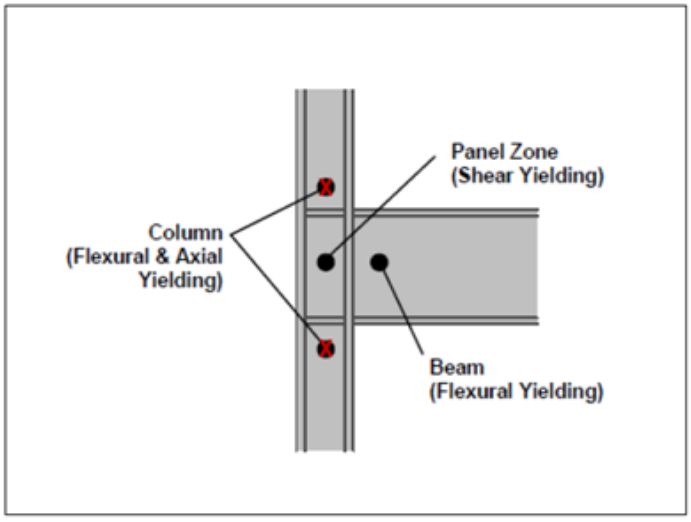

Figure 2.2: Possible plastic hinge locations [20].

2.2.2 Dual Systems

These systems consist of braced or infilled moment-resisting frames where the shear and moment diagrams of the walls and frames are completely affected by the coupling of the moment resisting frames with braces or shear/infill walls (Fig. 2.3 and 2.4). Hence, the difference in shear between the floors displays small variation because large displacements are inhibited by the braces or infill walls. The total design force can be resisted by the use of these two systems together in accordance with their lateral stiffness values.

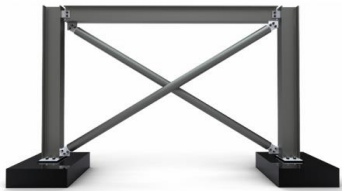

Figure 2.3: Diagonally braced frame [21].

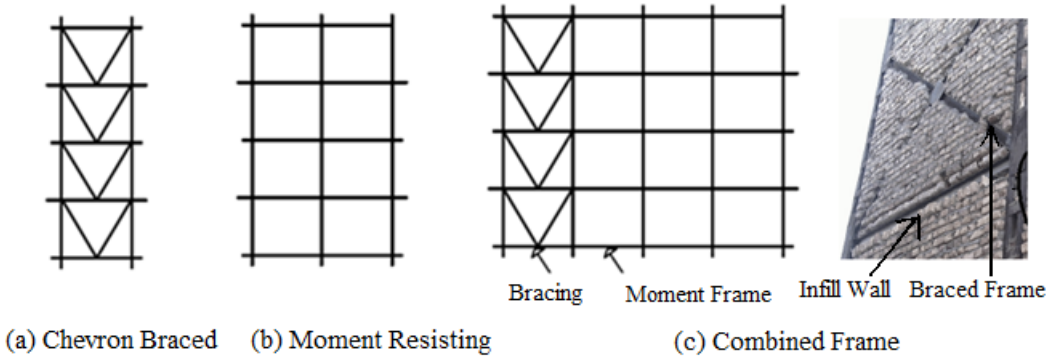

Figure 2.4: (a) Chevron braced frame system, (b) moment frame system and, (c) dual multi-storey frame system.

2.3 Seismic Methods of Analysis

After setting the structural model and performing the structural analysis then it is possible to determine the seismic forces induced on the structure. The types of structural model selected, external actions, the behaviour of structure and the

structural materials, indicate which analysis method can be used. According to the nature of the considered variables, methods of analysis can be categorized as shown in Figure 2.5.

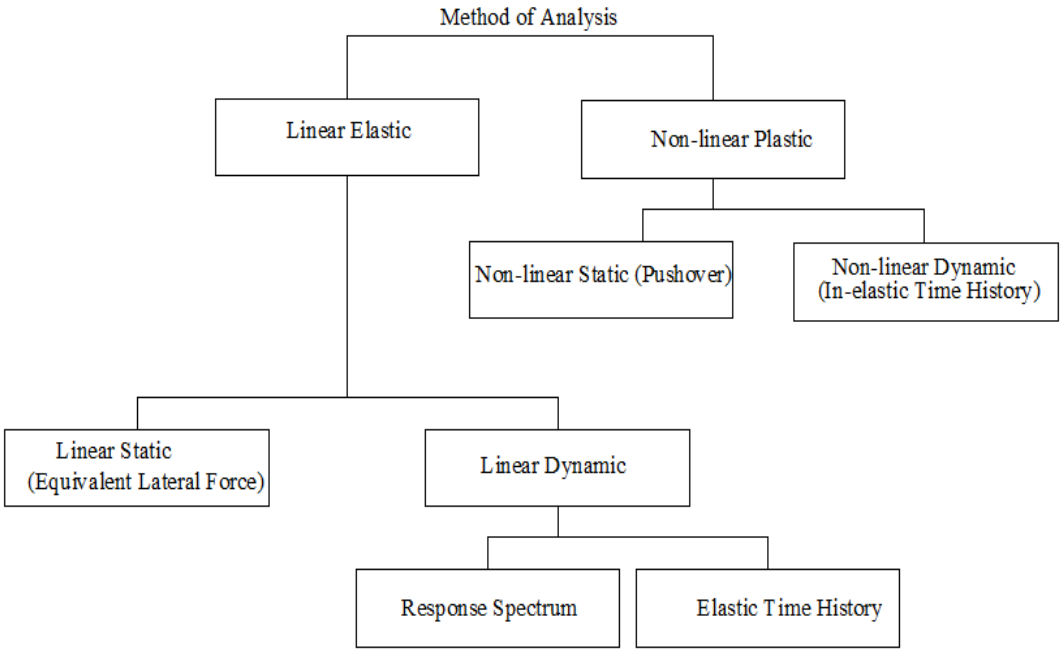

Figure 2.5: Seismic methods of analysis.

The regular structures with limited height can be analyzed by using linear static (or equivalent static) analysis. The response spectrum method and the elastic time history method are the two ways in which linear dynamic analysis can be performed. The level of forces and the distribution of them through the height of the structure distinguish linear static analysis from linear dynamic analysis.

Non-linear static analysis involves inelastic structural behaviour and can be considered as improved method over linear static and linear dynamic analysis. However, the actual response of a structure to seismic forces can only be described precisely by non-linear dynamic (or inelastic time history) analysis.

2.3.1 Elastic/Linear Analysis

This type of analysis is performed by the equivalent lateral force method (static) and response spectrum or more refined time history method (dynamic) of static and dynamic analysis respectively. Such analysis methods are used to determine forces and resulting displacements due to each horizontal component of ground motion for an idealized building that has one lateral degree of freedom per floor in the considered direction of ground motion. The preliminary design of the building can be held by equivalent lateral force procedure and then response spectrum and elastic time history methods can be applied.

2.3.1.1 Linear Static Analysis

This method considers structure's fundamental period of vibration and corresponding modal shape. It is applied by calculating base shear on the structure according to its mass which is then distributed over the height of the structure. This type of analysis is appropriate for regular buildings of medium height.

2.3.1.2 Linear Dynamic Analysis

The linear dynamic analysis can be either performed by response spectrum or elastic time history methods. The former is suitable to use with structures essentially remaining in their linear range of behaviour when their response is substantially affected by the modes other than the fundamental one. On the other hand, the latter overcomes all the deficits in the response spectrum method by involving non-linear behaviour. The response spectrum method is applied for the elastic analysis of structures by considering the response of a single degree of freedom oscillator in each vibration mode independently and later combining them to calculate the total response. The elastic time history method is applied in a way that mathematical model of the building is subjected to accelerations obtained from past earthquake

records to find expected earthquake at the structure's base. This method requires greater computational efforts because the response of a structure is calculated at discrete times. It is advantageous over the probabilistic response spectrum method because while combining different modal contributions, actual behaviour of the structure may be represented incorrectly. Also, the most sophisticated dynamic analysis methods are represented by the time history analysis techniques.

2.3.2 Inelastic/Non-linear Analysis

In general, linear analysis methods are feasible when the response of structure is expected to remain almost elastic. However, uncertainties can arise by the application of linear analysis for non-linearly responding structures because of the fact that inelastic behaviour is implied when performance objective of structures is considered. These uncertainties can be minimized by incorporating non-linear analysis that is performed by non-linear static (pushover) and non-linear dynamic analysis.

2.3.2.1 Non-linear Static Analysis

It is also known as pushover analysis and despite some deficiencies, reasonable estimation on the global behaviour and capacity is provided for the structures essentially responding in the first mode. In this method, gradually increased load with a definitive pattern is imposed on the structure while yielding of various components is allowed. Normally, a target displacement (in general the top of the structure is chosen to be the indicator) is set before the application of the load and then loading is continued until the target is reached. The method is capable of providing information on the strength, ductility and deformation of the structure. Thus, critical members which are prone to reach limit states under earthquake forces can be identified during the design and detailing processes.

2.3.2.2 Non-linear Dynamic Analysis

In this method, integration of differential equations of motion is done by taking into account elasto-plastic deformation of structure.

It is considered as the most rigorous approach because a detailed structural model is combined with past earthquake records. However, response of the structural model can be very sensitive to the characteristics of the individual earthquake under consideration, thus a reliable estimation on the probabilistic distribution of the structural response can be achieved by using different earthquake records.

2.4 Failure Modes of Infill Walls and Frames

Evaluation of the infilled structure is a difficult issue due to difficulties relating the evaluation of the type of infill-frame interaction that significantly affects the load resisting mechanism and the structural behaviour. An infilled frame behaves as a monolithic system at low lateral load levels, with increase in load levels infill starts separating from the surrounding frame forms diagonal compression mechanism.

Infill and infilled frame system failures have been studied to establish a universally accepted general approach for their consideration through the design phase. For this purpose, researchers have been investigated out-of-plane failure of infills in addition to in-plane failure [25]. Also, classical diagonal strut models have been subjected to modifications with further experimental data. In addition, more sophisticated finite element models have been developed to obtain reliable results on non-linear behaviour of infilled frames. Depending on the strength and stiffness of the infills relative to those of the surrounding frames, a number of different possible failure modes have been observed in previous studies. Failure modes associated with infill and frame can be categorized as follows:

2.4.1 Infill Wall Failure

2.4.1.1 In-plane Infill Wall Failure

When infills are designed to contribute to the load carrying capacity they are tightly placed into the surrounding frame. Hence, additional forces will be attracted to the frame area due to their large in-plane stiffness, and this will eventually, partially or as a whole influence the behaviour of the frame system [10]. Partial failure includes in-plane and out-of-plane failure of the infill, failure of the beam and/or column elements, and soft/weak storey formation, where system failure includes total collapse of the building. Some of the very common types of in-plane infill failure can be listed as corner crushing (CC), diagonal compression (DC), diagonal cracking (DK) and sliding shear (SS) (Fig.2.6).

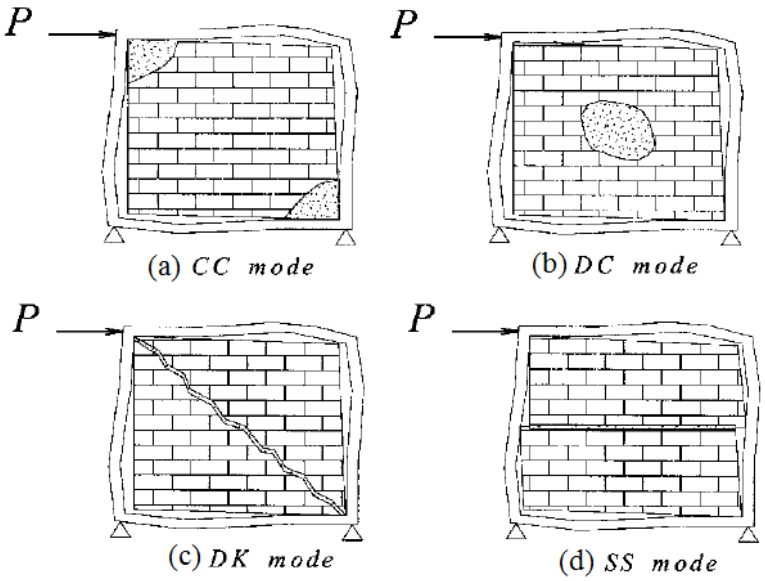

Figure 2.6: Failure modes of masonry infills: (a) corner crushing mode; (b) diagonal compression mode; (c) diagonal cracking mode; and (d) sliding shear mode [22].

The following are the detailed information for each failure mode.

i. The Corner Crushing

This failure mode is observed with weak infill bounded by strong frame members having weak infill-frame interface joints. Infill crush occurs at least at the loaded corner zone.

ii. The Diagonal Compression

This failure mode is observed in the form of panel crushing within its central region. This type of failure requires an infill subjected to in-plane loading with a high slenderness ratio to undergo out-of-plane buckling which happens rarely.

iii. The Diagonal Cracking

This failure mode is observed, in the form of a crack passing through two loaded diagonally opposite corners. It can also take a stepped diagonal shape along the mortar head and bed joints (Fig. 2.7). Weak frames or frames having weak joints and strong frame bounding strong infill are proned to this kind of failure mode. It can be distinguished from other failure modes due to the fact that infill is still capable of carrying loads after cracks occur.

iv. The Sliding Shear

This failure mode is observed in the form of a horizontally sliding crack through bed joints of a masonry infill having weak mortar joints i.e. mortar joints having low coefficient of friction and bond strength. Diagonal cracking and sliding shear failure modes may take place as a combined mode of failure.

2.4.1.2 Out-of-plane Infill Wall Failure

During earthquakes, infill walls are subjected to combined effects of inertial forces coming perpendicular to them and high in-plane drift demands along out-of-plane and in-plane directions respectively (Fig.2.7).

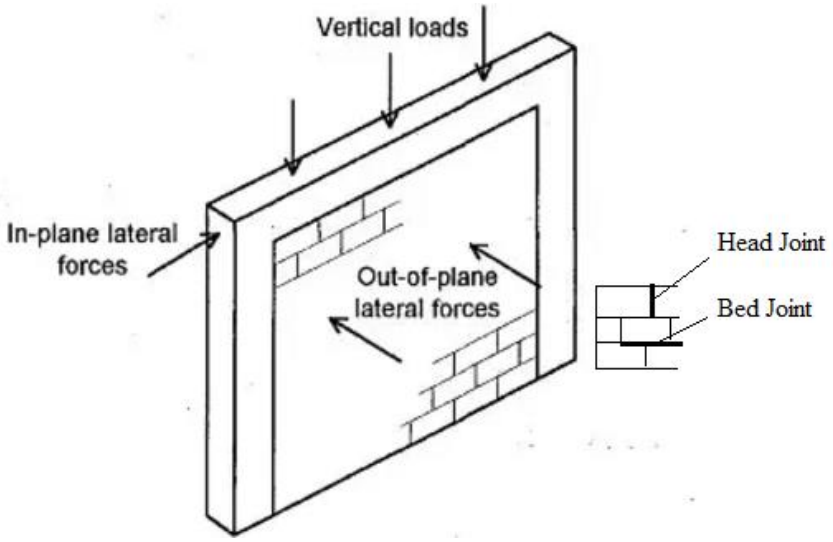

Figure 2.7: Forces acting on structures during earthquakes.

In-plane damage of infill walls triggers out-of-plane failures. Similarly, inappropriate support conditions within the frame create the same problem. High out-of-plane and in-plane demands due to stiffer infill walls relative to the frames in structures lead to sudden changes in the lateral stiffness which may form soft/weak storey mechanism by sudden brittle infill failure. On the other hand, out-of-plane oscillation of infill walls can positively affect the structure's fundamental mode of vibration by reducing the mass contributed within the system [15]. Although, it is expected that larger out-of-plane loads act on infill walls located at upper stories as a result of higher level of acceleration, field investigations in the places which were hit by earthquakes showed that impacts of these loads were more destructive on the lower and middle stories.

Figure 2.8: Out-of-plane infill wall failure after the Abruzzo, Italy earthquake [1, 23].

2.4.2 Frame Failure

The reasons behind the frame failure are related to the mechanical, physical and geometrical properties of infill panels, frame and other structural components. Strong infills surrounded by strong frame and weak frame with weak joints cause plastic hinges to form in the columns and the beams near the joints, the beam column connections or, although occurs very few, at the mid-height of columns[24].

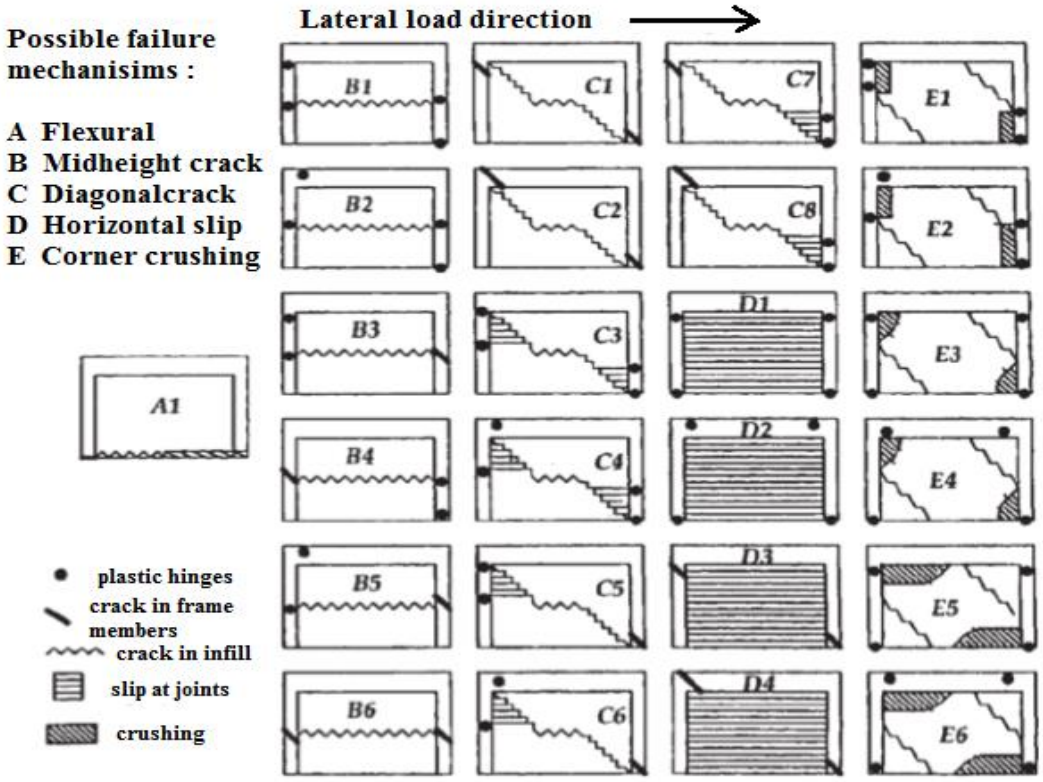

Figure 2.9: Failure mechanisms of infilled frames [25].

Failure of steel frame infilled with unreinforced hollow concrete masonry blocks is rarely observed compared to the case of infilled RC frames [24]. The possible failure modes of surrounding frame are related with shear failure of columns, beam-column connections, flexural collapse mechanism and failure due to axial loads.

i. Column Shear Failure (Shear Yielding)

Design of structural systems is carried out in a way that frames undergo flexural behaviour when seismic forces are present. Although, infill walls provide higher strength, stiffness and better energy dissipation capacity than that of bare frames, most of the lateral loads are compensated by shear action of the columns. However, infills having relatively larger strength and stiffness than the surrounding frame may cause shear failure of columns due to their local destructive effects.

The compression moving downward into the column due to corner crushing of strong infill causes end-region of the columns to bear large shear. The frame members that are no confined by masonry may exhibit localized shear deformations and web buckling for thin webbed steel members. However, shear yielding in steel is ductile and damage arising from this behaviour mode is not serious compared to RC structures. In addition, the same problem takes place when contact is only on one side of the outer columns or infill wall is cut short due to window openings that the effective length of the column is decreased, thus, it cannot resist inter-story drift completely, especially in the ground storey [7].

ii. Bolted or Riveted Connection Failure

The beam-to-column connection of infilled steel frame systems usually have bolted or reverted semi-rigid connections encased in concrete. In the regions of loaded corners, tangential and normal stresses develop highly which puts the connection under considerable axial tension. The prying in the connection angles may occur but ductility of these connections are capable of sustaining many cycles of loading before a low cycle fatigue failure.

iii. Flexural Failure of Frames

Plastic hinges developing in columns are generally located at the ends of these members; in the regions that are exposed to maximum bending moments. It is possible to observe plastic hinges in both columns of a frame at the same time when sliding shear type of infill failure takes place. In this case, one column member fails at the end and the other one at mid height. In the region of plastic hinges, inelastic deformation capacity should be ensured because deformation capacity of plastic hinges determines the deformation capacity of frames [7].

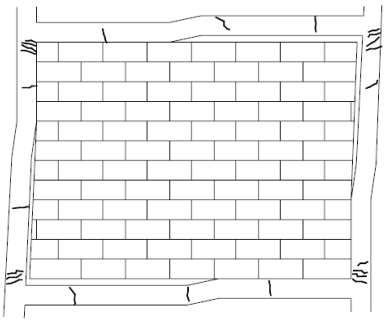

Figure 2.10: Flexural collapse mechanism.

iv. Axial Load Failure

Column compressive failure might occur when frames are subjected to severe axial loading resulting in buckling of the column. In addition to this, as the lateral forces increase so do the tensile axial stresses due to buckling. The large flexural buckling and hence bending of the columns leads to violation of the infill-frame integrity.

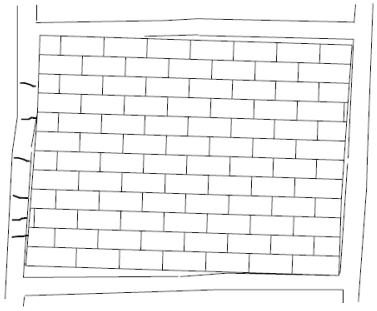

Figure 2.11: Axial load failure of the frame member.

2.5 Vertical Discontinuities and Formation of Soft/Weak Storey

The setbacks (e.g. pent houses), changes in storey height, changes over the height of a structural system (e.g. discontinuous shear/infill walls), changes in materials, and unforeseen participation of non-structural elements lead to sudden changes in stiffness and strength between adjacent storeys [26]. Hence, distribution of lateral forces and deformations under such vertical or horizontal discontinuities can differ

from those of regular structure, eventually resulting in inelastic structural deformations concentrating at or near these discontinuities. As a result, radical changes should be avoided in the vertical configuration for minimizing stiffness and strength differences between the adjacent floors. Overall structural failure due to vertical elements discontinuity of the lateral load-resisting system has been the most common and notable. The buildings having vertical setbacks (Fig. 2.12(a)) [26], are exposed to sudden jump of earthquake forces at the level of discontinuity when forces are transmitted from top to bottom which causes a large vibrational motion to develop. Hence, a large diaphragm action is demanded in these regions. A decrease in the number of walls or columns in a particular storey, or remarkably tall storey (Fig. 2.12(b)) [26] is more likely to cause collapse or damage. The most prevailing mode of vertical elements discontinuity belongs to those buildings where shear/infill walls are only present in the upper storeys and discontinued on the lower storeys resulting in so-called soft storey formation (Fig. 2.12(c)). The reason behind the collapse under this formation is simply reduced stiffness due to geometrical non-linear effects of the soft storey.

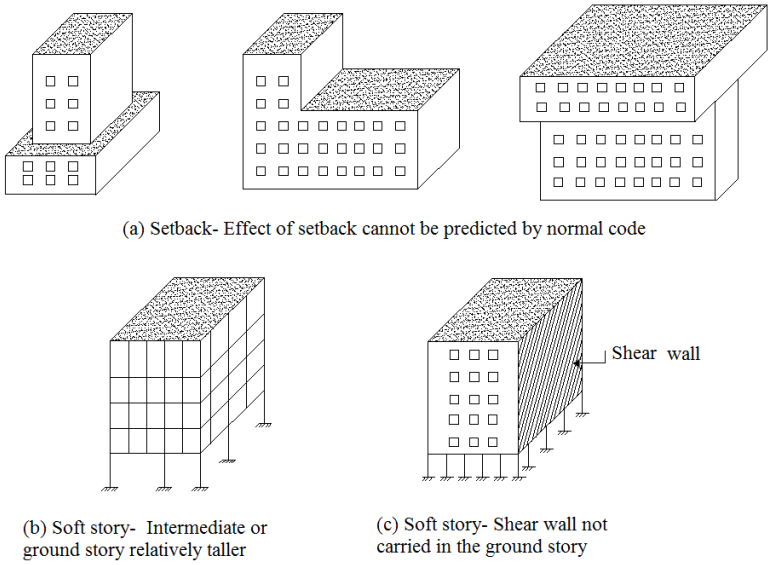

(a) Setback- Effect of setback cannot be predicted by normal code

(b) Soft story- Intermediate or ground story relatively taller

(c) Soft story- Shear wall not carried in the ground story

Figure 2.12: Discontinuation in vertical configuration of buildings [19].

2.6 Modelling of Infill Walls

A highly non-linear inelastic behaviour of infilled frames arises from interaction between the infill panel and the surrounding frame which makes their analytical modelling a complicated issue in turn. Procedures that are used to analyse infilled frames fall into two main groups of simplified or macro-models and local or micro-models namely, according to number of elements considered. In the former group, infill wall is represented with a few number of elements with the aim of understanding global physical behaviour where in the second group, large number of elements are considered to simulate local effects precisely by dividing structure into numerous parts. Equivalent compression strut(s) and the plane finite element modelling are the typical examples for abovementioned models respectively.

2.6.1 Micro Models

The first study included finite element method for modelling structures with infills was conducted by Mallick and Severn in 1967 [26] and since then it has been used extensively by other researchers. However, this model requires a number of different elements to be included due to the composite characteristics of the infilled frames such as: beam or surrounding frame continuum elements, interface and the infill panel continuum elements for the enclosure of the frame-panel interaction. Local effects of cracking, crushing and contact interaction as well as the behaviour of infilled frame can be displayed in more detail by the advantage of the finite element model. More time and greater computational effort is implied in the preparation of the input data and the analysis than the simplified macro models. Non-linear behaviour of infill must be considered by defining constitutive properties of different elements (i.e. infill and frame-panel interface elements) for reliable results and to avoid vain great computational effort.

2.6.2 Macro Models (Equivalent Diagonal Strut(s) Model)

Polyakov (1960) [27] was the first to conduct analytical studies to investigate effects of infill panels. For this purpose he loaded masonry infilled frames laterally and observed diagonal compression failure mode. Then, he suggested that infill elements of frames could be replaced with single diagonal strut acting in compression (Fig.2.13). Holmes' (1961) [28] study followed that idea by proposing a width to the equivalent diagonal strut as one third of the panel length. This was proceeded with a more refined approach by Smith (1962) [29] by assigning a more definitive width to the equivalent diagonal strut. Later on, Mainstone and Weeks (1970) [30] conducted experimental tests to determine the effective diagonal width. Cyclic behaviour of the infill panels with dimming stiffness was taken into account by Bertero and Klinger (1978) [31] and similarly, Hobbs and Saneihejad (1995) [32] used a numerical model to detect strength and stiffness degradation of the infills. Kwan and Liauw (1984) [33] developed strut width in relation to other geometrical parameters of the infill panel. Other studies included investigation of ultimate shear strength, corner crushing strength and post capping strength respectively [34]. For the understanding the effects of infill panels on the overall behaviour of the structures, diagonal strut approach can be accepted as the simplest rational way. However, this approach assumes that diagonal struts be activated in the presence of compressive forces in the infill panel.

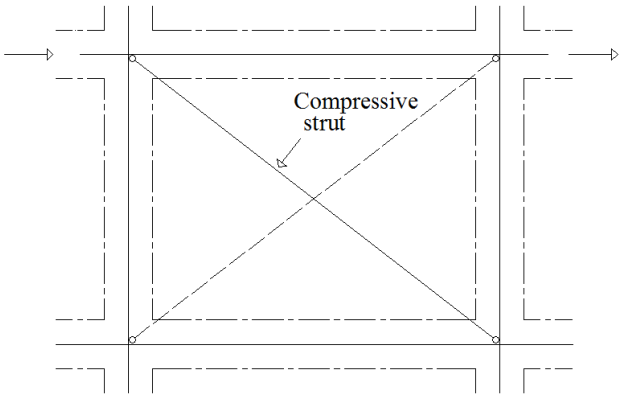

Figure 2.13: Equivalent diagonal strut model for infilled frames.

Also, one equivalent strut aimed for resisting tensile and compressive forces under dynamic and cyclic loading is insufficient to represent internal forces developed in the frame members, describe the infill-frame interaction and the resulting local effects. Hence, shear forces and the bending moments arising in the surrounding frame members as well as the location of plastic hinges cannot be sufficiently estimated. As a result, many researchers modified the single diagonal strut method. First modified approach was proposed to be in the form of two diagonal struts in each direction having the half equivalent strut area by the Flanagan et al. [35] as a primitive approach. Then, Schmidt (1989) [36] implemented a double strut model to include strength and stiffness of the infill as well as the frame-infill interaction. Syrmakesis and Vratsanou (1986) [37] and later San Bartolomé (1990) [38] used increased number of parallel struts ranging between five and nine in number, respectively for each direction. Chrysostomou (1991) [39] used three parallel struts to understand behavior of the frame. Crisafully (1997) [40], first investigated double strut model (Fig. 2.14) for its accuracy in dealing with complexity of the multi strut approaches and later with Carr (2007) [41] adopted a new macro model by modifying his first approach. In this new model, infill panel was represented with

two parallel struts and a shear spring in each direction that were connected to the frame at the column-beam joints by means of four nodes (Fig.2.15). By doing so shear forces of the infill panel was included with the compressive forces at the same time.

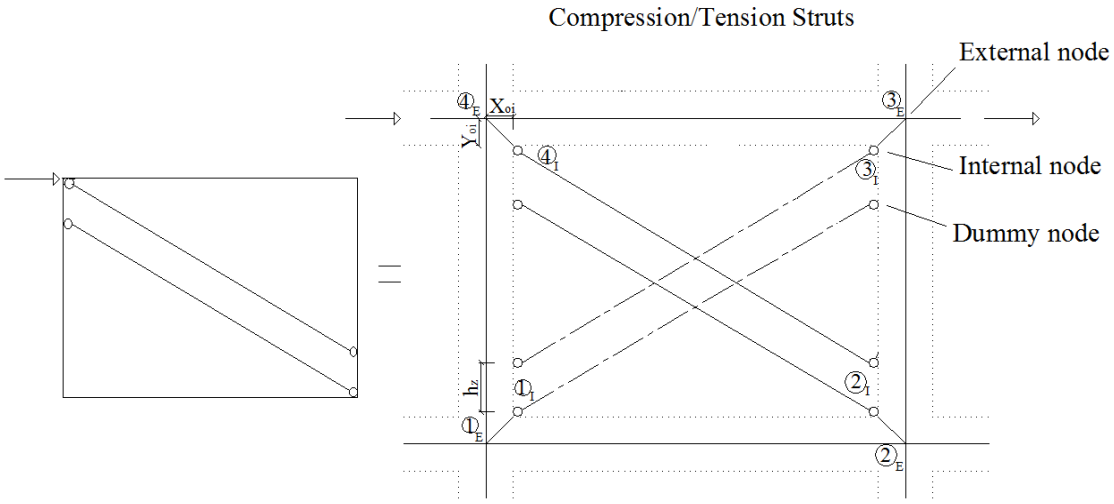

Figure 2.14: Crisafulli double strut model (1997).

2.6.3 Crisafulli & Carr Model

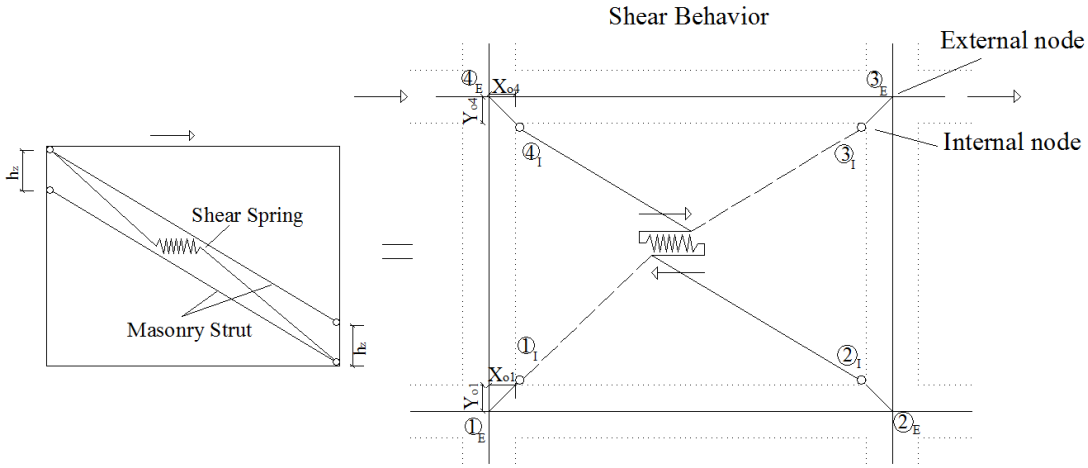

Figure 2.15: Modified Crisafulli double strut model by Carr.

2.6.3.1 Introduction to Crisafulli Model

The model is first proposed by Crisafulli (1997) [40], and shed light upon the following studies of the researchers to develop new macro models or improvement on existing models. Multi-strut models have been proposed to include local effects, such as, shear forces and the bending moments arising in the surrounding frame members resulting from the frame panel interaction. Hence, this model has been found capable of detecting such effects without going through complex analysis.

2.6.3.2 Overview and Implementation of the Model

This model can be accounted for an elaborated version of triple-strut model that compromises with simplified diagonal strut approach while featuring double strut model. The use of this model gives comparatively good insight into the effects of panel-frame interaction at a fair modelling and computational effort [41].

In each direction, tension/compression forces and deformations across the two opposite diagonal corners are accounted by employing two parallel axial struts. Resistance of bed joint and sliding are accounted by one shear spring that, when both directions are considered, makes up four axial struts and two shear springs in total. The spring is active only in compression region i.e. across the diagonal, thus, panel deformation type directly empowers its activation.

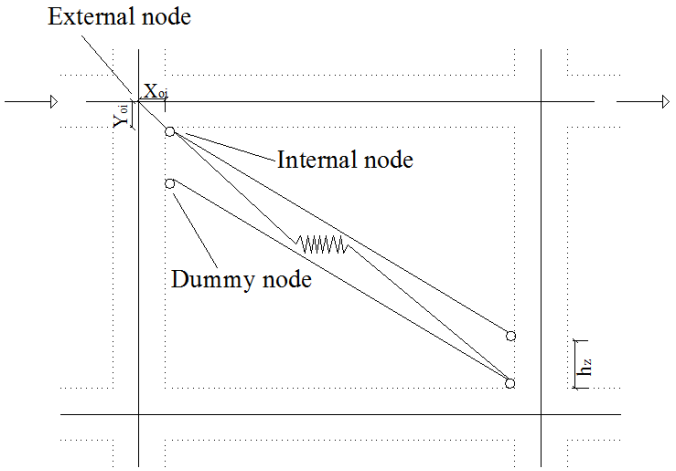

Figure 2.16: Crisafulli and Carr (2007) model for masonry infill panel.

Panel element is developed by considering three different sets of nodes, namely, internal nodes, external nodes and dummy nodes. The frame and infill contact is represented by four internal nodes that are located at the beam column joints of the frame with a vertical and horizontal offset Y_{oi} and X_{oi} respectively measured from the external node i. Contact length between the infill panel and frame elements is represented by four dummy nodes. The forces and displacements developed in the dummy nodes are first transmitted to the neighbouring internal nodes and then all the internal forces are transmitted to the exterior four nodes [41]. The double strut model is employed with the objective of capturing shear forces and moments which are normally introduced in the columns due to compression of infill panels on the contiguous frame members.

2.6.3.3 Parameters of Inelastic Infill Panel Element

Equivalent diagonal strut approach is a highly practical tool for representing infill panels in comparison to more complex micro models from practical viewpoint. As a result, many researchers have been tried to govern parameters to relate infill characteristics with this simplified model. Type of analysis and loading define the required properties for the modelling of the strut i.e. linear-elastic or non-linear type

of analysis and cyclic/dynamic or monotonic type of loading. However, complete material hysteretic behaviour must be defined for dynamic or cyclic loading which yields complexity of the analysis to arise and increases the uncertainties. In order to characterise an infill panel element, depending on the scope of the study, some or all of the following mechanical, geometrical and empirical parameters in Figure 2.17 need to be defined.

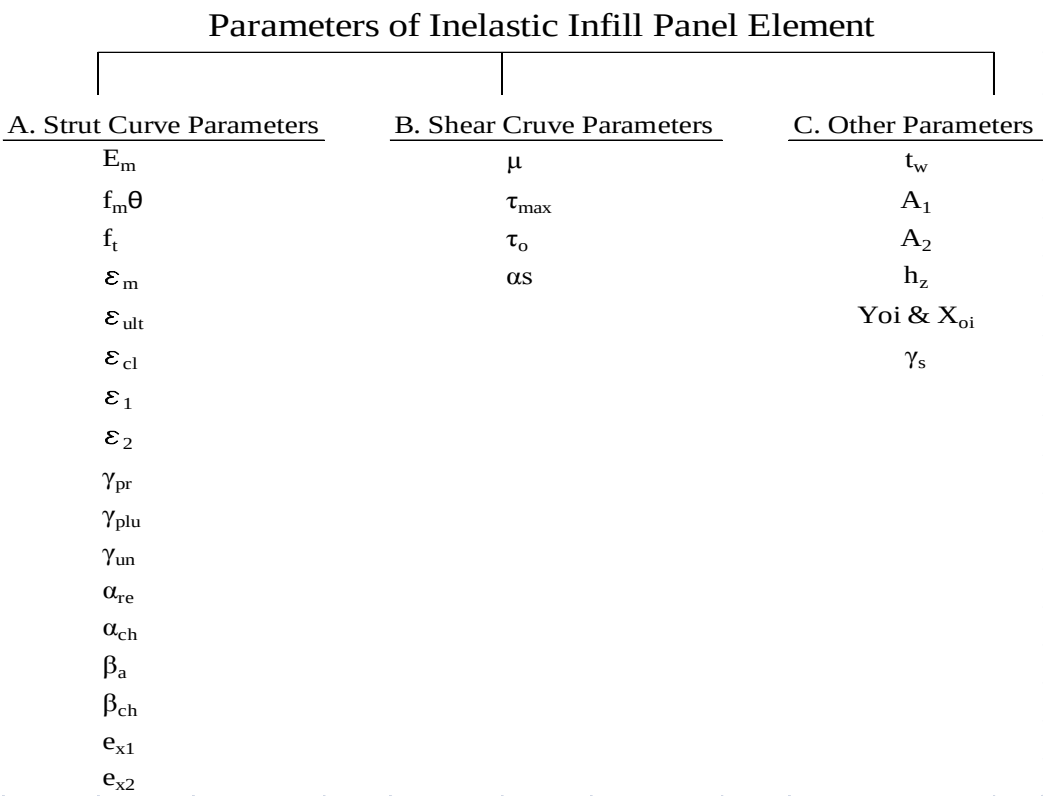

Figure 2.17: Mechanical, geometrical and empirical parameters required in SeismoStruct model.

For the scope of this thesis, parameters at utmost importance are explained in detail below. In other words, majority of the parameters are explained to let reader understand the model easily. However, not all the explained parameters were used to define infill panel elements for this study. Majority of them were left as default values and in the methodology chapter (section 3.2) default values of these

parameters are given in a table. For more detailed information readers can refer to SeismoStruct user manual and studies of Crisafulli et al. [40, 41, 42].

A. Strut Curve Parameters

i. Elastic Modulus, E_m

It is used to describe relationship between stress and strain of linear-elastic solid materials. Thus, slope of the stress-strain curve in the linear region (i.e. initial slope) is used to measure it. However, its value displays high variation and many researchers had proposed a variety of approaches for its calculation. Majority of them related modulus of elasticity with the material compressive strength [40] which has a range between $400f_m\theta < E_m < 1000f_m\theta$.

ii. Compressive strength, $f_m\theta$

It is used to define infill panel (strut) compressive resistance capacity.

iii. Tensile strength, f_t

It represents the masonry tensile strength or the frame infill panel interface bond-strength. Although it provides generality in the model, due to the fact that it is much smaller than the compressive strength, $f_m\theta$, can be accepted as equal to zero.

iii. Strain at maximum stress, ε_m

It is used to represent the ultimate strain at the maximum strength and has a varying value between 0.001-0.0005 [40].

iv. Ultimate strain, ε_{ult}

It is used to represent descending part of the stress-strain curve and often accepted as equal to $20\varepsilon_m$.

There are other parameters in addition to aforementioned material mechanics parameters. Brief information is given about the meanings of these empirical

parameters in the following pages. Also, their suggested values are given in the Table 2.1.

Table 2.1: Empirical parameters and their suggested values for SeismoStruct software programme [41].

Empirical parameters	Suggested values
ε_{cl}	0.000 - 0.003
ε_1	0.003 - 0.0008
ε_2	0.006 - 0.016
γ_{pr}	1.100 - 1.500
γ_{plu}	0.500 - 0.700
γ_{un}	1.500 - 2.500
α_{re}	0.200 - 0.400
α_{ch}	0.100 - 0.700
β_a	1.500 - 2.000
β_{ch}	0.500 - 0.900
e_{x1}	1.500 - 3.000
e_{x2}	1.000 - 1.500

ε_{cl}: it defines strain after which cracks partially close allowing compression stresses to develop.

ε_1 & ε_2: it is assumed that axial strain affects the strut area and these two strain parameters are related to the reduction of the strut area.

γ_{pr} or γ_{plr} : it defines the modulus of the reloading curve after total unloading.

γ_{plu}: it defines the modulus of the hysteretic curve at zero stress after complete unloading in proportion to E_m.

γ_{un}: it defines the unloading modulus in proportion to E_m

α_{re}: it predicts the strain at which the loop reaches the envelope after unloading.

α_{ch}: it predicts the strain at which the reloading curve has an inflexion point, controlling the loops' "fatness".

β_a: it defines the auxiliary point used to determine the plastic deformation after complete unloading.

β_{ch}: it defines the stress at which the reloading curve exhibits an inflection point.

e_{x1}: it controls the influence of ε_{un} in the degradation stiffness.

e_{x2}: it increases the strain at which the envelope curve is reached after unloading and represents cumulative damage inside repeated cycles, important when there are repeated consecutive cycles inside same inner loops.

All these empirical parameters are demanded by non-linear dynamic or cyclic analysis to detect complex behaviour of infill panels for the generation of a sound model for representing them.

B. Shear Curve Parameters

i. Coefficient of friction, μ

It is used to describe the degree of friction between rigid bodies of infill panel and the surrounding frame.

King and Pandey [43] proposed values in Table 2.2 after an experimental study. But these values are considered unreliable due to the fact that friction for brick on concrete is apparently greater than that of concrete on concrete which is not the real case.

Table 2.2. Coefficient of friction for different materials [43].

Materials	Coefficient of friction, μ
Brick on steel	0.50
Mortar on steel	0.44
Concrete on steel	0.41
Brick on concrete	0.62
Mortar on concrete	0.42
Concrete on concrete	0.44

Instead, Atkinson et. Al. [44] proposed 0.7 to be the lower bound estimate of a bed joint friction coefficient for a variety of mortar types and masonry units.

ii. Maximum shear stress, τ_{max}

It represents the maximum mobilized shear stress in the infill panel and it is dependent on the development of failure mechanism, such as, diagonal tension, sliding shear and compression failure. Its value is assumed to be 0.6 MPa, that is, 0.3 MPa coming from friction-induced shear resistant and 0.3 MPa from shear bond strength. The other two shear curve parameters include shear bond strength, τ_o, and reduction shear factor, α_s. Their suggested values are given in Table 2.3.

Table 2.3: Suggested values of shear bond strength, τ_o, and reduction shear factor, α_s [41].

Shear curve parameters	Suggested values
Shear bond, τ_o	0.10 - 1.50
Reduction shear factor, α_s	1.40 - 1.65

Other Parameters

i. Infill panel thickness, t_w

Width of the infill panel elements (bricks) alone, can be considered to define this parameter and preferentially thickness of the plaster can also be included.

ii. Strut Area 1, A_1

It is found by the product of equivalent strut width, b_w, and the infill panel thickness, t_w, where equivalent strut width, b_w, is defined by:

$$b_w = d_m/3 \qquad \text{Eq. (2.1)}$$

and d_m is the masonry panel diagonal length (Fig. 2.18).

However, based on the latest experimental results and analytical data, b_w varies in the range of 10-40% of the panel diagonal length, d_m [45].

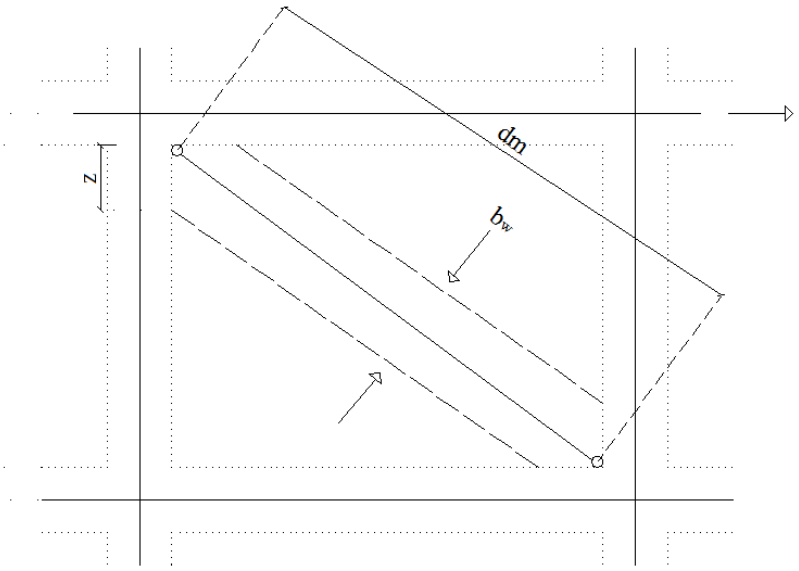

Figure 2.18: Effective width, b_w, of the diagonal strut [45].

iii. Strut Area 2, A_2

It is defined as percentage of strut area 1, and used to account decreasing contact length through the interface of the infill and the frame due to lateral and axial displacements of the infill which consequently affect the equivalent strut area [40].

iv. Equivalent Contact Length, h_z

It is defined as percentage of the panel vertical height, which was first introduced by Stafford Smith [46] as a fraction of the contact length between the infill panel and the

frame, z (Fig.2.18). Later this length is demonstrated using the distance between the dummy and internal nodes by Crisafulli model.

v. Vertical and Horizontal Offsets, Y_{oi} and X_{oi}

They are defined as percentage of the vertical and horizontal dimensions of the infill panel and represented by the distance between the internal corner nodes and the external ones. These parameters are introduced to account for the reduction in the dimensions of the infill panel due to the depth of the surrounding frame members because the ends of the diagonal members are normally assumed to coincide with the intersection of the centre lines of the columns and beams (see Fig. 2.13-16). This means that the length of the diagonal in the model is longer than that of the masonry panel.

vi. Proportion of Stiffness Assigned to Shear, γ_s

It is used to indicate the proportion of stiffness of the infill panel (computed automatically by the programme) that should be assigned to the shear spring. Its value is defined between 0.2 and 0.6.

Chapter 3

NUMERICAL MODELLING OF INFILL WALLS WITH SEISMOSTRUCT

3.1 Introductions

The analytical study presented in this thesis aimed to investigate structural behaviour of steel moment frames with and without infill walls, when subjected to lateral loads e.g. wind loads or earthquake loads. Once the results of the past experimental study were validated with SeismoStruct analytical models, then modifications were made to the steel frame, e.g. number of bays, stories and location of infill walls, to monitor the possible changes to frame behaviour due to these modifications.

3.2 Past Experimental Study

Experimental test results of Milad [11] were used to validate the analytical models by using the SeismoStruct software programme. Hence, the steel beam and column sections used for experimental test were used to create the analytical models and the same material and geometrical properties were used for the models with and without infill walls.

The experimental study was conducted using 2D half scale models that were extracted from a full scale one-story office building having plan dimensions of 4m x 3m. Then eight test frames including moment frames (major-MAJ and minor-MIN axis) and braced frames (major and minor axis) with and without infill wall were constructed.

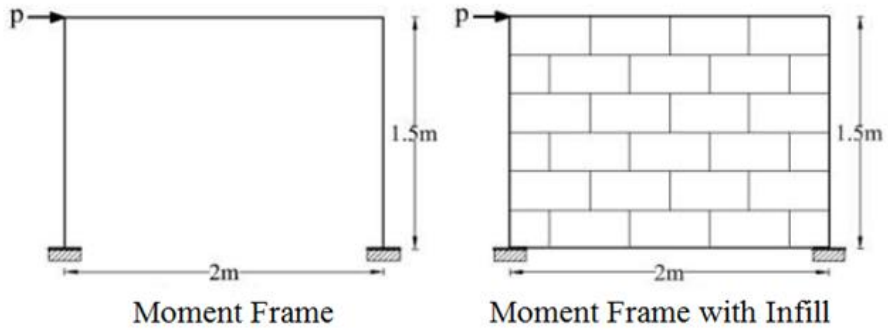

Figure 3.1: Experimental Moment and braced frames with and without infill wall [11].

The design was done according to Eurocode EN 3-1993 requirements. Then the systems were analysed with software programme ETABS, version 13.2.0. The test set-up of experimental models is shown in Figure.3.2. It must be noted that the braced frames are not in the scope of this study, hence, they will not be mentioned in the following sections. The experimental models considered in this study include MAJ-1B-1S, MAJ-1B-1S-INF and MIN-1B-1S, MIN-1B-1S-INF (Fig. 3.2). All the frames were constructed with HEB120 and IPE120 steel sections for column and beam members respectively, and the frame did not have any restraint in out-of-plane direction. The column-beam connections were provided with stiffened extended end plates and via the base plates the columns were connected to stiff steel bearings that are connected to 1.4 m thick strong floor. The infill walls were constructed with BIMs block (hollow concrete block) and cement mortar.

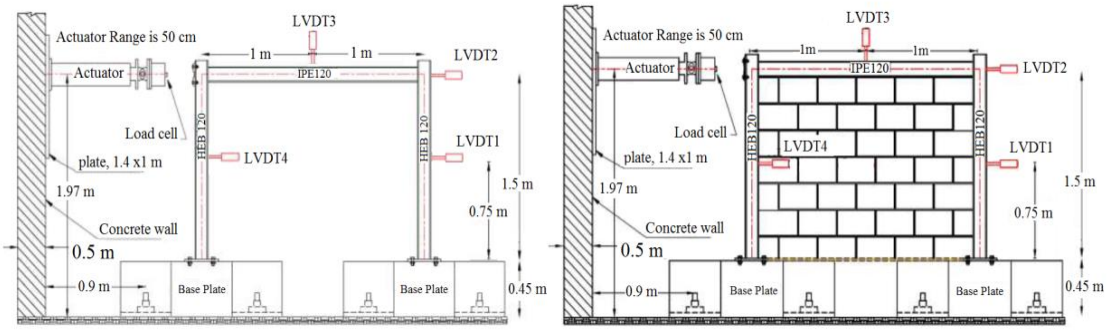

Figure 3.2: The experimental test set-up of (a) major and minor axis moment frame without infill wall (MAJ-1B-1S, MIN-1B-1S) and (b) major and minor axis moment frame with infill wall (MAJ-1B-1S-INF, MIN-1B-1S-INF) [11].

The section details, material properties and dimensions are shown in Fig. 3.4 and Tables 3.1 and 3.2 respectively. The mechanical properties of the column and beam sections were obtained from the coupon tensile tests. The lateral load was applied at a rate of 5 kN per minute by a hydraulic jack having 1000 kN capacity (Fig. 3.2) on the column flange or perpendicular to the column web depending on the orientation (major axis or minor axis) of the column members (Fig. 3.3).

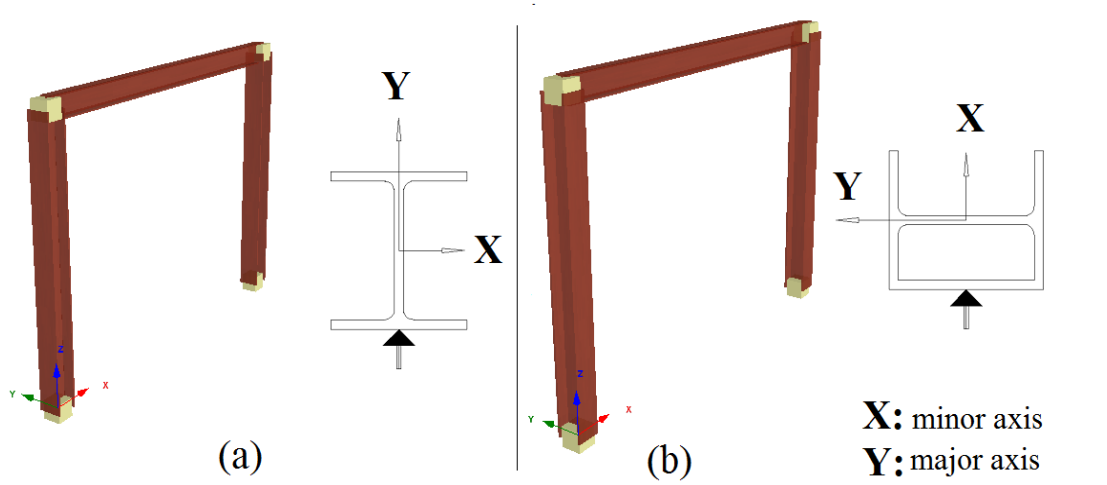

Figure 3.3: Load directions for (a) major and (b) minor axis frames.

The load application point was coinciding with the column web centreline and mid-depth of the beam. The load and corresponding frame top drifts were measured by

linear variable displacement transducers (LVDT) having 50-100 mm capacity that were placed at locations shown in Figure. 3.2. The load cell and LVDT readings were recorded at 0.1 seconds interval by using an electronic data acquisition system. It must be noted that, for this study readings of LVDT 2 (top right) and (for only one graph) LVDT 3 were considered. The former was used to measure lateral top displacement and the latter was used to measure beam displacement in the vertical direction (Fig.3.2). The LVDT 2 readings were represented with Node 2 and Node 3 readings of 1 bay and 2 bay SeismoStruct models respectively (Chapter 4).

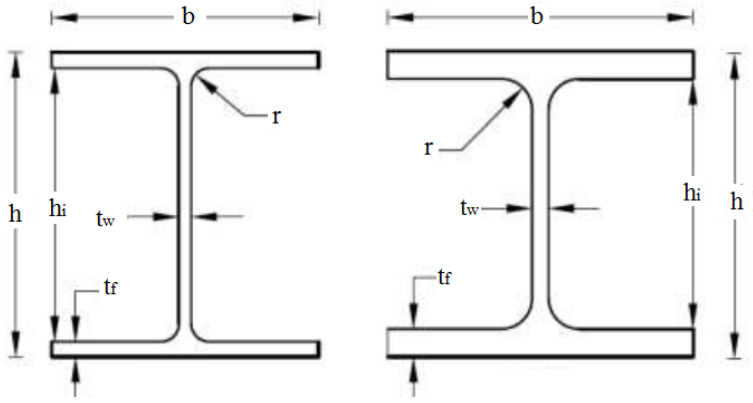

Figure 3.4: Colum and beam section dimension details [11].

Table 3.1: Mechanical properties of the steel sections [11].

Steel section	Yield stress	Ultimate stress	Ultimate Stain
	N/mm^2	N/mm^2	%
HEB120	339.70	474.77	26.67
IPE120	318.93	480.37	22.33

Table 3.2: Dimensions of the steel sections [11].

	HEB 120 (mm)				IPE120 (mm)			
Model No	Flange thickness	Web thickness	Height	Width	Flange thickness	Web thickness	Height	Width
	t_f	t_w	h	b	t_f	t_w	h	b
MAJ-1B	10	6.50	123	121	7.00	5.60	120	64
MAJ-1B-INF	10	6.50	122	121	7.00	5.50	120	64
MIN-1B	10	7.00	122	121	6.40	6.50	120	64
MIN-1B-INF	10	6.50	122	121	6.40	6.50	120	64

3.3 Numerical Modelling of the Experimental Test

The infill panel model of Crisafulli & Carr (section 2.6) is employed in Finite Elements software SeismoStruct, version 7.0.6., which considers material inelasticity and geometrical nonlinearities to predict the large deformation behaviour of space frames under static or dynamic loading. The accuracy of the model was evaluated by comparison of numerically modelled frames with experimental test results (section 3.1) obtained from non-linear static (pushover) analysis of 2D half-scale frames in which were all featuring the same material and geometrical properties, as well as loading conditions. The verification of the test results was first done by the investigation of the response of frames (in both major and minor axes) with no infill to ensure that infill panel would be left as the only "verification variable" and continued with infilled frames. The analytical models were formed in order of defining analysis type, materials, sections, element classes, nodes, constraints, restrains, applied load and performance criteria. First, the static pushover analysis was selected to define incremental load, P, in the following steps, to simulate the experimental test. Later, material type was selected as bilinear steel model (stl_bl) to define mechanical properties (strength, modulus of elasticity, strain-hardening etc.) of the steel sections according to Table 3.1. Then, symmetric I or T section (sits)

were selected to define steel sections by modifying programme defined HEB120 and IPE120 steel profile dimensions with respect to experimental test model dimensions (Table 3.2).

The material types are used to define sections, similarly, the element classes are needed for element connectivity module to create the actual elements that form-up the structural model being built. By using this module, the inelastic force-based frame element type (infmFB) and inelastic infill panel element were chosen for structural members (columns and beams) and non-structural components (infill walls) respectively. This stage was followed by the creation of four structural nodes (two for the base supports and two for the beam-column connections). These nodes were used in the previously mentioned element connectivity and loading steps. Top displacement readings for the validation procedure were obtained from Node 2. The column members were oriented in the major and minor axis (for MAJ-1B-1S and MIN-1B-1S respectively) and then beam and infill panel (for MAJ-1B-INF and MIN-1B-INF) were connected to them by using predefined structural nodes. Frames were fully restrained at the supports (fixed support) and they were not restrained in the out-of-plane direction as it was the case with experimental test. The formation of numerical models was finalized with defining laterally applied incremental load, P, until performance criteria's to frame members so that the yielding and failure loads can be detected. Among all the steps mentioned above the most time demanding step was the definition of the infill wall due to the fact that it requires a large number of parameters to be defined. The infill wall parameters are explained in section 2.6.3.3. However, for the scope of this study the default values were used for most of the parameters including empirical parameters mainly and only panel thickness, t_w, strut

area 1, A_1, strut area 2, A_2, compressive strength $f_m\theta$ and elastic Modulus, E_m were changed with respect to experimental test values. The default values of unmodified parameters are given in Table 3.3 with their available suggested values. Panel thickness, t_w, was measured 12 cm without plaster, A_1 was calculated 28502.8 mm^2 and A_2 was 21 % of the A_1. Referring to the experimental study of Ahmad et. al. [47] on masonry walls made of BIMs, compressive strength $f_m\theta$ was chosen 1.17 MPa and E_m was chosen 1170 MPa by staying in the range of $400f_m\theta < E_m < 1000f_m\theta$. In the same study, strain at maximum stress, ε_m, and the ultimate stain, ε_{ult}, were found 0.0012 and 0.024 respectively which were the same with programme default values.

Table 3.3. Infill wall suggested and programme default values [41].

Parameter	Suggested values	Default values	Unit
e_{cl}	0.000 - 0.003	0.004	-
e_1	0.003 - 0.0008	0.001	-
e_2	0.006 - 0.016	0.001	-
γ_{pr}	1.100 - 1.500	1.500	-
γ_{plu}	0.500 - 0.700	1.000	-
γ_{un}	1.500 - 2.500	1.500	-
α_{re}	0.200 - 0.400	0.200	-
α_{ch}	0.100 - 0.700	0.700	-
β_a	1.500 - 2.000	1.500	-
β_{ch}	0.500 - 0.900	0.900	-
e_{x1}	1.500 - 3.000	3.000	-
e_{x2}	1.000 - 1.500	1.400	-
f_t	0.000 - 0.575	0.000	MPa
μ	0.100 – 1.200	0.700	-
τo	0.100 - 1.500	0.300	MPa
αs	1.400 - 1.650	1.500	-
τ_{max}	0.300 - 0.600	0.600	MPa
h_z	-	23.000	-
X_{oi}	-	2.400	-
Y_{oi}	-	10.000	-
γ_s	-	20.000	-
γ	20.00	20.000	kN/m^3

3.4 Verification of the Experimental Test Results

3.4.1 Major Axis Frame Tests

These frames are formed by placing major axes of the vertical members in the direction of applied load. The load is applied laterally on the column flange at a level coinciding with the column web centreline and mid-depth of the beam (Fig. 3.5). Thus, column members were subjected to bending around their major axes.

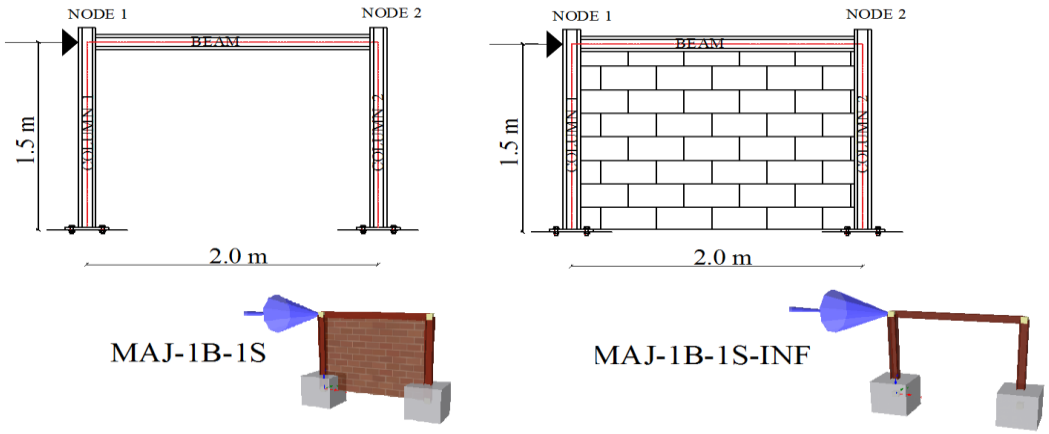

Figure 3.5: SeismoStruct models of major axis moment frame without infill, MAJ-1B-1S and major axis moment frame with infill, MAJ-1B-1S-INF.

3.4.1.1 Moment Frame without Infill Wall, MAJ-1B-1S

During experimental study lateral load was monotonically applied to the moment frame by using a hydraulic jack having 1000 kN capacity and the corresponding displacement readings were recorded by LVDT 2. For verification of these experiments, SeismoStruct software was used to apply similar load defined by the user. Also the corresponding node displacement was recorded at different load levels from LVDT 2 representative Node 2. The load and displacements are given in Table 3.4.

Table 3.4. Load and corresponding displacement readings of the experimental and analytical studies of MAJ-1B-1S.

Experimental Study		Analytical Study		Ratio of Anlytical/Exp	
Lateral Load P kN	Displacement Δ mm	Lateral Load P kN	Displacement Δ mm	Lateral Load	Displacement
0.00	0.00	0.00	0.00	0.000	0.000
1.33	0.45	1.32	0.39	0.992	0.867
5.00	1.32	5.06	1.52	1.012	1.152
10.17	2.64	10.12	3.04	0.995	1.152
16.17	3.70	16.17	4.87	1.000	1.316
20.00	4.75	20.02	6.03	1.001	1.269
26.01	6.48	26.07	7.85	1.002	1.211
30.84	8.06	30.80	9.27	0.999	1.150
35.67	9.47	35.64	10.73	0.999	1.133
40.01	10.97	40.04	12.06	1.001	1.099
45.01	12.60	45.10	13.57	1.002	1.077
50.01	14.18	50.05	15.06	1.001	1.062
55.18	15.88	55.11	16.59	0.999	1.045
60.18	17.32	60.17	18.11	1.000	1.046
65.01	19.07	65.01	19.57	1.000	1.026
70.18	21.12	70.18	21.12	1.000	1.000
75.01	23.28	75.02	22.60	1.000	0.971
80.18	26.11	80.19	24.25	1.000	0.929
85.01	29.07	85.03	26.08	1.000	0.897
90.35	33.13	90.31	28.41	1.000	0.857
95.02	37.08	95.04	31.00	1.000	0.836
100.19	42.81	100.10	40.45	0.999	0.945
105.69	69.30	102.30	58.68	0.968	0.847
104.19	69.61	102.52	66.96	0.984	0.962
102.85	69.65	102.63	67.59	0.998	0.970
			μ =	0.958	0.993
			σ =	0.200	0.245
			c.o.v.=	0.208	0.246

The experimental test specimen MAJ-1B-1S displayed an elastic behaviour up to the lateral load of approximately 60.18 kN and the corresponding displacement of LVDT2 was 17.32 mm (Fig. 3.6). On the other hand, analytical model behaviour was elastic up to a higher lateral load of approximately 70.18 kN and the corresponding

lateral displacement was recorded as 21.12 mm at Node 2. Hence, the yielding load of analytical model was higher than the experimental one and the maximum displacement achieved at maximum lateral load was 67.59 to 69.65 mm for experimental and analytical studies respectively. Analytical model behaved more elastically than the experimental specimen and their behaviour was somewhat varied in their plastic region.

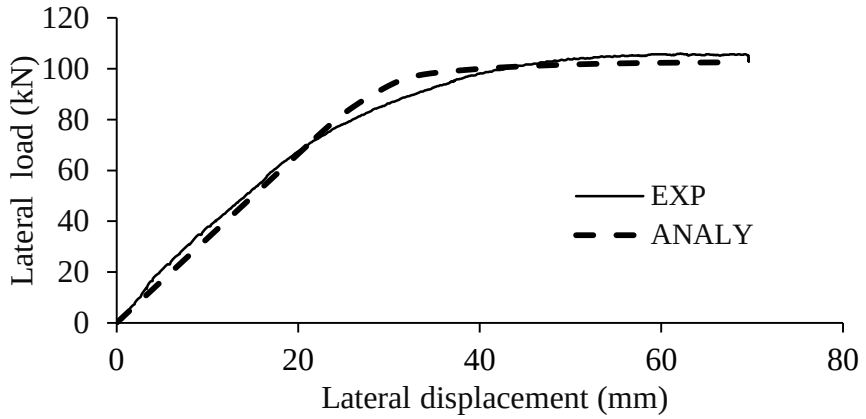

Figure 3.6: Comparison of the lateral load versus displacement curves of experimental (EXP) and analytical (ANLY) studies of MAJ-1B-1S.

Loading procedure was continued until failure of the experimental specimen and analytical model. Experimental specimen reached slightly higher load level than the analytical one at the failure. Frames of both studies were not restrained in out-of-plane direction and the deficiencies in the results are attributed to the possible behavioural differences caused by the lateral torsional buckling of columns and out-of-plane movement of the beam (Fig. 3.7).

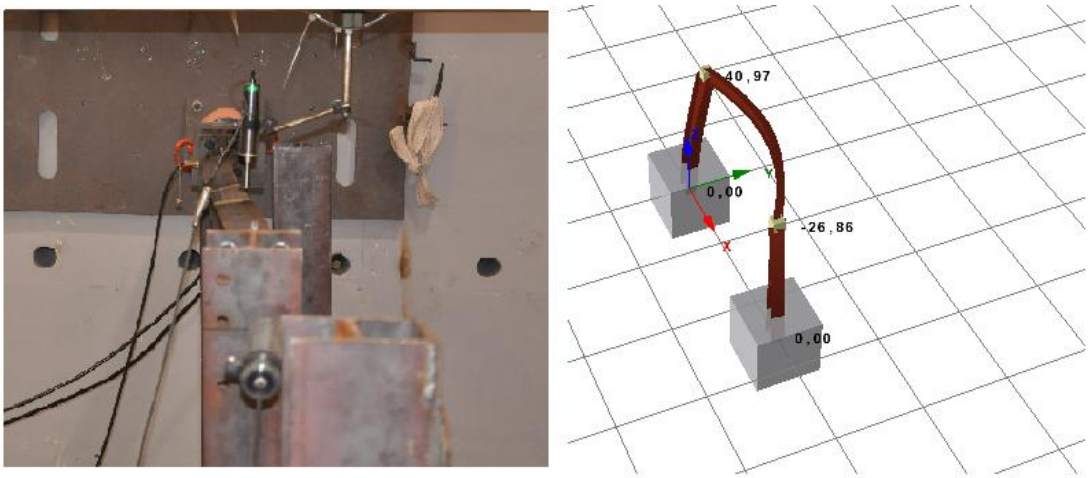

Figure 3.7: Lateral torsional and flexural buckling and out-of-plane displacements of the experimental specimen (on the left) and the analytical model (on the right) [11].

In reality, when the top beam rotates then it cannot properly transmit the lateral force in the initially applied direction. Hence this behaviour may cause the two components of the force (Fig. 3.8 (a)) to be transferred to the column member on which LVDT2 was placed Consequently, the column exposed to this kind of force tends to rotate and this is highly likely to alter displacement readings that are obtained from LVDT. However, the out-of-plane movement of the frame members were not measured during experimental study. On the other hand, analytical model experienced (in y-plane) positive 40.97 mm and negative 26.86 mm out-of-plane movement at the load application (Node 1) and Node 2 locations respectively (Fig. 3.7). In addition, during the experiments the base plate experienced upward bending due to developed high moments at that point which could not be accounted by the computer model due to columns being considered totally restrained at the base (Fig.3.8 (b)).

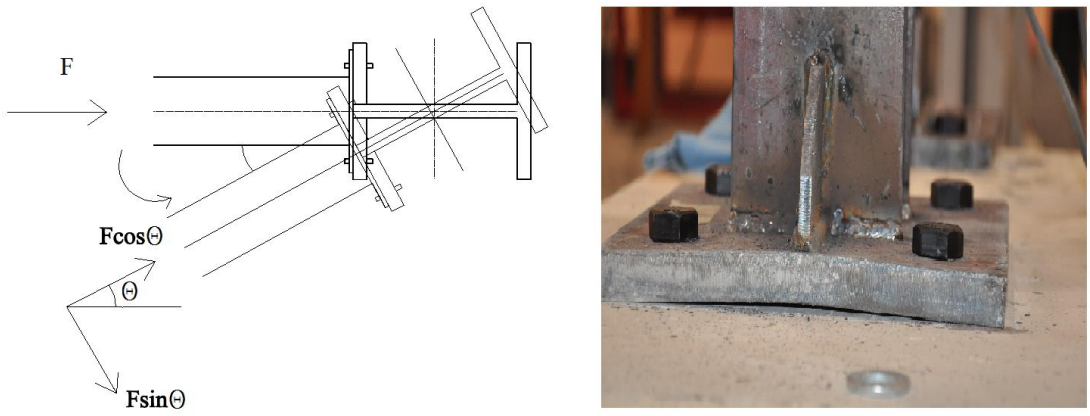

Figure 3.8: (a) Resulting two components of the applied force due to lateral torsional and flexural of-plane displacement of the frame, (b) base plate deformation (prying action) of the experimental test [11].

3.4.1.2 Moment Frame with Infill Wall, MAJ-1B-1S-INF

The experimental test specimen was subjected to lateral monotonic loading by using a hydraulic jack of 1000kN capacity and the displacement readings were recorded by LVDT 2 at different load levels. Then the same procedure was repeated for the analytical model and results of both studies are represented in Table 3.5.

Table 3.5. Load and corresponding displacement values of the experimental and analytical studies of MAJ-1B-1S-INF.

Experimental Study		Analytical Study		Ratio of Anlytical/Exp	
Lateral Load P kN	Displacement Δ mm	Lateral Load P kN	Displacement Δ mm	Lateral Load	Displacement
0.00	0.00	0.00	0.00	0.000	0.000
2.33	0.00	2.31	0.16	0.991	0.000
9.17	0.00	9.24	0.80	1.008	0.000
11.84	0.16	11.76	0.99	0.993	6.188
14.67	1.13	14.71	1.10	1.003	0.973
20.34	1.97	20.37	1.39	1.001	0.706
25.51	2.64	25.41	1.96	0.996	0.742
30.51	3.52	30.45	2.58	0.998	0.733
35.17	4.02	35.07	3.18	0.997	0.791
40.17	4.58	40.11	3.88	0.999	0.847
43.17	4.78	43.05	4.37	0.997	0.914
46.17	5.56	46.20	4.86	1.001	0.874
48.51	6.11	48.51	5.29	1.000	0.866
51.84	6.64	51.87	5.84	1.001	0.880
54.84	7.49	54.81	6.34	0.999	0.846
58.85	8.10	58.80	7.22	0.999	0.891
60.51	13.48	60.55	14.20	1.001	1.053
62.34	13.89	62.39	14.75	1.001	1.062
64.01	14.41	64.01	15.12	1.000	1.049
66.18	14.79	66.18	15.69	1.000	1.061
68.35	15.49	68.35	16.21	1.000	1.046
70.01	16.09	70.01	16.76	1.000	1.042
69.85	16.26	74.29	17.83	1.064	1.097
75.01	17.48	77.52	18.60	1.033	1.064
77.52	18.82	78.84	19.07	1.017	1.013
78.84	19.38	79.80	19.32	1.012	0.997
80.84	19.89	80.84	19.55	1.000	0.983
82.84	20.39	82.86	20.14	1.000	0.988
85.18	20.96	85.14	20.86	1.000	0.995
93.52	28.02	93.54	23.81	1.000	0.850
92.52	28.00	94.78	24.35	1.024	0.870
95.85	28.31	95.81	24.82	1.000	0.877
100.02	29.39	100.27	27.65	1.002	0.941
103.69	31.83	103.68	33.35	1.000	1.048
99.19	32.17	108.02	41.10	1.089	1.278
			μ =	0.978	1.016
			σ =	0.171	0.946
			c.o.v.=	0.175	0.931

The experimental test specimen did not show a considerable lateral movement up to 9.86 kN and then behaved elastically up to approximately 57.18 kN with 7.84 mm displacement (Fig. 3.9).

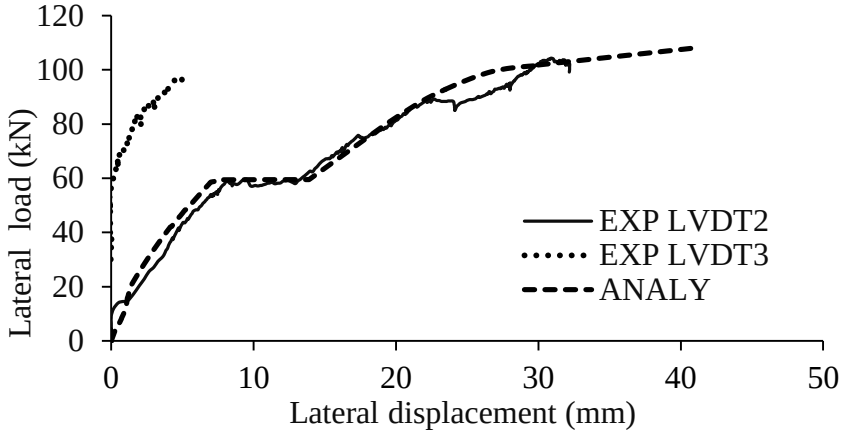

Figure 3.9: Comparison of the lateral load versus displacement curves of experimental (EXP LVDT2 and EXP LVDT3) and analytical studies of MAJ-1B-1S-INF.

The infill failure was initially started with the formation of diagonal cracks and then at higher loads corner crushing was developed (Fig.3.10 (b)). [11]. The frame was loaded until it was not capable of resisting higher loads (reaching plastic stage) and the final load recorded was 103.69 kN at 31.83 mm displacement. The analytical model exhibited elastic behaviour up to 58.17 kN and the corresponding displacement was 6.91 mm. The load was applied until the frame failed at 108.02 kN with 41.10 mm displacement. Despite the experimental study, the type of infill failure was not possible to be identified for analytical model since SeismoStruct software models infill walls as equivalent diagonal and shear struts as mentioned in section 2.6.3. However, yielding loads of column and beam were obtained as 86.23 kN and 94.78 kN respectively. The load-displacement curves of both study displayed similar pattern with slight differences. In addition to the load displacement curve by using LVDT2, the displacement curve obtained by using LVDT3 of the experimental

study is also included in the graph (Fig. 3.9). Unfortunately it was not possible to include the same curve from the analytical study since displacement readings at nodes can only be obtained from analytical models. The curve obtained from LVDT3 was included to show the effect of the upward movement of the beam member on the load-displacement curve. It is obvious that the load-displacement curve became parallel to x-axis when LVDT3 readings started increasing at a considerable rate. Although, it was not possible to obtain upward movement readings from the analytical study, its load-displacement curve displayed similar behaviour. This behavioural similarity together with the diagonal failure of the experimental specimen's infill wall can be attributed to effectiveness of the equivalent diagonal strut approach.

(a) (b)

Figure 3.10: The experimental specimen MAJ-1B-INF in the structures laboratory (a) before the test, (b) after the test with diagonal cracks and corner crush [11].

3.4.2 Minor Axis Frame Tests

These frames are formed by placing minor axes of the vertical members in the direction of applied load. The load is applied perpendicular to the column web, at a level coinciding with the column web centreline and mid-depth of the beam (Fig. 3.11). Thus, column members were subjected to bending around their minor axes.

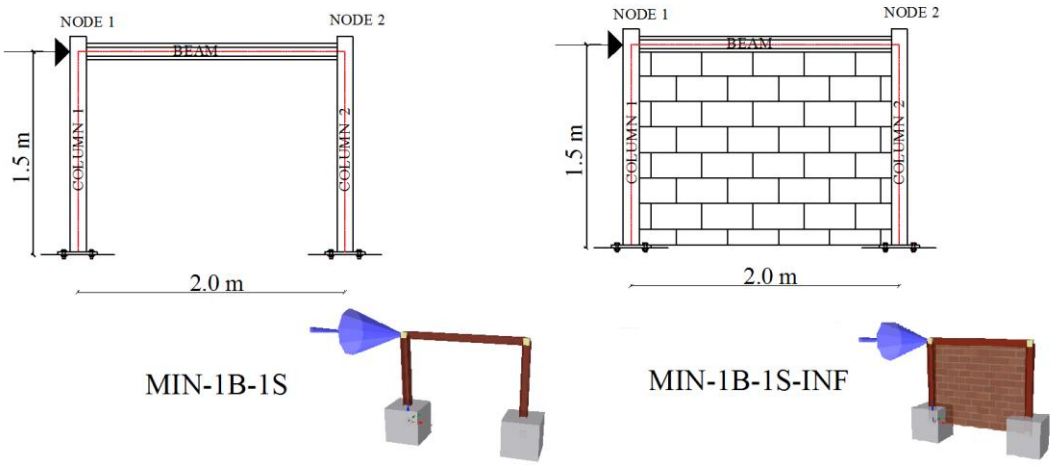

Figure 3.11: SeismoStruct models of minor axis moment frame without infill, MIN-1B-1S and minor axis moment frame with infill, MIN-1B-1S-INF.

3.4.2.1 Moment Frame without Infill Wall MIN-1B-1S

During experimental study monotonic lateral load was applied to the moment frame by using a hydraulic jack having 1000 kN capacity and the corresponding displacement readings were recorded by LVDT2. In a similar manner, user defined same load is applied by the SeismoStruct software and corresponding displacement at Node 2 was recorded at different load levels. The displacement readings for both studies are shown in Table 3.6.

Table 3.6: Load and corresponding displacement values of the experimental and analytical studies of MIN-1B-1S.

Experimental Study		Analytical Study		Ratio of Anlytical/Exp	
Lateral Load P kN	Displacement Δ mm	Lateral Load P kN	Displacement Δ mm	Lateral Load	Displacement
0.00	0.00	0.00	0.00	0.000	0.000
1.33	0.94	1.41	0.65	1.060	0.691
4.83	2.17	4.78	2.21	0.990	1.018
6.00	2.91	5.91	2.73	0.985	0.938
9.66	4.43	9.57	4.42	0.991	0.998
12.83	6.10	12.72	5.85	0.991	0.959
15.00	6.87	14.91	6.89	0.994	1.003
18.00	8.31	18.00	8.32	1.000	1.001
20.83	9.74	20.82	9.62	1.000	0.988
22.00	10.15	22.00	10.12	1.000	0.997
25.00	11.48	25.00	11.63	1.000	1.013
27.84	12.87	27.86	12.95	1.001	1.006
30.84	14.21	30.68	14.27	0.995	1.004
32.34	15.25	32.37	15.01	1.001	0.984
34.67	16.56	34.62	16.07	0.999	0.970
38.67	18.39	38.54	17.82	0.997	0.969
40.01	19.21	40.18	18.68	1.004	0.972
42.51	20.85	42.60	19.84	1.002	0.952
45.01	22.04	45.10	21.15	1.002	0.960
47.17	23.73	47.15	22.24	1.000	0.937
50.01	26.52	49.96	24.14	0.999	0.910
52.51	29.49	55.52	28.71	1.057	0.974
55.01	33.25	56.01	30.00	1.018	0.902
57.51	37.83	57.51	32.62	1.000	0.862
60.01	43.90	60.01	41.20	1.000	0.938
62.51	53.23	62.51	57.34	1.000	1.077
65.01	67.77	65.01	82.27	1.000	1.214
66.01	72.29	65.42	86.83	0.991	1.201
67.01	86.83	65.57	88.35	0.979	1.018
67.51	90.09	65.76	90.09	0.974	1.000
66.68	90.39	65.79	90.39	0.987	1.000
				μ = 0.968	0.950
				σ = 0.181	0.197
				c.o.v.= 0.186	0.208

The experimental test specimen MIN-1B-1S displaced an elastic behaviour up to the lateral load of approximately 44.5 kN and the corresponding displacement was recorded to be approximately 22.26 mm (Fig 3.12). Lateral load is applied until the frame fails (Fig.3.12 and 3.13) and the lateral displacement at the maximum load of 67.51 kN was 90.09 mm. A slight tide on the load-displacement curve occurred at the time when plasticity started.

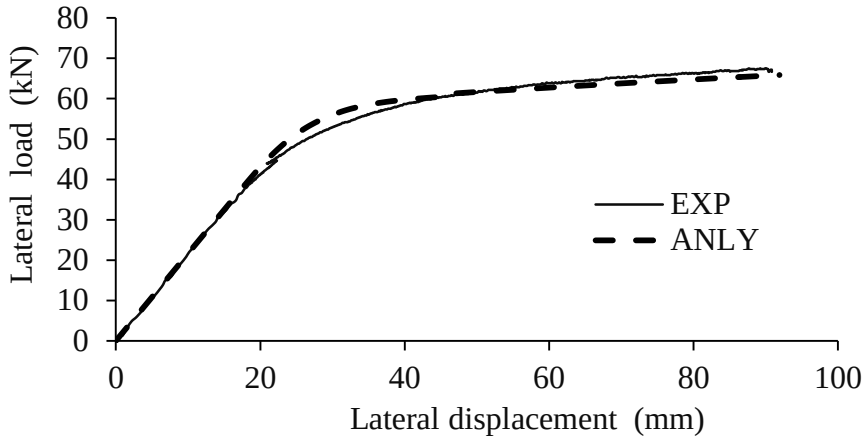

Figure 3.12: Comparison of the lateral load versus displacement curves of experimental (EXP) and analytical (ANLY) studies of MIN-1B-1S.

A similar behavioural pattern is exhibited by the analytical model and the plasticity started at approximately 19.96 mm displacement and 42.75 kN load with the yielding of one column member. Loading was continued until the failure of the analytical model.

Figure 3.13: Experimental specimen MIN-1B-1S before and after the test [11].

In general, pattern of the curves are similar to each other and they coincide at low load levels, i.e. in the elastic region. Also, the plasticity starting load and the displacement readings were very close to each other. It must be noted that, neither the experimental specimen nor the analytical model was restrained against out-of-plane movement and at the end of the experimental test where analytical model experienced zero out-of-plane displacement even at high load levels. This behavioural difference might have altered the results of the two studies.

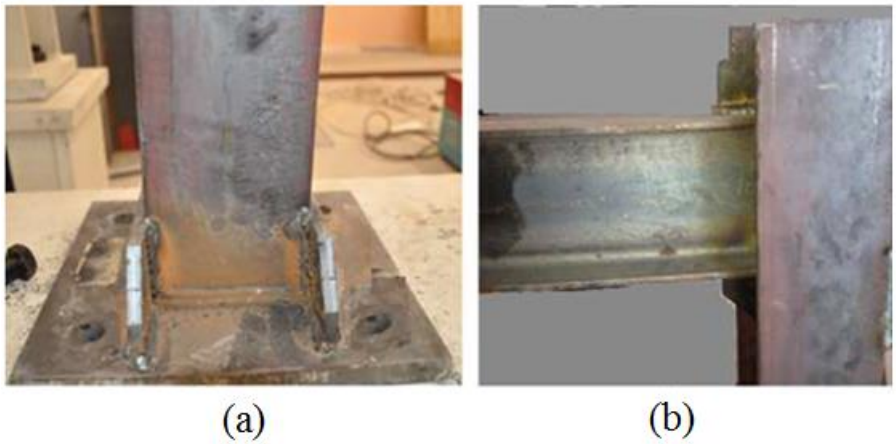

Figure 3.14: MIN-1B-1S at the end of the test; (a) column and column base, (b) beam end near column connection.

3.4.2.2 Moment Frame with Infill Wall, MIN-1B-1S-INF

The experimental test specimen was subjected to lateral monotonic load by using a hydraulic jack of 1000 kN capacity and the displacement readings were recorded by LVDT 2 at different load levels. Then the same procedure was repeated for the analytical model and results of both studies are given in Table 3.7.

Table 3.7: Load and corresponding displacement values of the experimental and analytical studies of MIN-1B-1S-INF.

Experimental Study		Analytical Study		Ratio of Anlytical/Exp	
Lateral Load P kN	Displacement Δ mm	Lateral Load P kN	Displacement Δ mm	Lateral Load	Displacement
0.00	0.00	0.00	0.00	0.000	0.000
1.60	0.00	1.77	0.14	1.106	0.000
4.93	0.36	4.78	0.41	0.970	1.139
6.23	0.36	6.59	0.57	1.058	1.583
9.81	0.67	9.60	0.86	0.979	1.284
16.43	1.62	15.57	1.44	0.948	0.889
15.00	1.62	16.17	1.50	1.078	0.926
21.00	2.02	21.58	2.04	1.028	1.010
26.67	2.44	26.38	2.54	0.989	1.041
30.34	3.05	30.58	2.99	1.008	0.980
32.67	3.46	32.48	3.19	0.994	0.922
35.51	3.95	34.50	3.45	0.972	0.873
34.84	3.99	35.38	3.90	1.015	0.977
39.34	4.47	38.38	5.15	0.976	1.152
38.34	4.50	39.58	5.42	1.032	1.204
42.51	5.33	42.60	6.41	1.002	1.203
44.51	6.07	44.40	7.12	0.998	1.173
46.34	7.05	46.20	7.88	0.997	1.118
47.01	7.16	46.80	8.14	0.996	1.137
46.51	7.31	47.40	8.41	1.019	1.150
47.34	7.61	47.99	8.68	1.014	1.141
48.68	10.78	48.60	8.96	0.998	0.831
52.34	12.99	52.20	10.72	0.997	0.825
54.01	15.97	54.00	11.70	1.000	0.733
52.01	16.08	59.99	13.86	1.153	0.862
51.01	16.11	67.98	17.25	1.333	1.071
			μ =	0.987	0.970
			σ =	0.215	0.336
			c.o.v.=	0.218	0.346

The experimental test specimen behaved elastically up to approximately 38.34 kN with 4.5 mm displacement reading on LVDT 2. The first visible crack on infill wall was noticed at approximately 47.0 kN that was corresponded to lateral 7.16 mm displacement (Fig 3.15). Later, this crack was grown into a longer diagonal crack

with a few short branches throughout its length and another diagonal crack developed into this initial crack (Fig 3.16). In addition to these two diagonal cracks corner hairline cracks in the top compression zone started to form with approximately 45^{o} inclination. The lateral displacement was recorded 15.97 mm at the maximum lateral load of 54.01 kN and only diagonal cracks were observed on the infill wall despite the expectation of corner crushing due to preformed corner hairline cracks. Although, load-displacement curve is inconsistent, there was no visible frame out of straightness during testing.

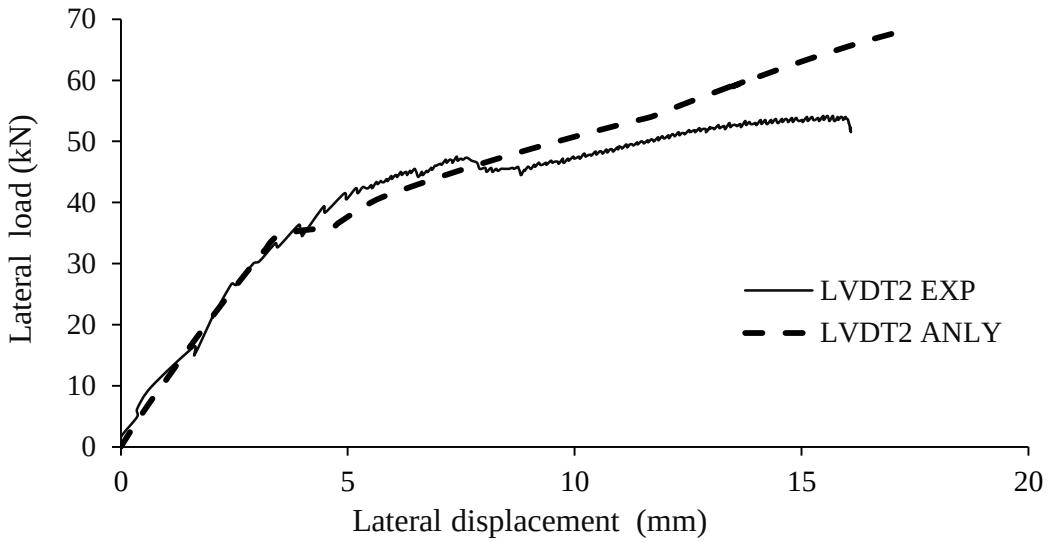

Figure 3.15: Comparison of the lateral load versus displacement curves of experimental (EXP) and analytical (ANALY) studies of MIN-1B-INF.

The analytical model exhibited elastic behaviour up to 34.50 kN and the corresponding displacement was 3.45 mm. The load continued to be applied until the frame failed at 67.98 kN with 17.25 mm displacement. Despite the experimental study, it was not possible to identify type of infill failure because SeismoStruct software models infill as equivalent diagonal and shear struts similar to the case of MAJ-1B-INF as explained previously.

Figure 3.16: The formation of diagonal and hairline cracks [11].

The load-displacement curves for both studies displayed a similar pattern in general, despite inconsistency of the experimental curve. However, it was clearer to see linear elastic and then plastic deformation of the system with the analytical model. Inconsistency in the experimental test readings might have contributed to the imperfections of the used material, workmanship and, most importantly, composite action of the frame-infill wall which could not be considered in the analytical model. As a result, analytical model failed at a higher lateral load level than that of the experimental specimen but their corresponding displacements were approximately equal at these maximum load levels.

Chapter 4

INVESTIGATION OF THE ANALYTICAL MODELS FOR THE EFFECTS OF INFILL WALL

4.1 Introduction

The results of the validation procedure had shown that SeismoStruct software is highly capable of modelling infilled frames. Hence, new models for the investigation of the effects of infill wall(s) on the structural behaviour could be formed. For this purpose six new groups of structural frames were modelled by using the same steel beam and column sections and mechanical properties of the experimental test frames. Simply the model frames of experimental program were used by adding more 2D frames. New models were formed by first, increasing the number of stories to 2 and the frames of this group are labelled with the notation of 2S. Later the number of bays was increased to 2 and these models were labelled with 2B.

The new models were formed by following the same approach as in experimental program. A reference model was formed without infill wall, then it was fully infilled and later it was symmetrically and regularly/irregularly infilled.

After the modelling had finished all model groups were studied on the bases of global structural performance parameters of top displacement, base shear, fundamental time period and out-of-plane displacement and local parameters of

inter-story drift ratio and member deformation capacities with applying linear pushover analysis.

The results of six new model groups are presented in the following sections. The validation models were also considered as two groups in the conclusion chapter for the comparison of all analytical models. However, in the previous chapter, parameters included in the validation models covered only top displacement, maximum lateral load and out-of-plane displacements. Hence, the load-displacement curves, base shear, fundamental time period, inter-story drift ratio and member deformation capacities for these models are given in Appendix A.

4.2 Major Axis Frame Models

The major axes of vertical members (column flanges) placed 90 degrees to the direction of applied load were modelled to investigate effects of infill wall(s) on the structural performance. For this purpose three different groups of models were created and infill wall was placed into the frames at different locations. These new models were grouped according to their number of bays and stories. Addition to 1 bay 1 story (1B-1S) (Fig. 3.4.) validation models, 1 bay 2 story (1B-2S) (Fig.4.1), 2 bay 1 story (2B-1S) (Fig.4.5.) and 2 bay 2 story (2B-2S) (Fig.4.9.) models were formed. After the modelling had finished all the members were studied on the bases of global structural performance parameters and local parameters.

4.2.1 One Bay Two Story (1B-2S) Frame Models

These models were created by using the validation model MAJ-1B-1S and increasing the number of story from one to two. After the modelling had finished all the members were studied on the bases of global structural performance parameters and local parameters. Node 1 and 2 represent locations of the top column to beam

connections, column 1, C1, column 2, C2, column 3, C3 and column 4, C4 are the column members and beam 1, B1 and beam 2, B2 are the two beams of the system (Fig. 4.1).

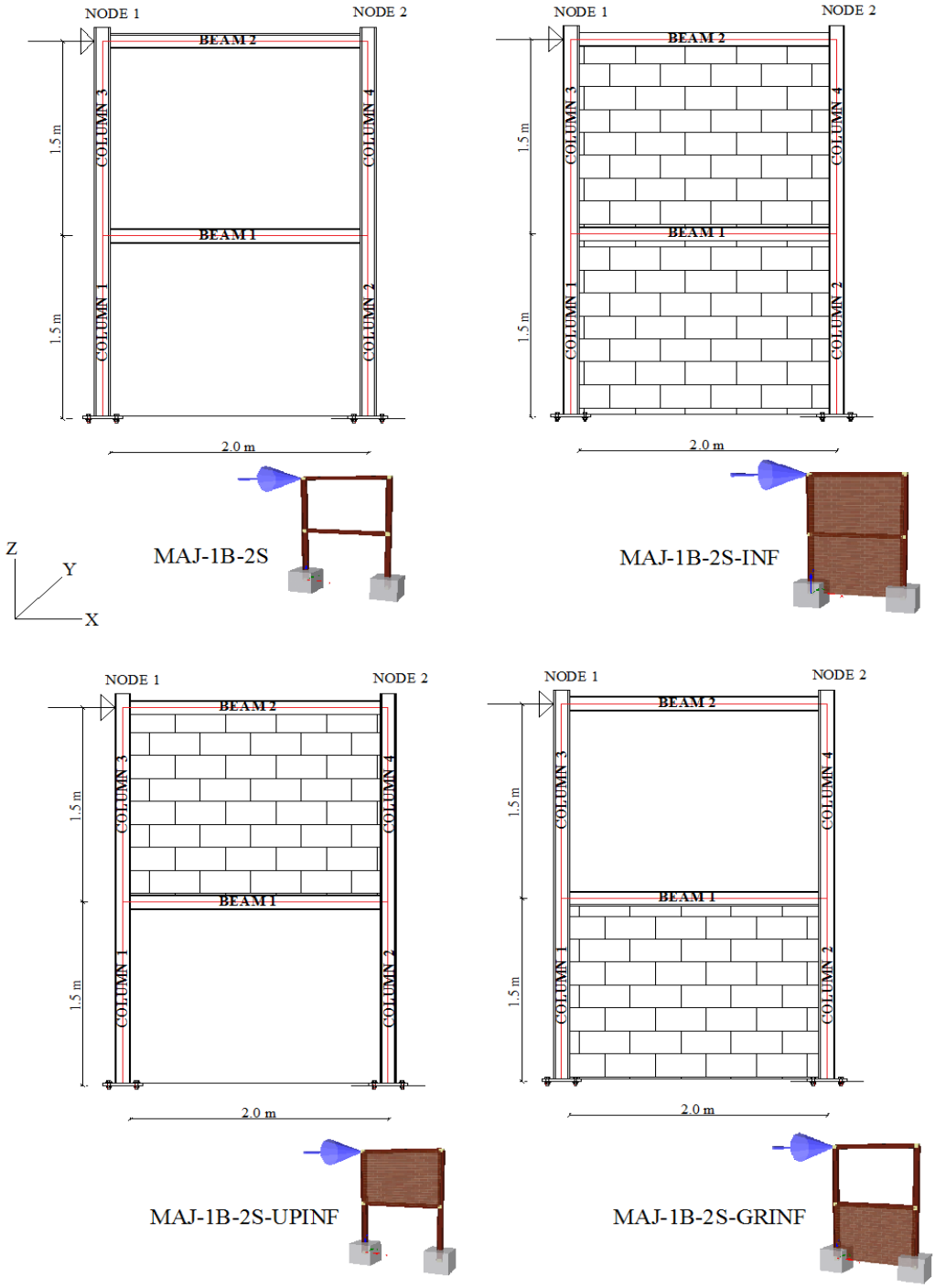

Figure 4.1: Details of major axis 1 bay 2 story (1B-2S) models with SeismoStruct illustrations.

Figure 4.2 shows the lateral load-displacement curves for all the major axis 1B-2S models. The curve for the MAJ 1B-2S model exhibited a non-linear behaviour. On the other hand all the other models followed similar behavioural pattern where the curve has a linear portion up to a certain load level then, there is a sudden increase in displacement while the load is constant. Then gradually the curve becomes non-linear with increase in both load and displacement. Finally, for some of the curves the rate of increase of load is considerably less than displacement and hence a fairly flat plateau is formed until failure.

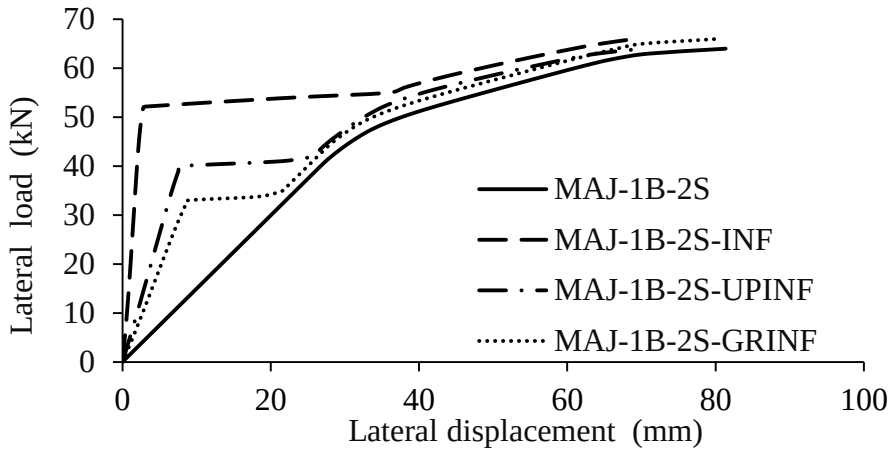

Figure 4.2: Load-displacement curves for major axis 1 bay 2 story (1B-2S) frame models.

The maximum top displacement hence drift ratio, was observed with MAJ-1B-2S but the variation of displacement values among all models were not so high. The maximum base shear and time period was exhibited by the heaviest model in weight, MAJ-1B-2S-INF (Fig.4.3). All the models had zero out-of-plane displacements at nodes 1 and 2 (Fig. 4.4).

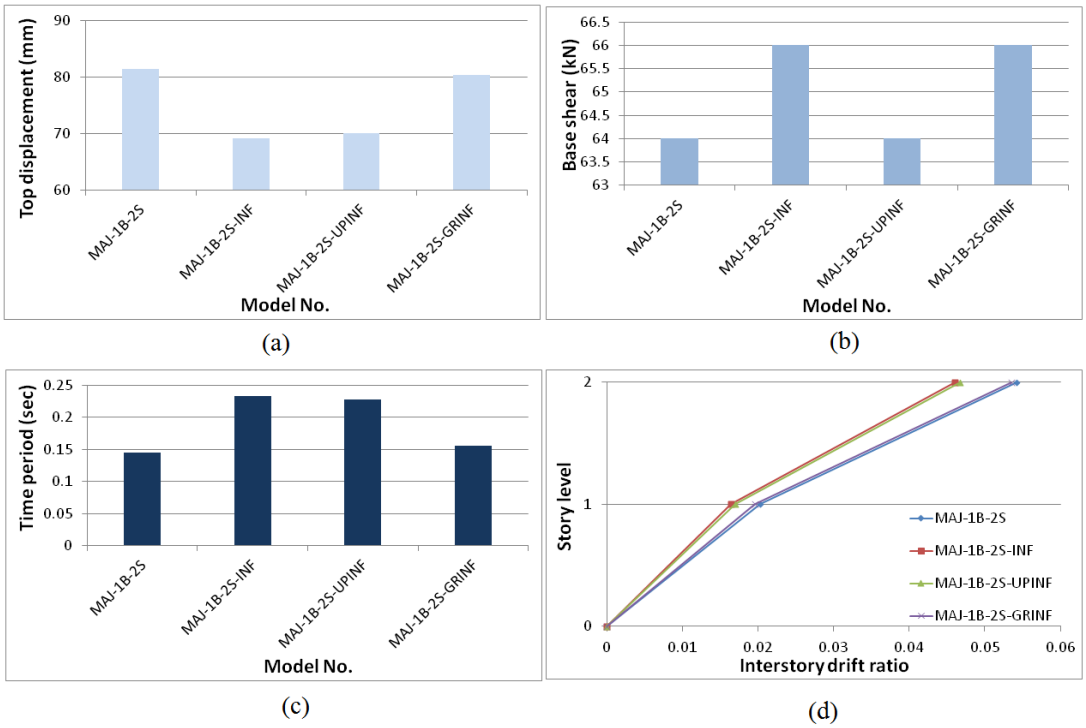

Figure 4.3: Global structural parameters of major axis 1 bay 2 story (1B-2S) models, (a) top displacement, (b) base shear, (c) time period and (d) drift ratio.

Locations of plastic hinges were the same in all models (see appendix, Fig. B.2) but demands on frame members were depended on the location of infill wall in general. However, both of the ground story columns were failed only in one model, MAJ-2B-2S-UPINF, which was indicating the formation of soft story resulting from vertical irregularities. Failure and yield loads of frame members are given in Table 4.1. Note that members which did not yield or failed leaved empty in Table. 4.1. and in member capacity tables of all other model groups in the following sections.

Figure 4.4: Plan view of major axis 1 bay 2 story (1B-2S) models illustrating zero out-of-plane displacement at nodes 1 and 2.

Table 4.1: Member capacities of major axis 1 bay 2 story (1B-2S) models.

Model No.	Member	Deformation Type	Load Level (kN)	Deformation Type	Load Level (kN)
MAJ-1B-2S	C1	Yielding	59	Failure	63
	C2	Yielding	61	Failure	63
	C3	Yielding		Failure	
	C4	Yielding		Failure	
	B1	Yielding	40	Failure	45
	B2	Yielding	46	Failure	50
MAJ-1B-2S-INF	C1	Yielding	64	Failure	66
	C2	Yielding	65	Failure	
	C3	Yielding		Failure	
	C4	Yielding		Failure	
	B1	Yielding	55	Failure	56
	B2	Yielding	55	Failure	56
MAJ-1B-2S-UPINF	C1	Yielding	61	Failure	64
	C2	Yielding	63	Failure	64
	C3	Yielding		Failure	
	C4	Yielding		Failure	
	B1	Yielding	43	Failure	48
	B2	Yielding	51	Failure	54
MAJ-1B-2S-GRINF	C1	Yielding	62	Failure	65
	C2	Yielding	64	Failure	66
	C4	Yielding		Failure	
	C3	Yielding		Failure	
	B1	Yielding	43	Failure	48
	B2	Yielding	48	Failure	51

4.2.2 Two Bay One Story (2B-1S) Frame Models

These models were created by using the validation model MAJ-1B-1S and increasing the number of bay from one to two. After the modelling had finished all the members were studied on the bases of global structural performance parameters and local parameters. Node 1, 2, and 3 represent locations of the column to beam connections, column 1, C1, column 2, C2, and column 3, C3 are the column from left to right respectively and beam 1, B1 and beam 2, B2 are the two beams of the system (Fig. 4.5).

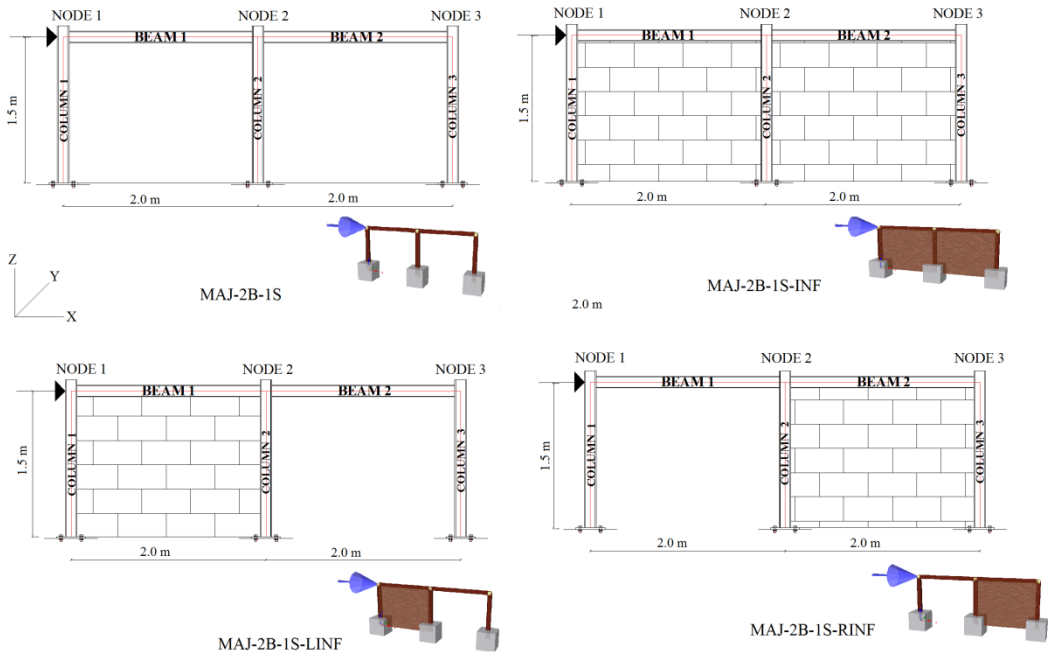

Figure 4.5: Details of major axis 2 bay 1 story (2B-1S) models with SeismoStruct illustrations.

Figure 4.6 shows the lateral load-displacement curves for all the major axis 2B-1S models. The curve for the MAJ-2B-1S model exhibited a non-linear behaviour. On the other hand all the other models followed similar behavioural pattern where the curve has a linear portion up to a certain load level, then there is a sudden increase in displacement while the load is constant. Then gradually the curve becomes non-linear with increase in both load and displacement. Finally, for all the curves the rate of increase of load is considerably less than displacement and hence a fairly flat plateau is formed until failure.

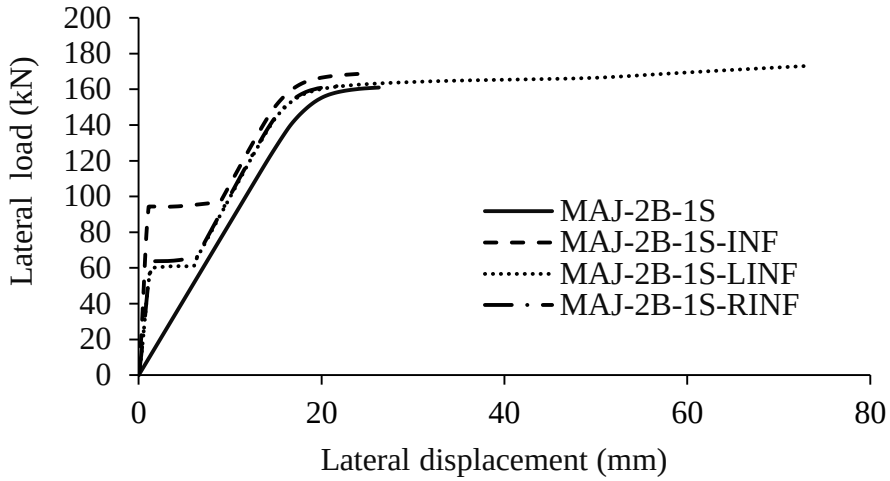

Figure 4.6: Load-displacement curves for major axis 2 bay 1 story (2B-1S) frame models.

The maximum top displacement was observed with MAJ-2B-1S-LINF with 72.83 mm and MAJ-2B-1S, MAJ-2B-1S-INF and MAJ-2B-1S-RINF had 26.26 mm, 25.25 mm and 22.15 mm respectively (Fig. 4.6 and 4.7 (a)). Also the maximum load and the maximum out-of-plane displacements at nodes 1, 2 and 3 were achieved by MAJ-2B-1S-LINF. This can be the reason behind extensive lateral displacement of MAJ-2B-1S-LINF when compared to the other three models. Out-of-plane displacement values of other models are shown in Figure 4.8 and given in Table 4.3.

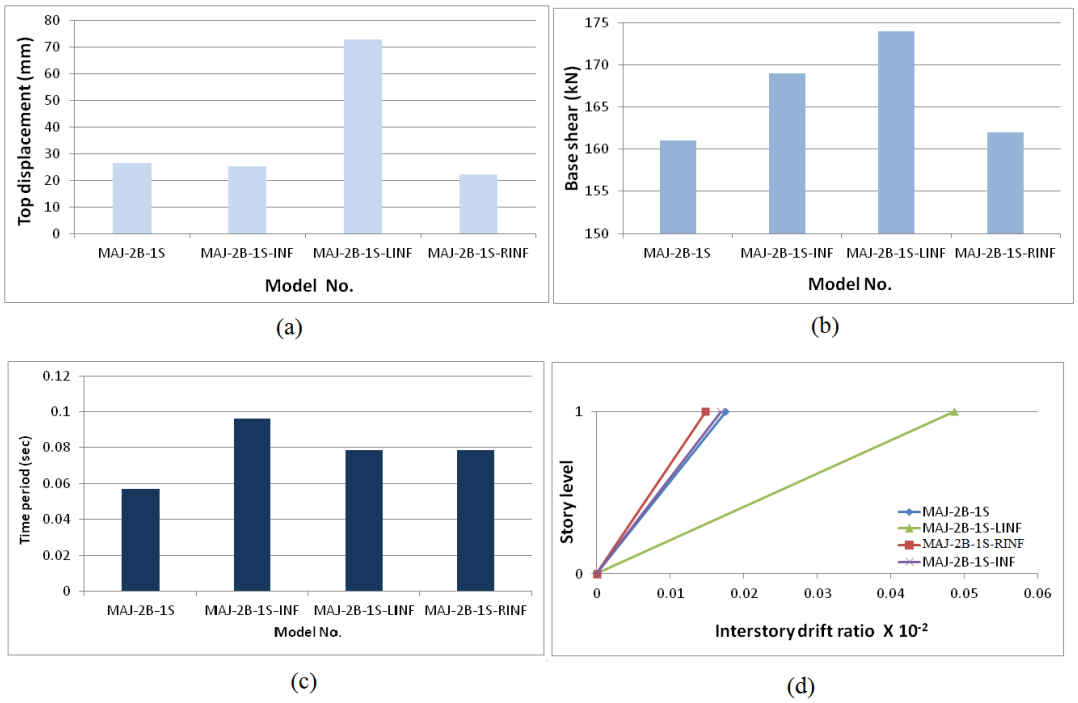

Figure 4.7: Global structural parameters of major axis 2 bay 1 story (2B-1S) models, (a) top displacement, (b) base shear, (c) time period and (d) drift ratio.

The heaviest model in weight, MAJ-2B-1S-INF, had the highest fundamental time period that was followed by MAJ-2B-1S-LINF, MAJ-2B-1S-RINF and MAJ-2B-1S. The time period was the same for MAJ-2B-1S-LINF and MAJ-2B-1S-RINF.

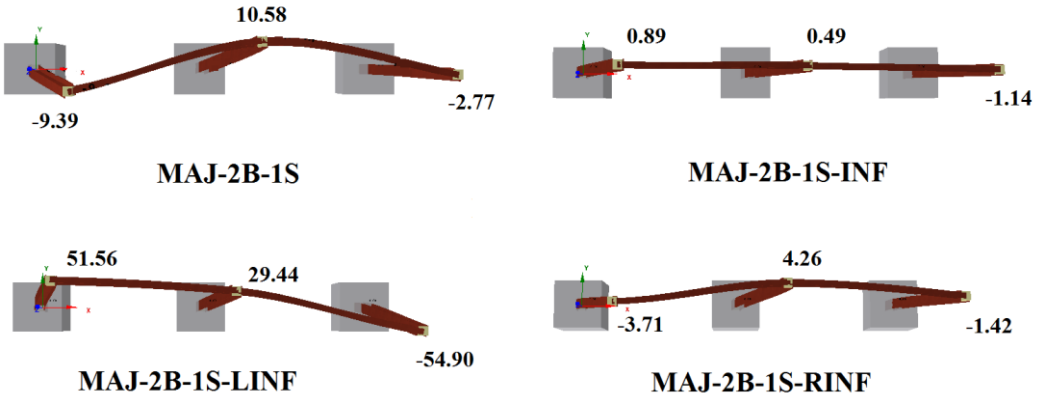

Figure 4.8: Plan view of major axis 2 bay 1 story (2B-1S) models illustrating out-of-plane displacements at node 1-3, without showing infills in frames.

When drift ratios are considered MAJ-2B-1S-RINF is observed to be the stiffest model and MAJ-2B-1S-LINF is observed to be the most flexible model among the other three models. Although, these two models were generated by changing the position of the infill wall only, it clearly shows how the presence of infill wall and its location in this system affects the flexural and lateral torsional buckling behaviour.of beams and hence non-uniform torsion of columns. All models experienced column failure at the base near supports and beam failures near the connections (see appendix B, Fig. B.4). Failure and yield loads of frame members are given in Table 4.2.

Table 4.2: Member capacities of MAJ-2B-1S, MAJ-2B-1S-INF, MAJ-2B-1S-LINF and MAJ- 2B-1S-RINF.

Model No.	Member	Deformation Type	Load Level (kN)	Deformation Type	Load Level (kN)
MAJ-2B-1S	C1	Yielding	124.5	Failure	152.5
	C2	Yielding	113	Failure	140.5
	C3	Yielding	136	Failure	
	B1	Yielding	126.5	Failure	150
	B2	Yielding	125.5	Failure	149
MAJ-2B-1S-INF	C1	Yielding	154	Failure	162
	C2	Yielding	142	Failure	154
	C3	Yielding	162	Failure	166
	B1	Yielding	153	Failure	164
	B2	Yielding	152	Failure	161
MAJ-2B-1S-LINF	C1	Yielding	148	Failure	157
	C2	Yielding	137	Failure	149
	C3	Yielding	156	Failure	
	B1	Yielding	147	Failure	158
	B2	Yielding	146	Failure	156
MAJ-2B-1S-RINF	C1	Yielding	149	Failure	158
	C2	Yielding	135	Failure	148
	C3	Yielding	156	Failure	161
	B1	Yielding	145	Failure	158
	B2	Yielding	146	Failure	156

Table 4.3: Out-of-plane displacement values of major axis 2 bay 1 story (2B-1S) models.

Model No.	Node No.	Out of plane disp. at failure (mm)
MAJ-2B-1S	1	0.89
	2	0.49
	3	-1.14
MAJ-2B-1S-INF	1	-9.39
	2	10.58
	3	-2.77
MAJ-2B-1S-LINF	1	51.26
	2	29.44
	3	-54.9
MAJ-2B-1S-RINF	1	-3.71
	2	4.26
	3	-1.42

4.2.3 Two Bay Two Story (2B-2S) Frame Models

These models were created in order of a 2 bay 2 story moment frames without infill wall, MAJ-2B-2S as a reference model and then followed by MAJ-2B-2S-INF, MAJ-2B-2S-LINF, MAJ-2B-2S-RINF, MAJ-2B-2S-UPINF, MAJ-2B-2S-GRINF, MAJ-2B-2S-ASYM1 and MAJ-2B-2S-ASYM2. After the modelling had finished, all the members were studied on the bases of global structural performance parameters and local parameters. Node 1, 2, and 3 represent locations of the top column to top beam connections, column 1, C1, column 2, C2, column 3, C3, column 4, C4, column 5, C5 and column 6, C6 are the column members and beam 1, B1, beam 2, B2, beam 3, B3 and beam 4, B4 are the beams of the system (Fig. 4.9).

Figure 4.9: Details of major axis 2 bay 2 story (2B-2S) models with SeismoStruct illustrations.

Figure 4.10 shows the lateral load-displacement curves for all the major axis 2B-2S models. The curve for the MAJ-2B-2S model exhibited a non-linear behaviour. On the other hand all the other models followed similar behavioural pattern where the curve has a linear portion up to a certain load level then, there is a sudden increase in displacement while the load is constant. Then gradually the curve becomes non-linear with increase in both load and displacement. Finally, for some of the curves the rate of increase for load is considerably less than displacement and hence a fairly flat plateau is formed.

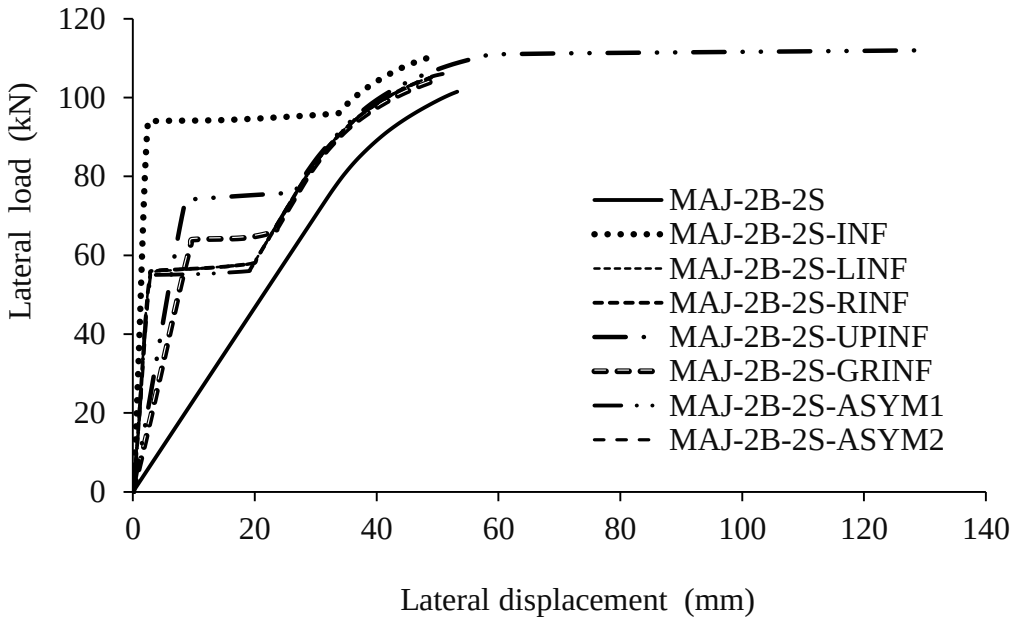

Figure 4.10: Load-displacement curves for all major axis 2 bay 2 story (2B-2S) frame models.

The maximum base shear and top displacement (drift ratio) was observed with MAJ-2B-2S-UPINF and this model exhibited higher value of out-of-plane displacements at nodes 1, 2 and 3 than all other major two bay two story models (Fig.4.11 and Table 4.6). Out-of-plane displacement values of all other models are shown in Figure 4.12 and given in Table 4.6.

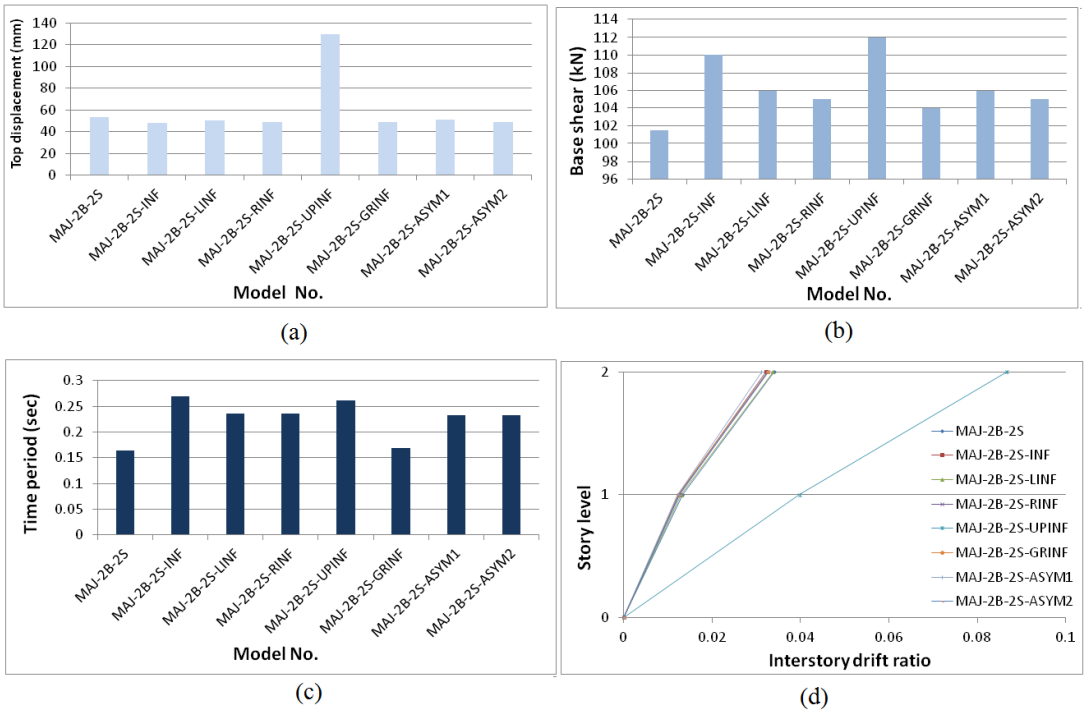

Figure 4.11: Global structural parameters of major axis 2 bay 2 story (2B-2S) models, (a) top displacement, (b) base shear, (c) time period and (d) drift ratio.

The heaviest model in weight, MAJ-2B-2S-INF, had the highest fundamental time period where the bare frame model MAJ-2B-2S had the lowest fundamental time period. The MAJ-2B-LINF and MAJ-2B-RINF and MAJ-2B-2S-ASYM1 and MAJ-2B-2S-ASYM2 had the same periods. However, MAJ-2B-2S-UPINF and MAJ-2B-2S-GRINF had different fundamental time periods although the only difference was the up and down placement of infill walls.

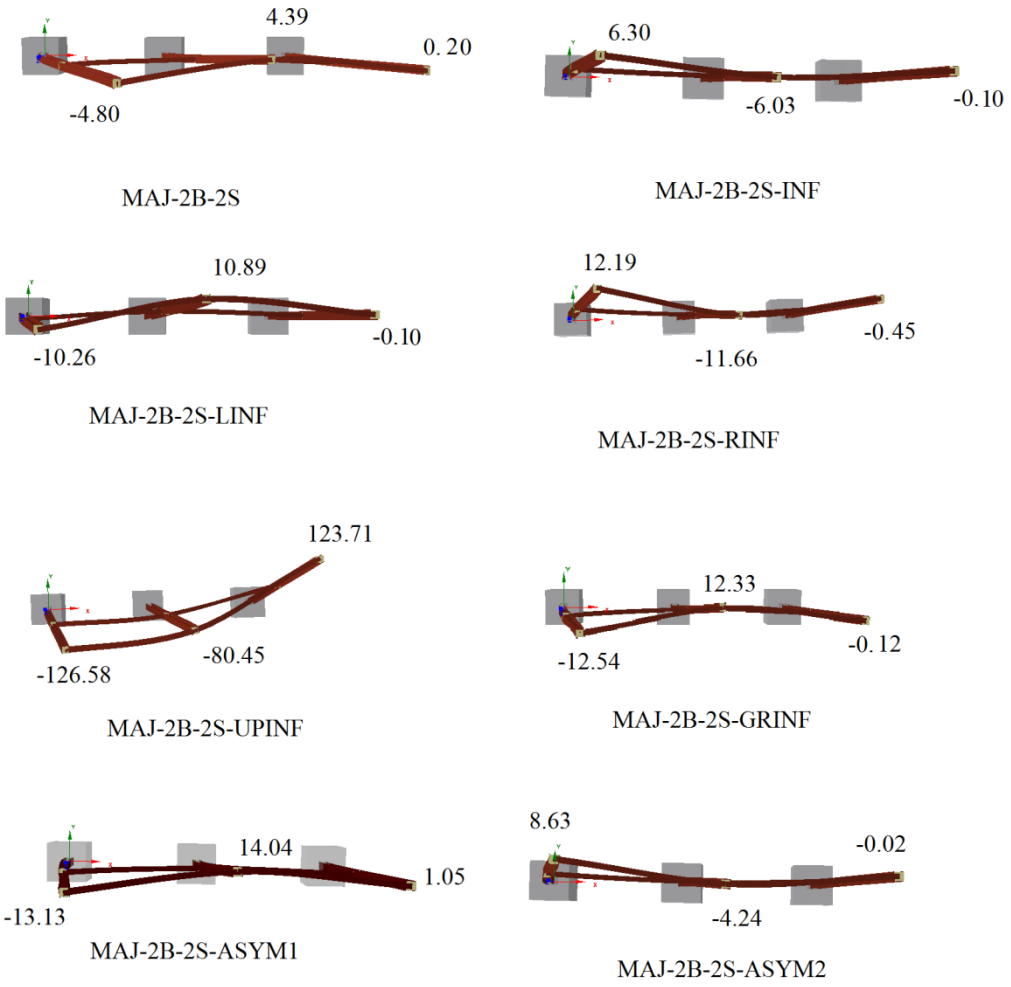

Figure 4.12: Plan view of major axis 2 bay 2 story (2B-2S) models illustrating out-of-plane displacements at nodes 1-3, without showing infills in frames.

Location of plastic hinges (see appendix B, Fig. B.5) and demands on frame members were depended on the location of infill wall in general. However, it was clearly observed that the ground story columns were all failed in only one model (MAJ-2B-2S-UPINF) which was indicating the formation of soft story caused by vertical irregularities. Failure and yield loads of frame members are given in Table 4.4. and Table 4.5.

Table 4.4: Member capacities of major axis 2 bay 2 story (2B-2S) models.

Model No.	Member	Deformation Type	Load Level (kN)	Deformation Type	Load Level (kN)
MAJ-2B-2S	C1	Yielding	96	Failure	
	C2	Yielding	94	Failure	
	C3	Yielding		Failure	
	C4	Yielding		Failure	
	C5	Yielding	100	Failure	
	C6	Yielding		Failure	
	B1	Yielding	60	Failure	78
	B2	Yielding	62	Failure	80
	B3	Yielding	82	Failure	94
	B4	Yielding	78	Failure	92
MAJ-2B-2S-INF	C1	Yielding	110	Failure	
	C2	Yielding	110	Failure	
	C3	Yielding		Failure	
	C4	Yielding		Failure	
	C5	Yielding		Failure	
	C6	Yielding		Failure	
	B1	Yielding	96	Failure	
	B2	Yielding	96	Failure	
	B3	Yielding	100	Failure	105
	B4	Yielding	104	Failure	
MAJ-2B-2S-LINF	C1	Yielding	105	Failure	
	C2	Yielding	105	Failure	106
	C3	Yielding		Failure	
	C4	Yielding		Failure	
	C5	Yielding		Failure	
	C6	Yielding		Failure	
	B1	Yielding	77	Failure	86
	B2	Yielding	78	Failure	87
	B3	Yielding	94	Failure	99
	B4	Yielding	93	Failure	98
MAJ-2B-2S-RINF	C1	Yielding	105	Failure	
	C2	Yielding	104	Failure	
	C3	Yielding		Failure	
	C4	Yielding		Failure	
	C5	Yielding		Failure	
	C6	Yielding		Failure	
	B1	Yielding	77	Failure	86
	B2	Yielding	78	Failure	87
	B3	Yielding	93	Failure	99
	B4	Yielding	93	Failure	98

Table 4.5: Member capacities of major axis 2 bay 2 story (2B-2S) models (continued).

Model No.	Member	Deformation Type	Load Level (kN)	Deformation Type	Load Level (kN)
MAJ-2B-2S-UPINF	C1	Yielding	107	Failure	111
	C2	Yielding	105	Failure	110
	C3	Yielding	110	Failure	112
	C4	Yielding		Failure	
	C5	Yielding		Failure	
	C6	Yielding		Failure	
	B1	Yielding	76	Failure	86
	B2	Yielding	78	Failure	87
	B3	Yielding	97	Failure	102
	B4	Yielding	95	Failure	101
MAJ-2B-2S-GRINF	C1	Yielding	104	Failure	
	C2	Yielding	103	Failure	
	C3	Yielding		Failure	
	C4	Yielding		Failure	
	C5	Yielding		Failure	
	C6	Yielding		Failure	
	B1	Yielding	77	Failure	86
	B2	Yielding	78	Failure	87
	B3	Yielding	90	Failure	96
	B4	Yielding	90	Failure	96
MAJ-2B-ASYM1	C1	Yielding		Failure	
	C2	Yielding	102.9	Failure	105
	C3	Yielding		Failure	
	C4	Yielding		Failure	
	C5	Yielding		Failure	
	C6	Yielding		Failure	
	B1	Yielding	90.1	Failure	
	B2	Yielding	90.1	Failure	92.24
	B3	Yielding	101.6	Failure	
	B4	Yielding	97	Failure	101
MAJ-2B-2S-ASYM2	C1	Yielding	105	Failure	
	C2	Yielding	104	Failure	
	C3	Yielding		Failure	
	C4	Yielding		Failure	
	C5	Yielding		Failure	
	C6	Yielding		Failure	
	B1	Yielding	77	Failure	86
	B2	Yielding	78	Failure	86
	B3	Yielding	93	Failure	100
	B4	Yielding	93	Failure	98

Table 4.6: Out-of-plane displacement values of major axis 2 bay 2 story (2B-2S) models.

Model No.	Node	Out-of-plane disp. (mm)
MAJ-2B-2S	1	-4.80
	2	4.39
	3	0.20
MAJ-2B-2S-INF	1	6.30
	2	-6.03
	3	-0.10
MAJ-2B-2S-LINF	1	-10.26
	2	10.89
	3	-0.10
MAJ-2B-2S-RINF	1	12.19
	2	-11.66
	3	-0.45
MAJ-2B-2S-UPINF	1	-126.58
	2	-80.45
	3	123.71
MAJ-2B-2S-GRINF	1	-12.54
	2	12.33
	3	-0.12
MAJ-2B-2S-ASYM1	1	-13.13
	2	14.04
	3	1.05
MAJ-2B-2S-ASYM2	1	8.63
	2	-4.24
	3	-0.024

4.3 Minor Axis Frame Models

The minor axes of vertical members (column webs) are placed 90 degrees to the direction of applied load were modelled to investigate effects of infill wall(s) on the structural performance. For this purpose three different groups of models were created and infill wall was placed into the frames at different orientations. These new models were grouped with respect to their number of bays and stories. Addition to 1 bay 1 story (1B-1S) (Fig.3.10) validation models, 1 bay 2 story (1B-2S) (Fig.4.13), 2 bay 1 story (2B-1S) (Fig.4.17) and 2 bay 2 story (2B-2S) (Fig.4.21) models were

formed. After the modelling had finished all the members were studied on the bases of global structural performance parameters and local parameters.

4.3.1 One Bay Two Story (1B-2S) Frame Models

These models were created by using the validation model MIN-1B-1S and increasing the number story from one to two. After the modelling had finished all the members were studied on the bases of global structural performance parameters and local parameters. Node 1 and 2 represent locations of the top column to beam connections, column 1, C1, column 2, C2, column 3, C3 and column 4, C4 are the column members and beam 1, B1 and beam 2, B2 are the two beams of the systems (Fig. 4.13)

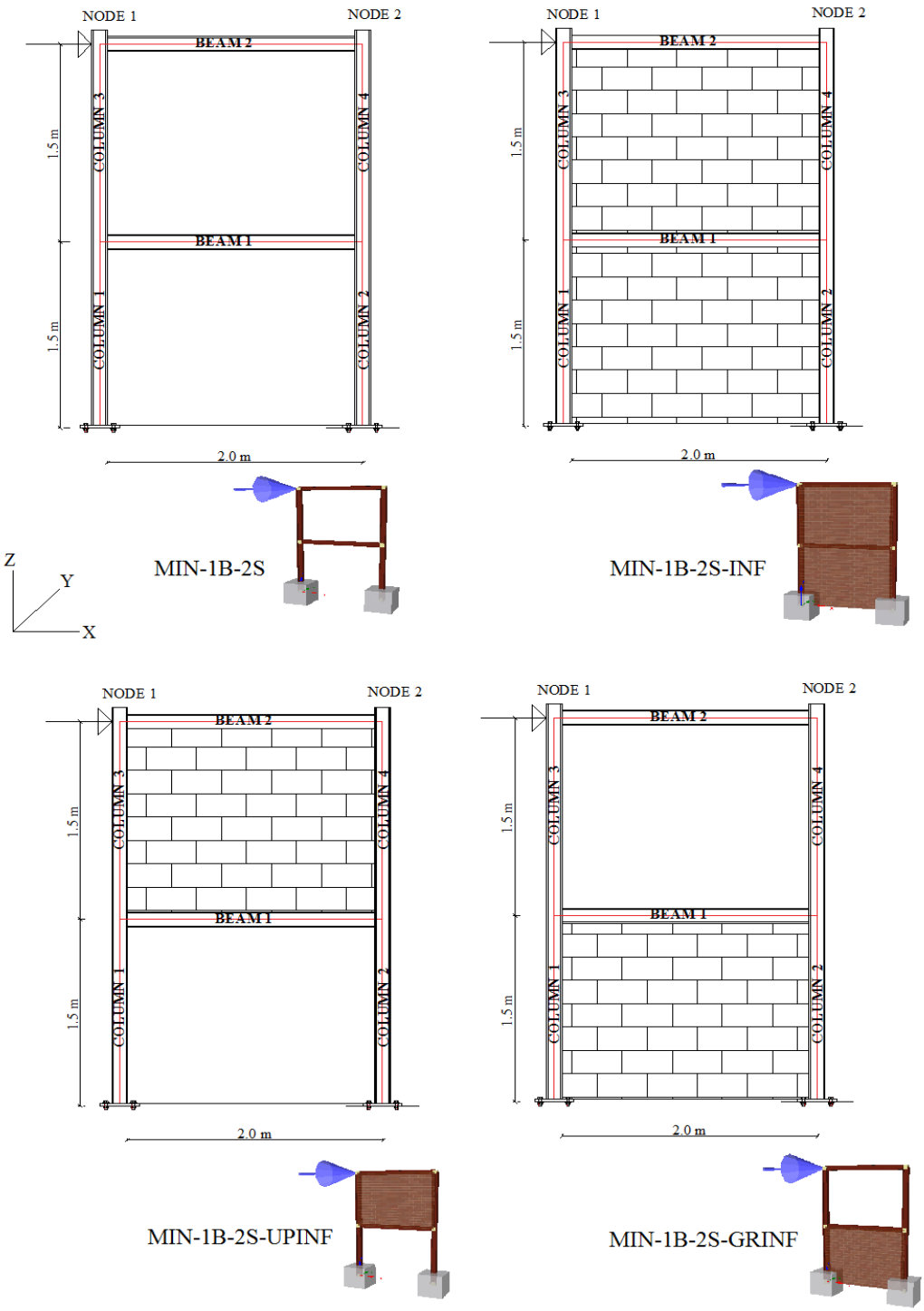

Figure 4.13: Details of minor axis 1 bay 2 story (1B-2S) models with SeismoStruct illustrations.

Figure 4.14 shows the lateral load-displacement curves for all the minor axis 1B-2S models. The curve for reference model, MIN-1B-2S, exhibited a non-linear

behaviour. On the other hand all the other models followed similar behavioural pattern where the curve has a linear portion up to a certain load level then there is a sudden increase in displacement while the load is constant. Then gradually the curve becomes non-linear with increase in both load and displacement until the failure load.

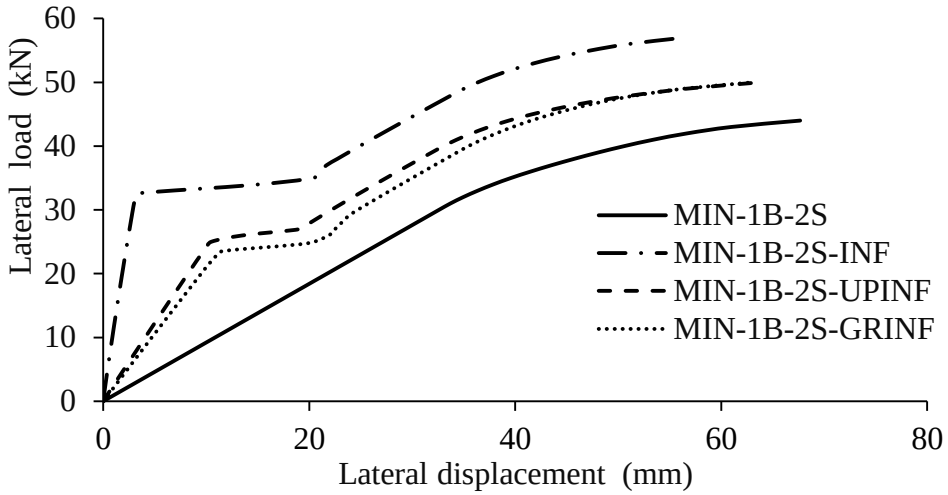

Figure 4.14: Load-displacement curves for minor axis 1 bay 2 story (1B-2S) frame models.

The maximum top displacement and drift ratio were observed with MIN-1B-2S but the variation of displacement values among all models was not so high. The maximum base shear and time period was exhibited by the heaviest model in weight, MAJ-1B-2S-INF (Fig.4.15). All the models exhibited zero out-of-plane displacements at nodes 1 and 2 (Fig. 4.16).

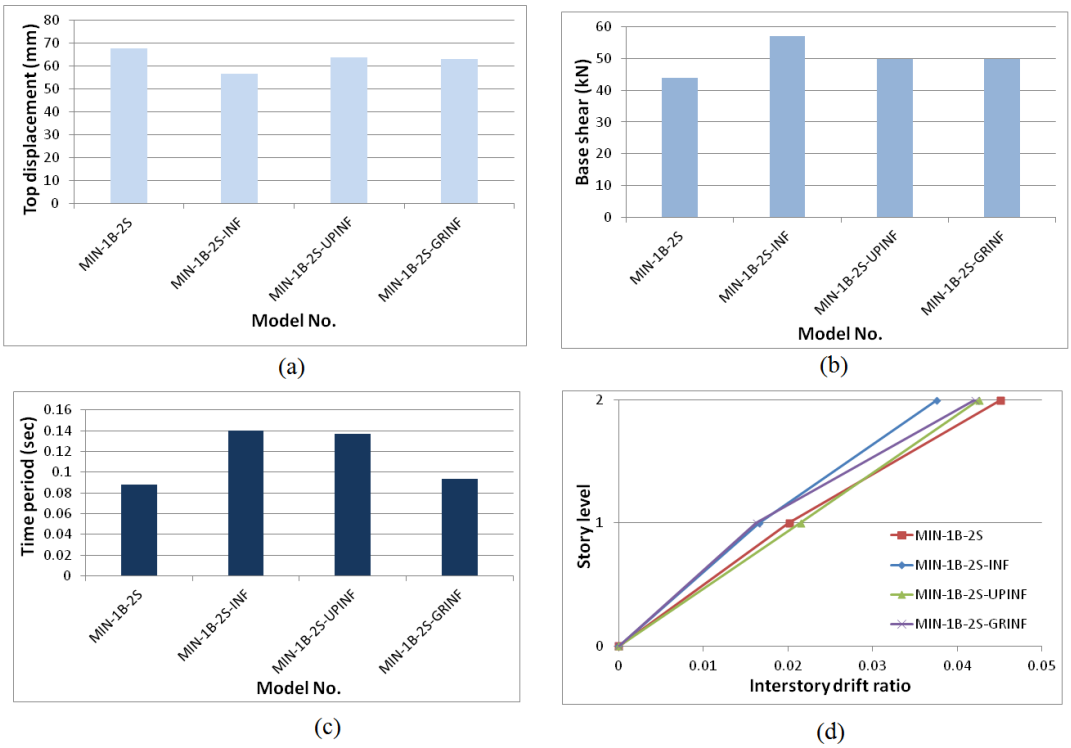

Figure 4.15: Global structural parameters of minor axis 1 bay 2 story (1B-2S) models, (a) top displacement, (b) base shear, (c) time period and (d) drift ratio.

Figure 4.16: Plan view of minor axis 1 bay 2 story (1B-2S) models illustrating out-of-plane displacements at nodes 1 and 2.

Location of plastic hinges (see appendix B, Fig. B.3) and demands on frame members were depended on the location of infill wall in general. However, both of the ground story columns failed for all models. Failure and yield loads of frame members are given in Table 4.7.

Table 4.7: Member capacities of minor axis 1 bay 2 story (1B-2S) models.

Model No.	Member	Deformation Type	Load Level (kN)	Deformation Type	Load Level (kN)
MIN-1B-2S	C1	Yielding	34	Failure	40
	C2	Yielding	36	Failure	40
	C3	Yielding		Failure	
	C4	Yielding		Failure	
	B1	Yielding	31	Failure	34
	B2	Yielding		Failure	
MIN-1B-2S-INF	C1	Yielding	50	Failure	55
	C2	Yielding	52	Failure	56
	C3	Yielding		Failure	
	C4	Yielding		Failure	
	B1	Yielding	48	Failure	52
	B2	Yielding		Failure	
MIN-1B-2S-UPINF	C1	Yielding	37	Failure	44
	C2	Yielding	38	Failure	45
	C3	Yielding		Failure	
	C4	Yielding		Failure	
	B1	Yielding	40	Failure	43
	B2	Yielding		Failure	
MIN-1B-2S-GRINF	C1	Yielding	46	Failure	50
	C2	Yielding	48	Failure	50
	C4	Yielding		Failure	
	C3	Yielding		Failure	
	B1	Yielding	39	Failure	43
	B2	Yielding	48	Failure	

4.3.2 Two Bay One Story Frame Models

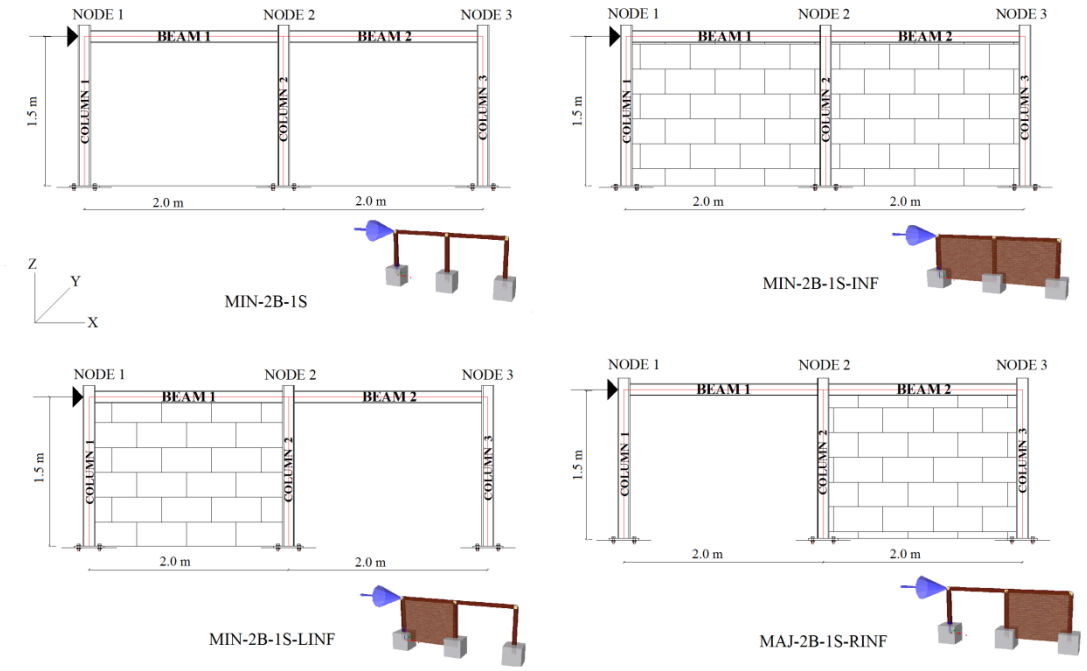

Figure 4.17: Details of minor axis 2 bay 1 story (2B-1S) models with SeismoStruct illustrations.

These models were created by using validation model MIN-1B-1S and increasing the number of bay from one to two. After the modelling had finished, all the members were studied on the bases of global structural performance parameters and local parameters. Node 1, 2, and 3 represent locations of the column to beam connections, column 1, C1, column 2, C2, and column 3, C3 are the column from left to right respectively and beam 1, B1 and beam 2, B2 are the two beams of the system (Fig. 4.17). Figure 4.18 shows the lateral load-displacement curves for all the minor axis 2B-1S models. The curve for the MIN-2B-1S model exhibited a non-linear behaviour. On the other hand all the other models followed similar behavioural pattern where the curve has a linear portion up to a certain load level then there is a sudden increase in displacement while the load is constant. Then gradually the curve

becomes non-linear with increase in both load and displacement. Finally for some of the curves the rate of increase for load is considerably less then displacement and hence a fairly flat plateau is formed

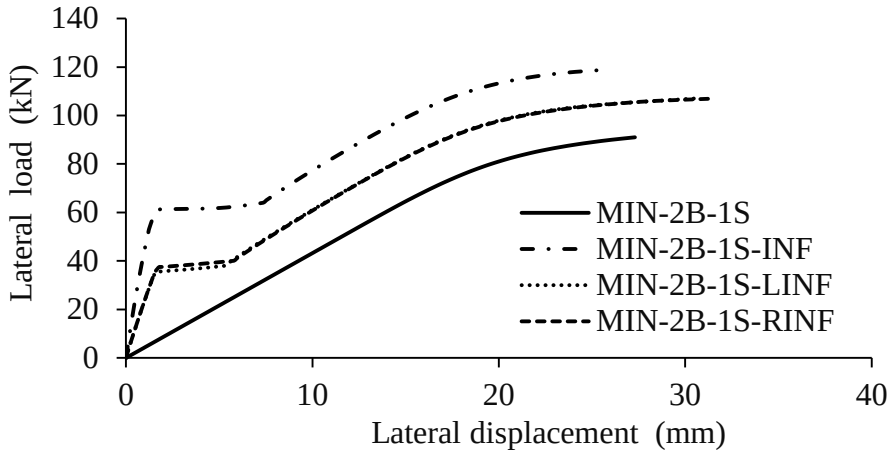

Figure 4.18: Load-displacement curves for minor axis 2 bay 1 story (2B-1S) frame models.

The maximum top displacement was observed with MIN-2B-1S-RLINF but the difference with other models was not so high (Fig. 4.18 and 4.19.(a)). The maximum load and the minimum top displacement, hence the maximum stiffness was exhibited by MIN-2B-1S-INF. Zero out-of-plane displacement at nodes 1, 2 and 3 were observed for all models as shown in Figure 4.20.

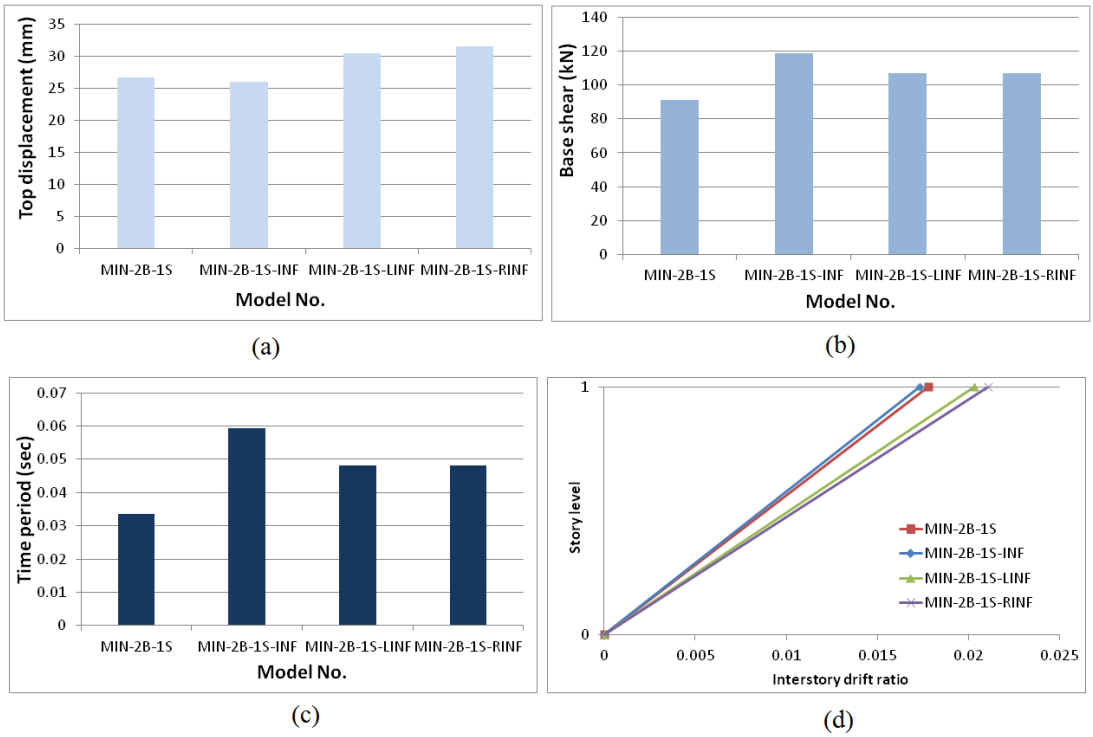

Figure 4.19: Global structural parameters of minor axis 2 bay 1 story (2B-1S) models, (a) top displacement, (b) base shear, (c) time period and (d) drift ratio.

The heaviest model in weight, MIN-2B-1S-INF, had the highest fundamental time period that was followed by MIN-2B-1S-LINF, MIN-2B-1S-RINF and MIN-2B-1S. The fundamental time periods were the same for MIN-2B-1S-LINF and MIN-2B-1S-RINF of the same weight.

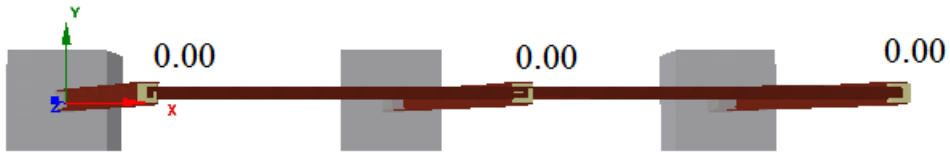

Figure 4.20: Plan view of minor axis 2 bay 1 story (2B-1S) models illustrating out-of-plane displacements at nodes 1-3, without showing infills in frames.

Locations of plastic hinges were the same for all models which occurred at the base of column members near supports and beam ends near the connections (see appendix

B, Fig. B.4). Failure and yield loads of all members are given in Table 4.8. that shows how demand on individual members changes with the presence and location of the infills.

Table 4.8. Member capacities of minor axis 2 bay 1 story (2B-1S) models.

Model No.	Member	Deformation Type	Load Level (kN)	Deformation Type	Load Level (kN)
MIN-2B-1S	C1	Yielding	63	Failure	76
	C2	Yielding	55	Failure	71
	C3	Yielding	66	Failure	78
	B1	Yielding	92	Failure	
	B2	Yielding	92	Failure	
MIN-2B-1S-INF	C1	Yielding	93	Failure	106
	C2	Yielding	86	Failure	99
	C3	Yielding	98	Failure	109
	B1	Yielding		Failure	
	B2	Yielding		Failure	
MIN-2B-1S-LINF	C1	Yielding	77	Failure	91
	C2	Yielding	71	Failure	84
	C3	Yielding	82	Failure	94
	B1	Yielding	107	Failure	
	B2	Yielding	106	Failure	107
MIN-2B-1S-RINF	C1	Yielding	79	Failure	92
	C2	Yielding	70	Failure	82
	C3	Yielding	81	Failure	93
	B1	Yielding	106	Failure	
	B2	Yielding	107	Failure	

4.3.3 Two Bay Two Story Frame Models

These models were created by using validation model MIN-1B-1S and increasing the number of bay and story from one to two. Node 1, 2, and 3 represent locations of the top column to beam connections, column 1, C1, column 2, C2, column 3, C3, column

4, C4, column 5, C5 and column 6, C6 are the vertical members and beam 1, B1, beam 2, B2, beam 3, B3 and beam 4, B4 are the beams of the systems (Fig. 4.21).

Figure 4.21: Details of minor axis 2 bay 2 story (2B-2S) models with SeismoStruct illustrations.

Figure 4.22 shows the lateral load-displacement curves for all the minor axis 2B-2S models. The curve for the MIN-2B-2S displayed a non-linear behaviour. On the other hand all the other models behaviour followed a similar pattern where the curve has a linear portion up to a certain load level then there is a sudden increase in displacement while the load is constant. Then gradually the curve becomes non-linear with increase in both load and displacement until failure.

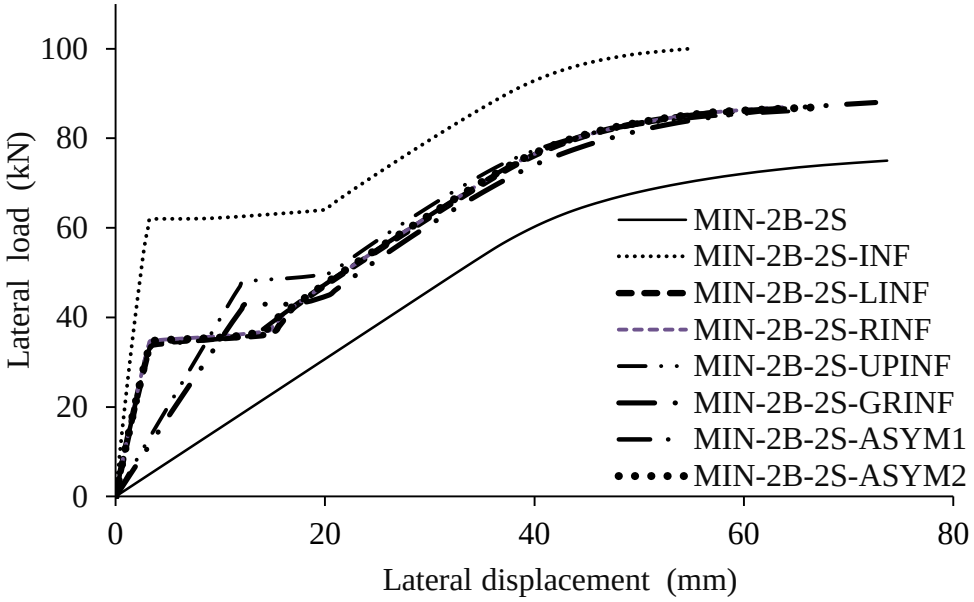

Figure 4.22: Load-displacement curves for all minor axis 2 bay 2 story (2B-2S) frame models.

The maximum top displacement (drift ratio) was observed with MIN-2B-2S but the displacement as well as base shear values remained in a narrow range (Fig.4.22 and 4.23 (a) and (b)).The heaviest model in weight, MIN-2B-2S-INF, had the highest fundamental time period where the bare frame model MAJ-2B-2S had the lowest. The MIN-2B-LINF together with MIN-2B-RINF and MAJ-2B-2S-ASYM1 together with MAJ-2B-2S-ASYM2 had the same fundamental time periods. However, MIN-

2B-2S-UPINF and MIN-2B-2S-GRINF had different fundamental time periods (Fig.4.23 (c)).

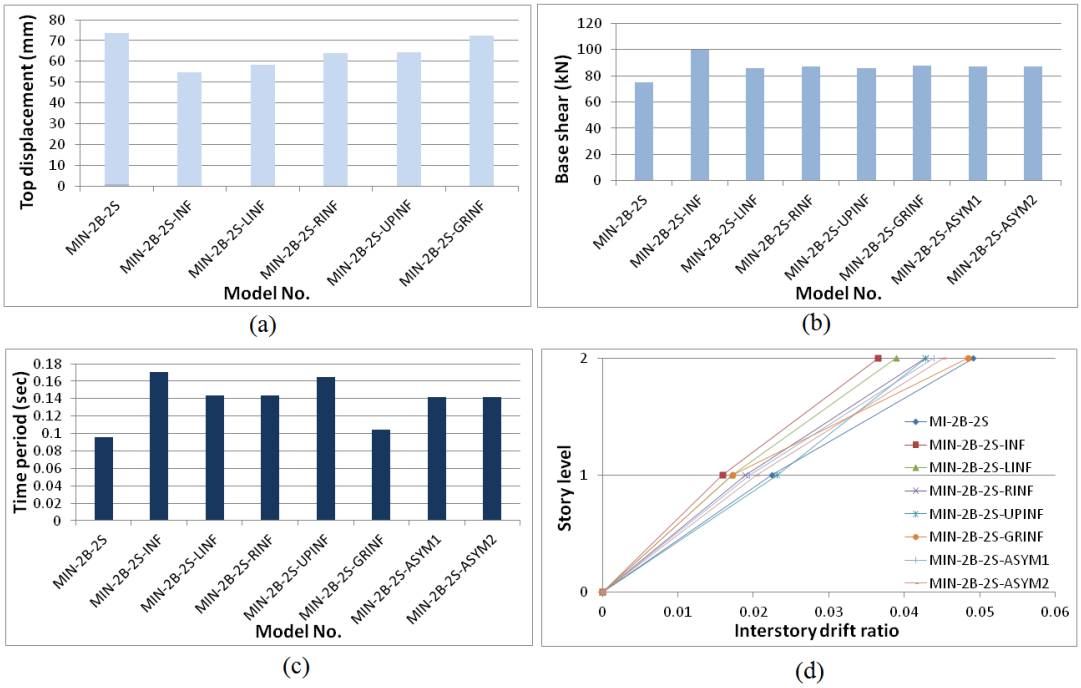

Figure 4.23: Global structural parameters of minor axis 2 bay 2 story (2B-2S) models, (a) top displacement, (b) base shear, (c) time period and (d) drift ratio.

There was not a definite pattern for the locations of plastic hinges but they were concentrated near column bases and around the beam ends (see appendix B, Fig. B.6). Almost all of the column members yielded for all models but none of them failed at maximum received load except bare frame model, MIN-2B-2S. Thus orientation of the column members and the presence of infill affect the demands on vertical load bearing members clearly. Failure and yield loads of frame members are given in Table 4.9 and Table 4.10. Finally, all models had zero out-of-plane displacements at the nodes 1, 2 and 3 (Fig.4.24).

Figure 4.24: Plan view of minor axis 2 bay 2 story (2B-2S) models illustrating out-of-plane displacements at node 1-3.

Table 4.9: Member capacities of minor axis 2 bay 2 story (2B-2S) models.

Model No.	Member	Deformation Type	Load Level (kN)	Deformation Type
MIN-2B-2S	C1	Yielding	57	Failure
	C2	Yielding	50	Failure
	C3	Yielding	59	Failure
	C4	Yielding	70	Failure
	C5	Yielding	48	Failure
	C6	Yielding	72	Failure
	B1	Yielding	54	Failure
	B2	Yielding	55	Failure
	B3	Yielding	73	Failure
	B4	Yielding	73	Failure
MIN-2B-2S-INF	C1	Yielding	88	Failure
	C2	Yielding	81	Failure
	C3	Yielding	91	Failure
	C4	Yielding	99	Failure
	C5	Yielding	78	Failure
	C6	Yielding	100	Failure
	B1	Yielding	89	Failure
	B2	Yielding	89	Failure
	B3	Yielding		Failure
	B4	Yielding		Failure
MIN-2B-2S-LINF	C1	Yielding		Failure
	C2	Yielding	66	Failure
	C3	Yielding	75	Failure
	C4	Yielding	83	Failure
	C5	Yielding	64	Failure
	C6	Yielding	86	Failure
	B1	Yielding	72	Failure
	B2	Yielding	72	Failure
	B3	Yielding		Failure
	B4	Yielding		Failure
MIN-2B-2S-RINF	C1	Yielding		Failure
	C2	Yielding	65	Failure
	C3	Yielding	75	Failure
	C4	Yielding	85	Failure
	C5	Yielding	62	Failure
	C6	Yielding	86	Failure
	B1	Yielding	71	Failure
	B2	Yielding	73	Failure
	B3	Yielding	87	Failure
	B4	Yielding	87	Failure

Table 4.10: Member capacities of minor axis 2 bay 2 story (2B-2S) models (continued).

Model No.	Member	Deformation Type	Load Level (kN)	Deformation Type
MIN-2B-2S-UPINF	C1	Yielding	61	Failure
	C2	Yielding	55	Failure
	C3	Yielding	62	Failure
	C4	Yielding		Failure
	C5	Yielding	74	Failure
	C6	Yielding		Failure
	B1	Yielding	71	Failure
	B2	Yielding	73	Failure
	B3	Yielding		Failure
	B4	Yielding		Failure
MIN-2B-2S-GRINF	C1	Yielding	84	Failure
	C2	Yielding	75	Failure
	C3	Yielding	85	Failure
	C4	Yielding	77	Failure
	C5	Yielding	52	Failure
	C6	Yielding	79	Failure
	B1	Yielding	72	Failure
	B2	Yielding	71	Failure
	B3	Yielding	81	Failure
	B4	Yielding	81	Failure
MIN-2B-2S-ASYM1	C1	Yielding		Failure
	C2	Yielding	65	Failure
	C3	Yielding	75	Failure
	C4	Yielding	84	Failure
	C5	Yielding	64	Failure
	C6	Yielding	86	Failure
	B1	Yielding	72	Failure
	B2	Yielding	73	Failure
	B3	Yielding		Failure
	B4	Yielding	87	Failure
MIN-2B-2S-ASYM2	C1	Yielding	72	Failure
	C2	Yielding	66	Failure
	C3	Yielding	75	Failure
	C4	Yielding	85	Failure
	C5	Yielding	62	Failure
	C6	Yielding	86	Failure
	B1	Yielding	72	Failure
	B2	Yielding	71	Failure
	B3	Yielding	87	Failure
	B4	Yielding	87	Failure

Chapter 5

COMPARISON OF RESULTS, CONCLUSIONS AND RECOMMENDATIONS FOR FUTURE WORK

5.1 Introduction

This analytical study has been concentrated on the investigation of the effects of infill walls on steel framed structures using BIMs block as infill under non-linear static (pushover) analysis. For this purpose, finite element software SeismoStruct was used. First, analytically formed four half-scale moment frames with and without infill by using the data of a previous experimental study of Milad [11] were validated. Later the results of experimental and analytical studies were compared. Then, six new groups of models were constructed by modifying the validation models e.g. increasing number of bays and stories and changing location of the infill walls. The models having the same number of bay and story are considered in the same group and models of the same group differ by means of the existence and the location of the infill walls only.

In total, thirty-six analytical models were studied on the bases of global structural performance parameters of top displacement, base shear, fundamental time period and out-of-plane displacement and local parameters of inter-story drift ratio and member deformation capacities to monitor the effect of plan and vertical irregularities and symmetrical/asymmetrical placement of infill walls. The following results have been derived from this study.

5.2 Comparison of the Results and Conclusions

- All bare frame models experienced higher top displacements when compared to fully infilled frames of the same group. On the other hand, when frames did not all have infill walls then the location of infill wall affects the top displacements (Fig.5.1).

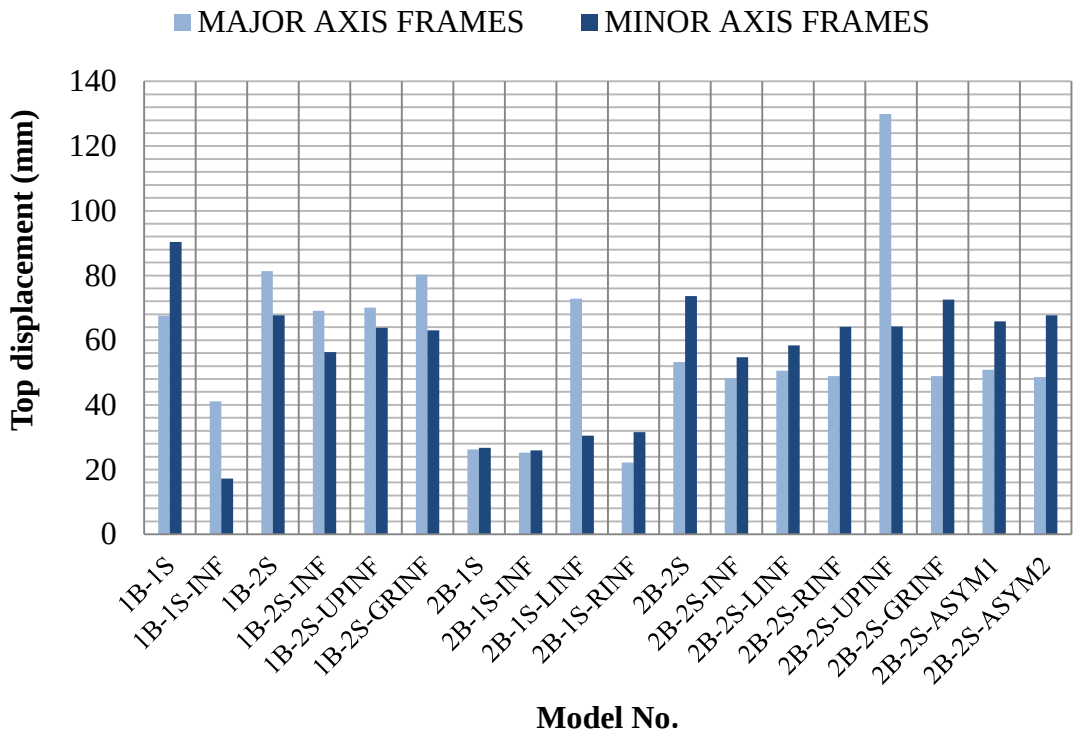

Figure 5.1: Top displacement values for major and minor axis frame models.

- In general, presence of out-of-plane displacement causes dramatic differences in the top displacement values of frames especially for major axis frames. Frames having the highest out-of-plane displacements in a group exhibited the highest top displacements (Fig. 5.1)

- All minor axis models experienced zero out-of-plane displacement. Hence, it was concluded that the orientation of the column members directly influences out-of-plane displacement.

- When out-of-plane displacement is zero or relatively low, top displacements of the same group models do not differ too much from each other except 1 bay 1 story model group which can be attributed to the effect of bay and story increase on these parameters. Minor axis frames have low variance in top displacements, hence, this can be related to zero out-of-plane displacement.

- For minor axis frames, the effect of plan irregularity and symmetrical placement of infills on top displacements and the resisted lateral loads are not as great as vertical irregularity.

- Fully infilled frames displayed the highest stiffness by receiving more loads for the same displacement values compared to other models in the same group.

- The highest time period belongs to fully infilled models where the lowest fundamental time period belongs to bare frame models (Fig.5.2). This conforms to the references [15, 16] that the presence of infill walls increases stiffness of the structure and consequently the natural period due to increased weight.

- The orientation of column members directly affect the fundamental time period of the models, all minor axis models have lower fundamental time

periods (approximately half) compared to their major axis group members (Fig. 5.2)

- Although, plan irregularity and asymmetrical placement of infills do not affect the fundamental time period of models having the same weight, the vertical irregularity causes increase or decrease of the fundamental time period depending on the location of infill.

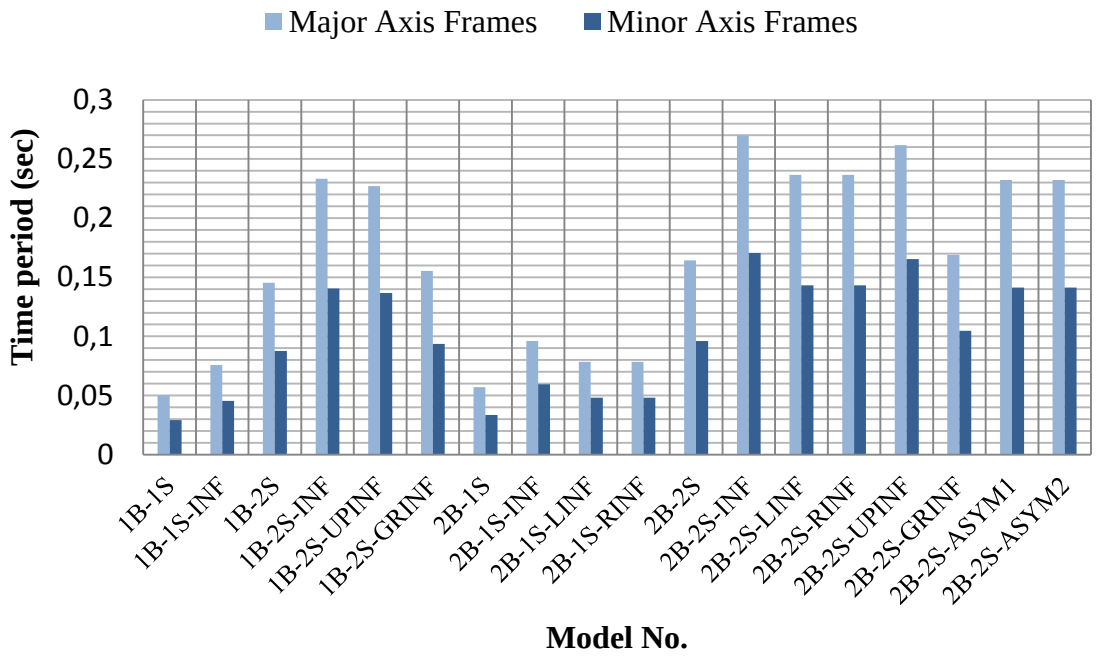

Figure 5.2: Fundamental time period for major and minor axis frame models.

- Load-displacement curves for all bare frame models exhibited a non-linear behavioural pattern where infilled frames showed a sudden loss in stiffness and then started receiving higher loads. This result reminds the phenomena that "infilled frame behaves as a monolithic system at low lateral load levels, with increase in load levels infill starts separating from the surrounding frame and forms diagonal compression mechanism" (section 2.4).

- The presence of infill wall on the second story only, caused failure of all ground story columns, hence, this was due to the formation of soft story in major axis 2 story frame models.

- Location of plastic hinges remain same for all models of 1B-1S and major axis 1B-2S frame models but for all other models, locations were altered due to the presence of infill (see Appendix B).

- As the number of bays increase the base shear increases for both major and minor axis frame models and all major axis frame models received higher loads compared to minor axis models (Fig. 5.3).

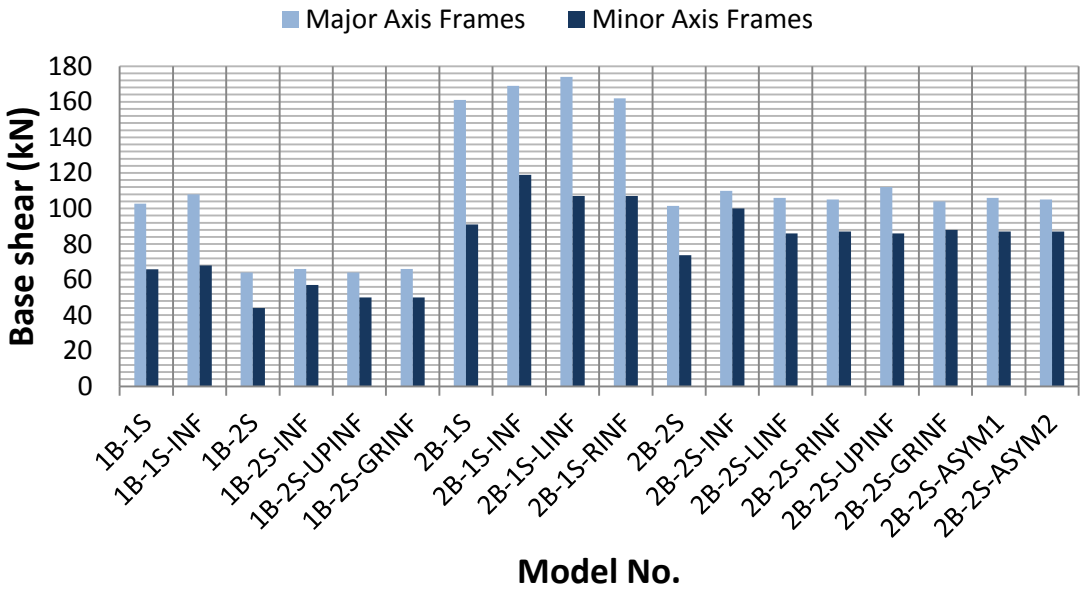

Figure 5.3: Base shear values for major and minor axis frame models.

- The existence of infill walls increase the received load since the bare models received the lowest. However, this phenomenon is mainly dependent on the location of infill walls.

- Out-of-plane displacement and fully infilled frames have greater effects on stiffness compared to vertical irregularity and asymmetrical placement of infills.

In the light of aforementioned results, it can be concluded that the presence and location of infill walls and orientation of the vertical frame members have both advantageous and disadvantageous effects on the behaviour of steel structures. Increased stiffness of fully infilled frames compared to bare and partially infilled frames can be accounted as positive effect of infills. However, higher fundamental time periods due to increased weight, alterations in top displacement, and base shear are accounted as their negative effects.

Similarly, effects of the orientation of the vertical members are significant. Major axis frames are more advantageous than minor axis frames by means of increased strength but they have higher fundamental time periods. Also, major axis models having infills on the upper story only, experience soft story formation. Minor axis frames decrease fundamental time period, has zero out-of-plane displacement and variation among top displacements due to vertical irregularities is not as high as that of major axis frames.

5.3 Recommendations

The following are the recommendations for future research work.

- Infill walls made of different materials can be used to evaluate effect of infill material on the behaviour of steel frames and then the results can be compared to find out which infill material is the most effective one to totally ignore or include infill walls during design.

- The non-linear dynamic analysis can be employed to monitor the most realistic response of structures to seismic forces by defining complete hysteretic behaviour of infill wall.

- The effect of out-of-plane displacement of frames can be tested with restrained and unrestrained frames. Similarly, effect of upward movement of top beams can also be studied.

- The effect of bay and story increase as well as plan and vertical irregularities on performance parameters can be studied with 3D, full-scale multi-storey buildings.

REFERENCES

[1] Arêde, A., Furtado, A., Rodrigues, H., & Varum, H. (2016). Experimental evaluation of out-of-plane capacity of masonry infill walls, *Journal of Engineering Structures,* 111, 48-63.

[2] Farshchi, H., Hajirasouliha, I., & Jazany, R. A. (2013). Influence of masonry infill on the seismic performance of concentrically braced frames. *Journal of Constructional Steel Research*, 88, 150-163.

[3] Sezen, H., Whittaker, A. S., Elwood, K. J., and Mosalam, K. M. (2003). Performance of reinforced concrete buildings during the August 17, 1999 Kocaeli, Turkey earthquake, and seismic design and construction practise in Turkey, *Engineering* Structures 25, 103–114.

[4] Jain, S. K., Kaushik, H. B. and Rai, D. C. (2006). Code approaches to seismic design of masonry-infilled reinforced concrete frames: A state-of-the-art review. *Earthquake Engineering Research Institute, Earthquake Spectra,* 22(4), 961-83.

[5] Jain, S. K., and Murty, C. V. R. (2000). Beneficial influence of masonry infills on seismic performance of RC frame buildings, *Proceedings, 12th World Conference on Earthquake Engineering*, New Zealand, Paper No. 1790.

[6] Bertero, V. and Brokken, S. (1983). Infills in seismic resistant building, *Journal of Structural Engineering, ASCE,* 109(6), 1337–1361.

[7] FEMA-306 (1999). Evaluation of earthquake damaged concrete and masonry wall buildings—Basic Procedures Manual, *Federal Emergency Management Agency*, Washington D.C.

[8] FEMA-273 (1997). Guidelines for the Seismic Rehabilitation of Buildings, *Federal Emergency* Management *Agency*, Washington, D.C.

[9] EUROCODE-8 (1998). Design Provisions for Earthquake Resistance of Structures. *European Committee of Standardization*, Brussels, Belgium.

[10] Chen, X., & Liu, Y. (2016). A finite element study of the effect of vertical loading on the in-plane behaviour of concrete masonry infills bounded by steel frames. *Journal of Engineering Structures*, 117, 118-129.

[11] Milad, A. M. L. (2015). Effect of infill wall on the seismic behaviour of steel framed structures. *Master Thesis, Department of Civil Engineering, Eastern Mediterranean University,* 116 p.

[12] Arêde, A., Furtado, A., Ramos, T., Rodrigues, H., Tavares, P., & Varum, H. (2015). In-plane response of masonry infill walls: experimental study using digital image correlation. *Procedia Engineering*, 114,870-6.

[13] Misir, I. S. (2015). Potential use of locked brick infill walls to decrease soft-story formation in frame buildings. *Journal of Performance of Constructed Facilities*, 29(5), *04014133*.

[14] Liu, Y., & Soon, S. (2012**).** Experimental study of concrete masonry infills bounded by steel frames**.** *Canadian Journal of Civil Engineering*, 39(2), 180-90.

[15] Girgin, S. C., Misir, I. S., Ozcelik, O., & Yucel, U. (2015). The behaviour of infill walls in RC frames under combined bidirectional loading, *Journal of Earthquake Engineering*, 00,1-28.

[16] Arêde, A., Furtado, A., & Rodrigues, H.(2015). Modelling of masonry infill walls participation in the seismic behaviour of RC buildings using OpenSees. *International Journal of Advanced Structural Engineering*, 7, 117-27.

[17] Basha, S. H., & Kaushik, H. B. (2016). Behaviour and failure mechanisms of masonry-infilled RC frames (in low-rise buildings) subject to lateral loading. *Journal of Engineering Structures,* 111, 233-45.

[18] Liu, Y., & Manesh, P. (2013). Concrete masonry infilled steel frames subjected to combined in-plane lateral and axial loading- An experimental study. *Engineering Structures*, 52, 331-9.

[19] Duggal, S. K. (2007). Earthquake resistant design of structures, Oxford University Press, New Delhi.

[20] Steel lateral load resisting systems. (2017, January 20). Retrieved from http://users.encs.concordia.ca/home/x/xiaom_h/Study/New%20folder/Steel%20Lateral%20Load%20Resisting%20Systems.pdf

[21] Cross braced frame with pinned bases. (2017, January 20). Retrieved from: http://expeditionworkshed.org/applets/2D_frames/sketch_19/sketch_19.html

[22] Zhang, B. (2006). Parametric study on the influence of infills on the displacement capacity of RC frames for earthquake loss estimation. *Master Thesis, Department of Earthquake Engineering, Rose School*, 86p.

[23] Bilgin, H., Binici, H., Kaplan, H., Öztas, A., Yılmaz, S. (2010). Structural damages of L'Aquila (Italy) earth-quake, *Natural Hazards and Earth System Sciences*, 10, 499–507.

[24] El-Dakhakhni, W. W. Elgaaly, M., & Hamid A. A. (2003). Three-strut model for concrete masonry-infilled steel frames. *J. Struct. Eng*. 129(2), 177-185.

[25] Mehrabi, A. B. & Shing, P. B. (2002). Behaviour and analysis of masonry-infilled frames. *Prog. Struct. Eng. Mater*, 4, 320-31.

[26] Mallick, D. V. & Severn, R. T. (1967). The behaviour of infilled frames under static loading. *Proceedings of the Institution of Civil Engineering*, 38, 639-56.

[27] Polyakov, S. V. (1966). Some investigations of the problem the strength of elements of buildings subjected to horizontal loads. *Symposium on Tall Buildings, University of Sourthampton,* 465-86.

[28] Holmes, M. (1961). Steel frames with brickwork and concrete filling. *Proc Inst Civ Eng Res Theory*, 19, 473–78.

[29] Smith, S. (1962). Lateral stiffness of infilled frames. *J. Struct. Div.,* 88, 183–199.

[30] Mainstone J., Weeks, G. (1970). The influence of bounding frame on the racking stiffness and strength of brick walls. *2nd International Brick Masonry Conference,* Watford.

[31] Bertero, V. V, & Klinger, R. E. (1978). Earthquake resistance of infilled frames. *J Struct Div.,* 104, 973–89.

[32] Hobbs, B. & Saneinejad, A. (1995). Inelastic design of infilled frames. *J. Struct. Eng.* 121, 634–50.

[33] Liauw, T., Kwan, K. (1984). Nonlinear behavior of non-integral infilled frames. *Comput. Struct.,* 18, 551–60.

[34] Dolsek, M., Fajfar, P. (2002). Mathematical modelling of an infilled RC frame structure based on the results of pseudo-dynamic tests. *Earthq. Eng. Struct. Dyn*., 31,1215–30.

[35] Bennett., R. M., Flanagan, R. D. & Tenbus, M. A. (1994). Numerical modelling of clay tile infills. *Proceedings from the NCEER Workshop on Seismic Response of Masonry,* San Francisco, California, 1, 63-8.

[36] Schmidt, T. (1989). An approach of modelling masonry infilled frames by the f.e. method and a modified equivalent strut model. *Annu. J. Concr. Struct*., 4, 171–180.

[37] Syrmakesis, C., Vratsanou, V. (1986). Influence of infill walls to RC frames response. *8th European Conference on Earthquake Engineering*, Istanbul, Turkey, 47–53.

[38] San Bartolomé, A. (1990). Colleción del Ingeniero Civi l, (in Spanish), Libro No. 4. Colegio de Ingenierios del Peru.

[39] Chrystomou, C. Z. (1991). Effects of degrading infill walls on the nonlinear seismic response two-dimensional steel frames. *Ph.D. Thesis,* Cornel University, Ithaca, New York.

[40] Crisafulli F. J. (1997). Seismic behaviour of reinforced concrete structures with masonry infills. *Ph.D. Thesis*, University of Canterbury, New Zealand.

[41] Crisafulli, F. J., & Carr, A. J. (2007). Proposed macro-model for the analysis of infilled frame structures. *Bull. NZ Soc. Earthq. Eng.,* 40(2), 69–77.

[42] Antoniou, A., Blandon, C., Crisafulli, F. J., Pinho, R., & Smyrou, E. (2011). Implementation and verification of a masonry panel model for nonlinear dynamic analysis of infilled RC frames. *Bull. Earthquake Eng.*, 9, 1519-34.

[43] King, G. J., W. & Pandey, P. C. (1978). The analysis of infilled frames using finite elements. *Proceedings of the Institution of Civil Engineers, 2(65), 749-60.*

[44] Atkinson, R. H., Amadei, B. P., Saeb, S. & Sture, S. (1989). Response of masonry bed joints in direct shear. *J. Struct. Eng.*, 115(9), 2276-96.

[45] Crisafulli, F. J., Carr, A. J. & Park, R. (2000). Analytical modelling of infilled frame structures - A general review. *Bull. NZ Soc. Earth. Eng.*, 33(1), 30-47.

[46] Smith, S. (1966). Behaviour of square infilled frames. *Proceedings of the American Society of Civil Engineering, Journal of Structural Division*, 92, 381-403.

[47] Ahmad, J., Ahmad, P., Ahmad, R., Jan, M. U., Malik, M. I. & Seth, H. (2014). Brick masonry and hollow concrete block masonry – A comparative study. *International Journal of Civil and Structural Engineering Research*, 1(1), 14-21.

APPENDICES

Appendix A: Structural Performance Parameters and Member Capacities of Validation Models

Figures A1 to A3 and Table A.1 give load-displacement curves, global and local performance parameters of 1 bay 1 story (1B-1S) validation models.

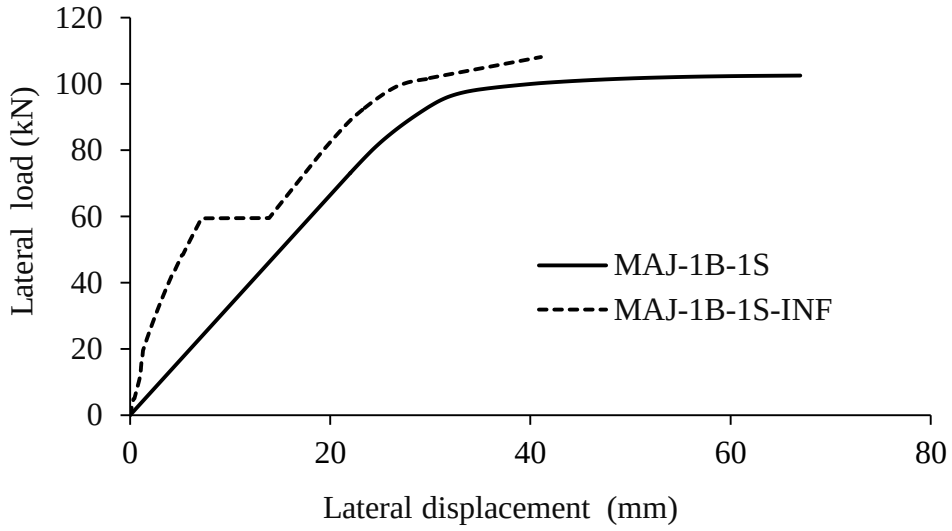

Figure A.1: Load-displacement curves for major axis 1 bay 2 story (1B-2S) frame models.

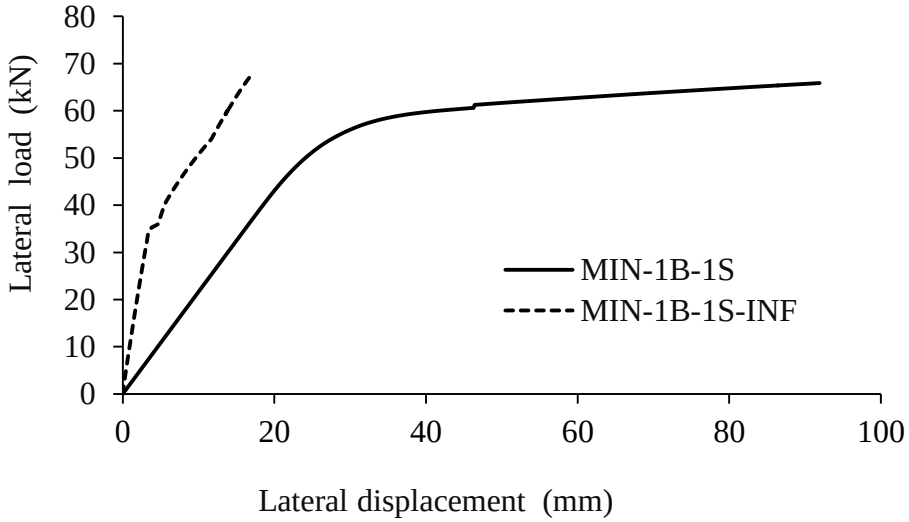

Figure A.2: Load-displacement curves for minor axis 1 bay 2 story (1B-2S) frame models.

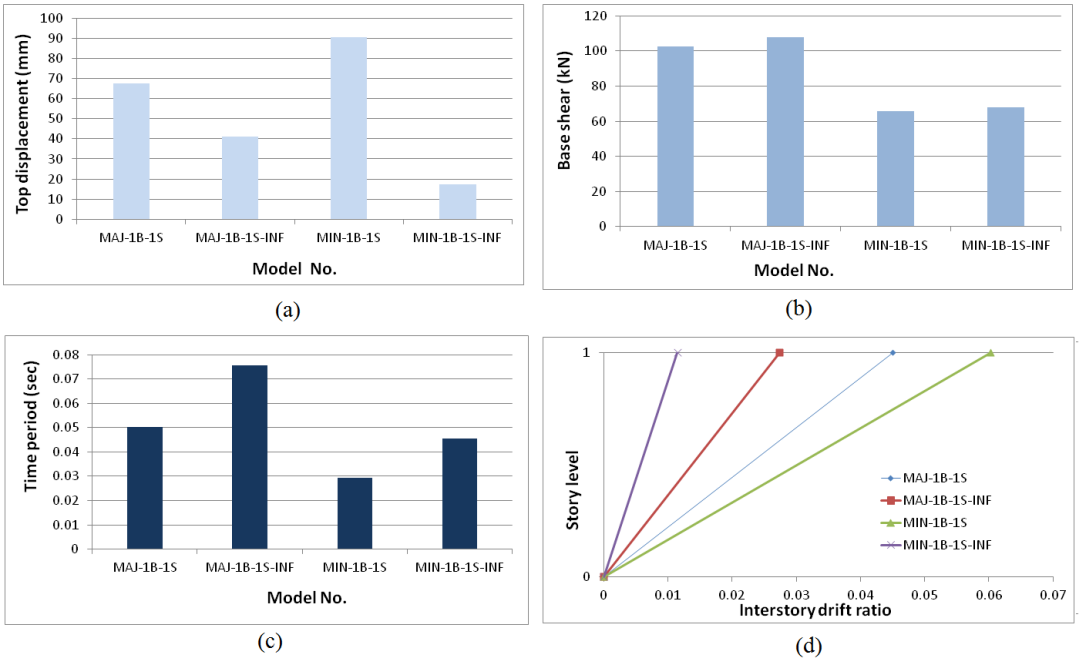

Figure A.3: Global structural parameters of 1 bay 1 story (1B-1S) validation models, (a) top displacement, (b) base shear, (c) time period and (d) drift ratio.

Table A.1: Member capacities of 1 bay 1 story (1B-1S) models.

	Member	Deformation Type	Load Level (kN)	Deformation Type	Load Level (kN)	Node	Load Level (kN)	Out of plane disp. (mm)
MAJ-1B-1S	C1	Yielding	82	Failure	99	1	102.63	40.97
	C2	Yielding	84	Failure	101	2		-26.86
	Beam	Yielding	98	Failure	100			
MAJ-1B-1S-INF	C1	Yielding	86	Failure	105	1	108.02	1.94
	C2	Yielding	95	Failure	108	2		-1.93
	Beam	Yielding	97	Failure	100			
MIN-1B-1S	C1	Yielding	50	Failure	64	1	65.79	0.00
	C2	Yielding	57	Failure	64	2		0.00
	Beam	Yielding	60	Failure	62			
MIN-1B-1S-INF	C1	Yielding	55	Failure	65	1	67.98	0.00
	C2	Yielding	58	Failure	65	2		0.00
	Beam	Yielding	62	Failure	60			

Appendix B: Location of Plastic Hinges

Figures B1 to B6 show the location of plastic hinges for all analytical models.

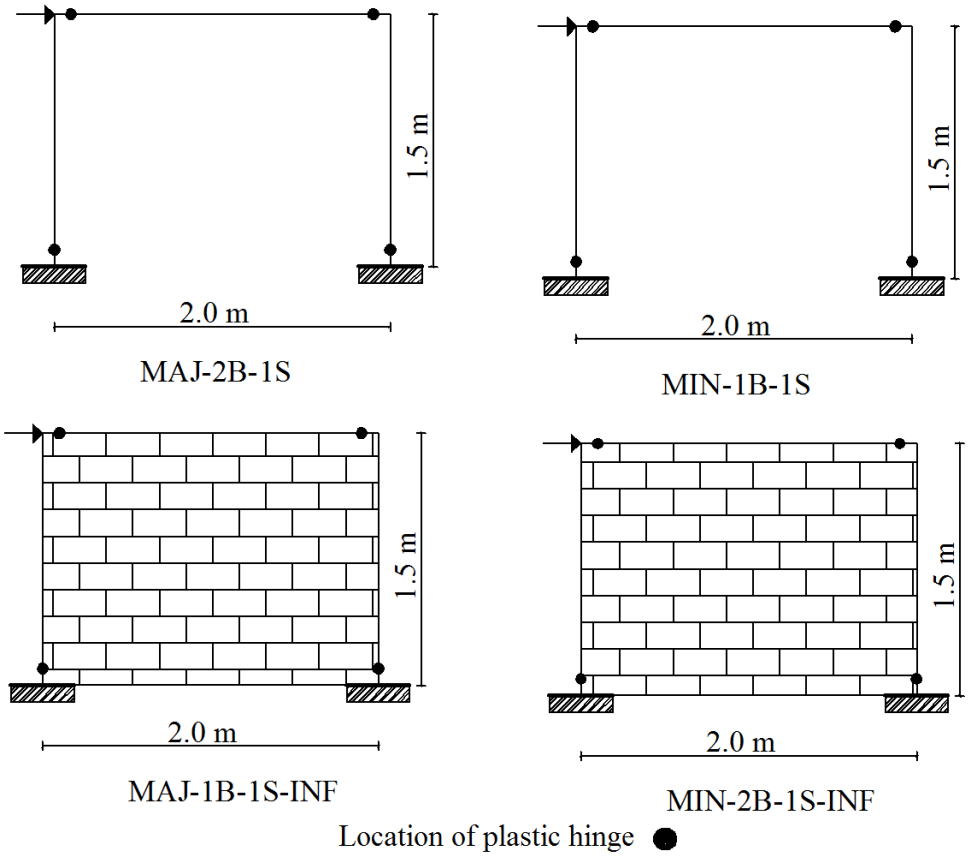

Figure B.1: Location of plastic hinges of 1 bay 1 story (1B-1S) frame models (validation models).

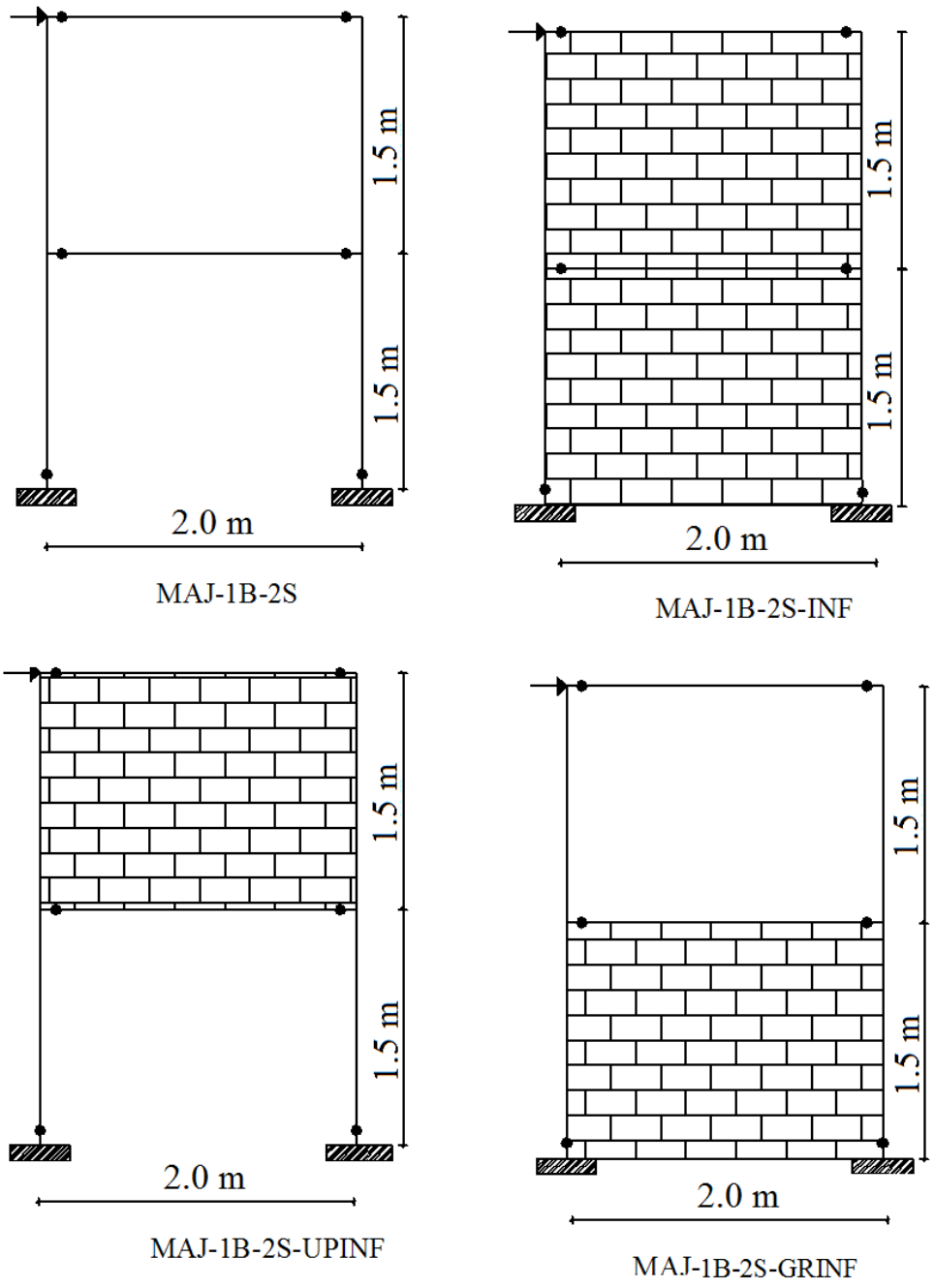

Figure B.2: Location of plastic hinges of major axis 1 bay 2 story (1B-2S) frame models.

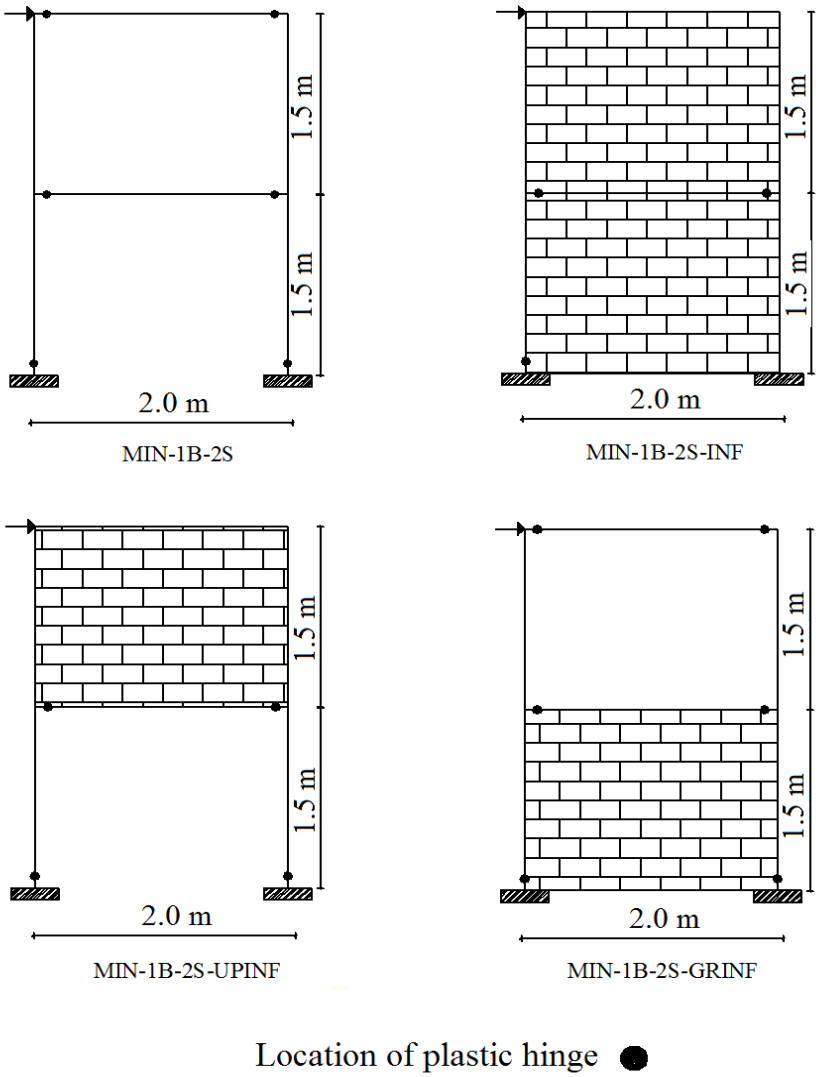

Figure B.3: Location of plastic hinges of minor axis 1 bay 2 story (1B-2S) frame models.

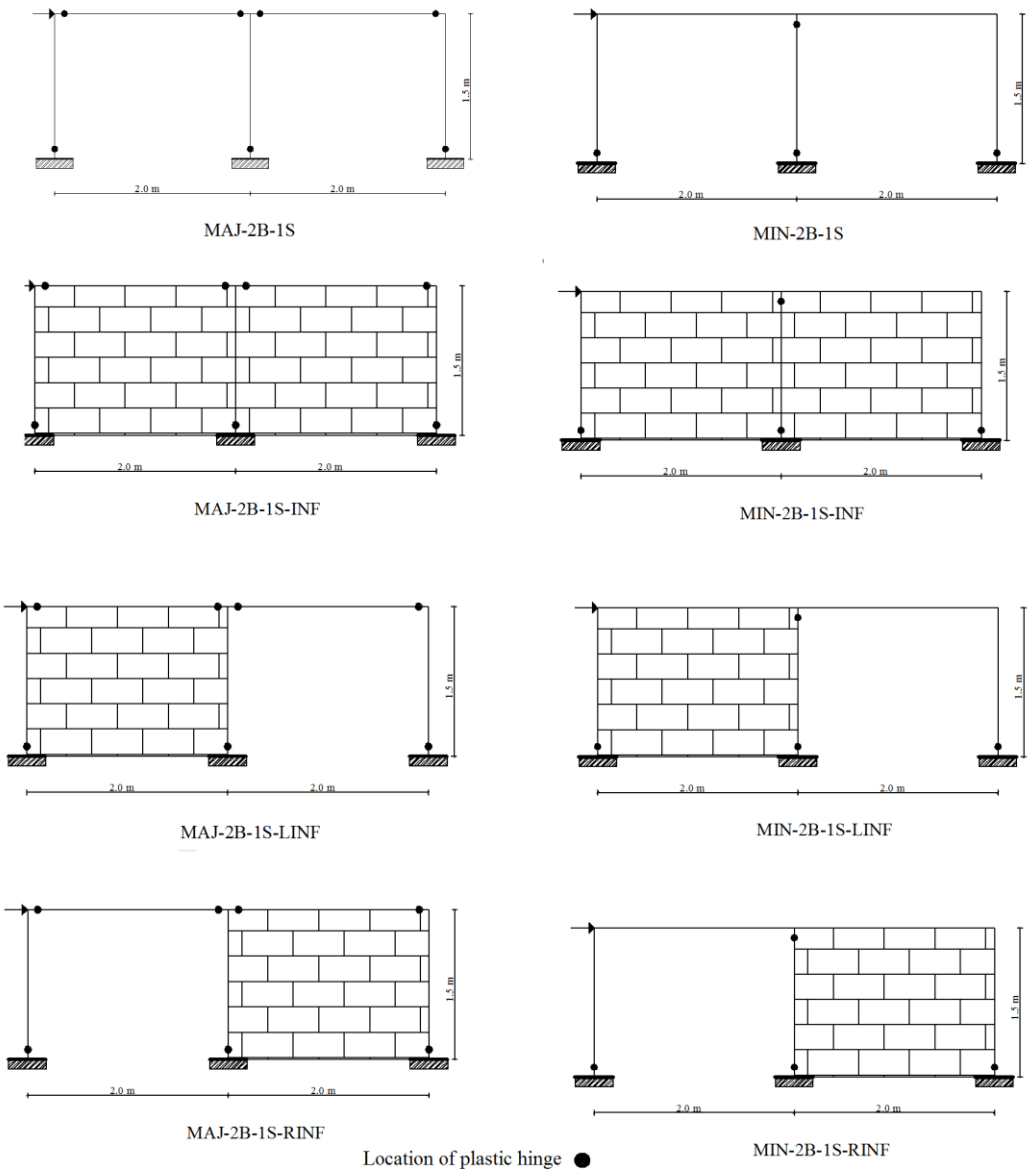

Figure B.4: Location of plastic hinges of 2 bay 1 story (2B-1S) frame models.

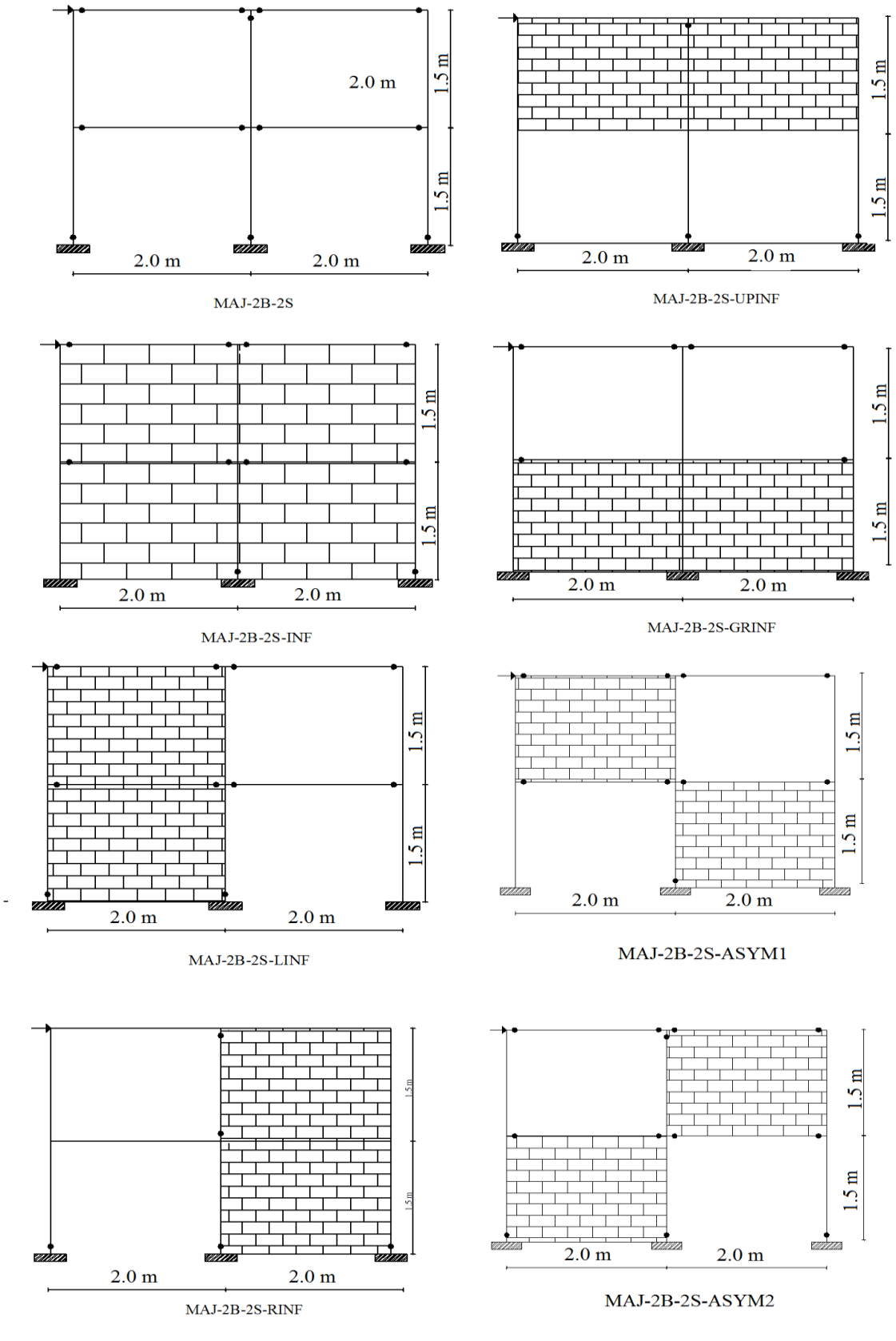

Figure B.5: Location of plastic hinges of major axis 2 bay 2 story (2B-2S) frame models.

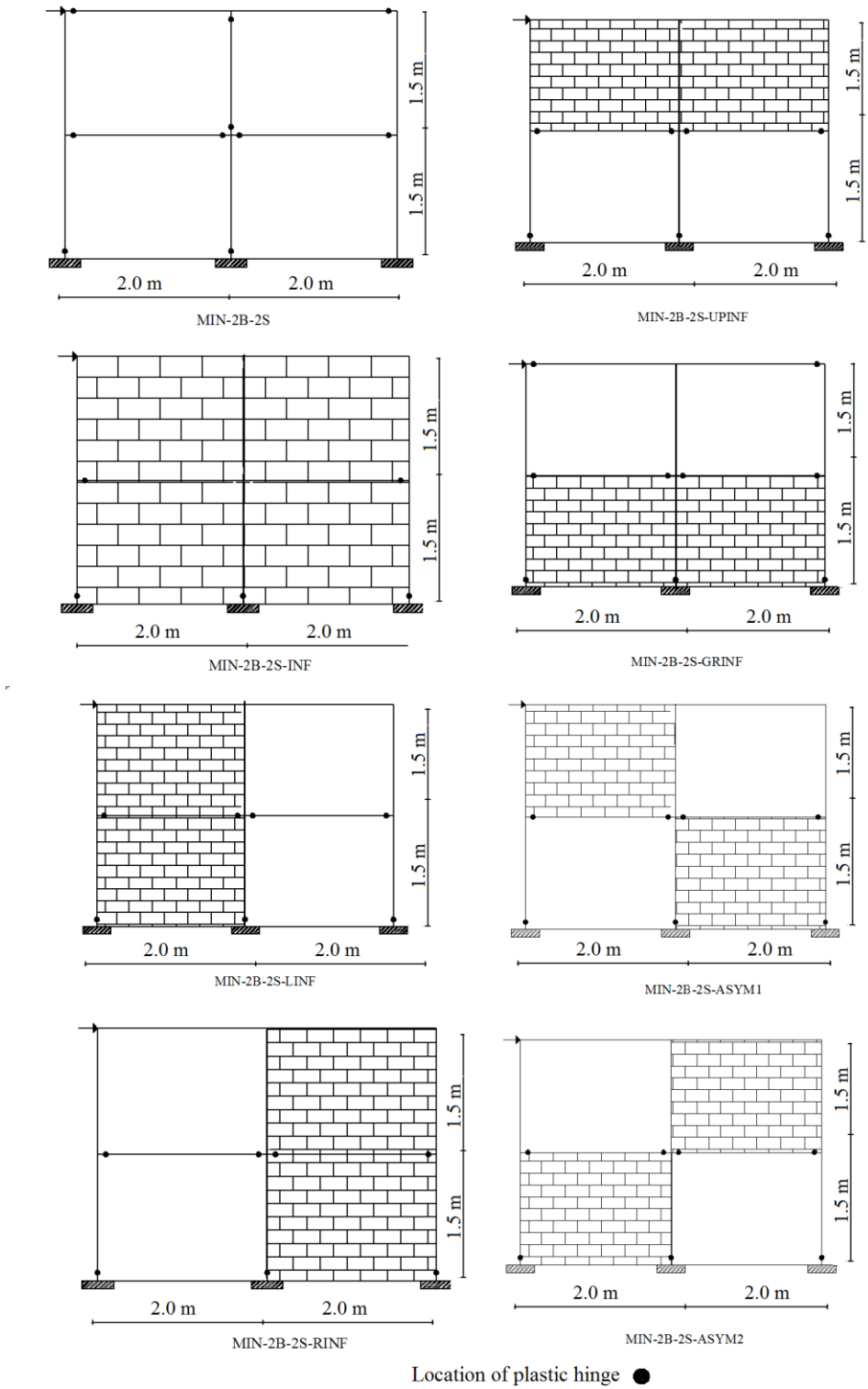

Figure B.6: Location of plastic hinges of minor axis 2 bay 2 story (2B-2S) frame models.